

Lateral Torsional Buckling of I-beams

A Parametric Study of Elastic Critical Moments in Structural Design Software

Master of Science Thesis in the Master's Programme Structural Engineering and Building Technology

MARTIN AHNLEN
JONAS WESTLUND

Department of Civil and Environmental Engineering
Division of Structural Engineering
Steel and Timber Structures
CHALMERS UNIVERSITY OF TECHNOLOGY
Göteborg, Sweden 2013
Master's Thesis 2013:59

Lateral Torsional Buckling of I-beams

A Parametric Study of Elastic Critical Moments in Structural Design Software

*Master of Science Thesis in the Master's Programme Structural Engineering and
Building Technology*

MARTIN AHNLEN

JONAS WESTLUND

Department of Civil and Environmental Engineering

Division of Structural Engineering

Steel and Timber Structures

CHALMERS UNIVERSITY OF TECHNOLOGY

Göteborg, Sweden 2013

Lateral Torsional Buckling of I-beams

A Parametric Study of Elastic Critical Moments in Structural Design Software

Master of Science Thesis in the Master's Programme Structural Engineering and Building Technology

MARTIN AHNLEN

JONAS WESTLUND

© MARTIN AHNLEN & JONAS WESTLUND, 2013

Examensarbete / Institutionen för bygg- och miljöteknik,
Chalmers tekniska högskola 2013:59

Department of Civil and Environmental Engineering

Division of Structural Engineering

Steel and Timber Structures

Chalmers University of Technology

SE-412 96 Göteborg

Sweden

Telephone: + 46 (0)31-772 1000

Cover:

Lateral torsional buckling of a cantilever beam (N.S Trahair cited in Atsuta & Chen 2008, p. 72)

Chalmers Reproservice, Göteborg, Sweden 2013

Lateral Torsional Buckling of I-beams

A Parametric Study of Elastic Critical Moments in Structural Design Software

Master of Science Thesis in the Master's Programme Structural Engineering and Building Technology

MARTIN AHNLEN

JONAS WESTLUND

Department of Civil and Environmental Engineering

Division of Structural Engineering

Steel and Timber Structures

Chalmers University of Technology

ABSTRACT

The elastic critical moment, M_{cr} , is an important parameter in design with regard to lateral torsional buckling. It can be calculated with analytical expressions, or more commonly, solved by structural design software. However, the complex nature of the lateral torsional buckling phenomenon makes it hard to embrace all the affecting factors and assumptions. Different programs use different methods to calculate M_{cr} , which leads to deviations in the results. One aim of this thesis was to study the assumptions and limitations of various design software with respect to this problem, and to explain the deviations between the results obtained from these programs. The programs included in this study are ADINA, COLBEAM, LTBeam and SAP2000.

A parametric study was carried out where single-spanned IPE500 steel beams were investigated. The differences in sectional constants and material properties were small. Thus, comparisons could be made directly by studying the C -factors in the *3-factor formula*. In finite element programs equivalent C -factors could be refracted from the expression of the critical moment.

Previous work has presented exact values of C_1 for some common load cases. When studying C_1 , these load cases were investigated with the exact values as references. When studying C_2 , two additional points of load application were considered; on the top flange, and on the bottom flange.

The main observation of the study was that C_1 not only depends on the moment distribution, but also on the lateral restraints and the length of the beam. This was expected and is in line with previous research. It was concluded that the deviation between the programs depends on to what extent these effects are accounted for. Generally, finite element programs gave solutions close to the exact values.

A general problem using programs based on the *3-factor formula* is to find accurate C -factors. The approximate expression by Lopez et al. (2006) is used by COLBEAM and provides satisfying results in most cases. However, if table values exist for the situation at hand, such values give better solutions.

Furthermore, it was observed that the point of load application has a great influence on M_{cr} , and that this influence is of greater magnitude when the beam is fixed about the major axis.

Key words: Lateral torsional buckling, elastic critical moment, 3-factor formula, C -factors, warping, lateral boundary conditions, ADINA, COLBEAM, LTBeam, SAP2000

Vippning av I-balkar

En parametrisk studie av det kritiska vippningsmomentet i beräkningsprogram

Examensarbete inom Structural Engineering and Building Technology

MARTIN AHNLEN & JONAS WESTLUND

Institutionen för bygg- och miljöteknik

Avdelningen för konstruktionsteknik

Stål- och träbyggnad

Chalmers tekniska högskola

SAMMANFATTNING

Det kritiska vippningsmomentet, M_{cr} , är en viktig parameter vid dimensionering av vippningsbenägna balkar. Det kan beräknas med hjälp av analytiska uttryck eller lösas med beräkningsprogram. Vippningsfenomenets komplexa natur gör det dock svårt att överblicka alla påverkande faktorer och antaganden. Olika program använder olika metoder för att beräkna M_{cr} , vilket leder till avvikelser i resultaten. Ett av syftena med det här examensarbetet var att förklara skillnaderna mellan programmen ADINA, COLBEAM, LTBeam och SAP2000.

En parametrisk studie genomfördes av IPE500-balkar med enkelt spann. Skillnaderna i tvärsnittskonstanter och materialdata var små, och därför kunde jämförelser göras direkt genom C -faktorerna i *3-faktorsformeln*. I finita element-program kunde ekvivalenta C -faktorer brytas ut ur uttrycket för det kritiska vippningsmomentet.

Serna et al. (2005) har presenterat exakta värden på C_1 för några vanliga lastfall. Dessa värden har använts som referens i undersökningen av C_1 . När C_2 studerades varierades lastangreppspunkten mellan överkant och underkant fläns.

Den viktigaste observationen i studien var att C_1 inte enbart beror på momentfördelningen, utan också på laterala randvillkor och balklängd. Detta var förväntat och stämmer överens med resultat presenterade av Lopez et al. (2006), Fruchtengarten (2006) etc. En slutsats som kunde dras var att avvikelserna mellan programmen berodde på hur hänsyn tas till dessa förhållanden. I regel gav finita element-program i stort sätt exakta lösningar.

Ett problem med program baserade på *3-faktorsformeln* är svårigheten att hitta korrekta C -faktorer. Det approximativa uttrycket av Lopez et al. (2006) används i COLBEAM och ger goda approximationer i många lastfall. Finns tabellvärden tillgängliga för det aktuella lastfallet ger dessa dock bättre lösningar.

Studien av C_2 visade att lastangreppspunkten har en stor inverkan på M_{cr} och att denna är större för balkar fast inspända kring huvudaxeln.

Nyckelord: Vippning, elastiskt kritiskt vippningsmoment, 3-faktorsformeln, C -faktorer, välvning, laterala randvillkor, ADINA, COLBEAM, LTBeam, SAP2000

Contents

1	INTRODUCTION	1
1.1	Background	1
1.2	Aim and objectives	2
1.3	Method	2
1.3.1	Motivation and discussion of chosen methodology	2
1.4	Limitations	3
2	LATERAL TORSIONAL BUCKLING	4
2.1	Definitions and description of concepts	4
2.1.1	Orientation of coordinate system	4
2.1.2	Degrees of freedom	5
2.1.3	Boundary conditions	6
2.1.4	Cross-section geometry	6
2.1.5	Centre of gravity, GC	7
2.1.6	Shear centre, SC	7
2.1.7	Centre of twist, TC	8
2.1.8	Point of load application, PLA	8
2.1.9	Saint Venant torsion	8
2.1.10	Warping	10
2.2	Classical theory of instability	13
2.2.1	Global buckling and buckling modes of loaded members	14
2.3	Mechanisms behind lateral torsional buckling	16
2.4	Measurements against lateral torsional buckling	18
2.4.1	Influence of the cross-section	18
2.4.2	Influence of the point of load application	18
2.4.3	Influence of lateral restraints	19
2.5	Behaviour of real beams	23
3	DESIGN WITH REGARD TO LATERAL TORSIONAL BUCKLING	24
3.1	Buckling curves	25
3.2	Comment	26
4	ANALYTICAL EVALUATION OF M_{CR}	27
4.1	Energy methods	27
4.2	The 3-factor formula	28
4.2.1	Comment	29
4.2.2	The equivalent uniform moment factor, C_1	29
4.2.3	Correction factor for the point of load application, C_2	36
4.2.4	Correction factor for cross-section asymmetry, C_3	37
4.2.5	Effective length factors k_z and k_w	38
4.3	American Institute of Steel Construction, <i>AISC LRFD</i>	40

4.3.1	Evaluation of M_{cr}	40
4.3.2	Equivalent Uniform Moment Factor, C_b	40
5	EVALUATION OF M_{CR} WITH FINITE ELEMENT METHODS	42
5.1	Linearized buckling analysis	42
5.1.1	Eigenvectors and eigenvalues	42
5.1.2	Eigenvalue problems applied on structural stability	43
5.1.3	The influence of the base load	44
5.2	Load-displacement control, LDC	45
6	PRESENTATION OF SOFTWARE	46
6.1	ADINA Solids & Structures, 900 Nodes Version 8.8	46
6.2	COLBEAM, EC3 v1.0.6	47
6.2.1	Implementation of C -factors	47
6.2.2	Implementation of lateral restraints	48
6.3	LTBeam, version 1.0.11	49
6.3.1	Implementation of lateral restraints	50
6.4	SAP2000, Ultimate 15.1.0, “design module”	51
6.4.1	Implementation of C -factors	52
6.4.2	Implementation of lateral restraints	52
6.5	Summary of software properties	53
7	PARAMETRIC STUDY	54
7.1	Background	54
7.2	Prerequisites and assumptions	54
7.2.1	Software	54
7.2.2	Material	54
7.2.3	Geometry	55
7.2.4	Point of load application, PLA	56
7.2.5	Lateral boundary conditions	56
7.2.6	Studied load cases	56
7.3	Procedure	57
7.3.1	The reference moment, $M_{cr,ref}$	57
7.3.2	Parametric study of the C_1 -factor	58
7.3.3	Parametric study of the C_2 -factor	59
8	RESULTS	61
8.1	The C_1 -factor	61
8.1.1	Comments	61
8.1.2	Load Case I	62
8.1.3	Load Case II	63
8.1.4	Load Case III	64
8.1.5	Load Case IV	65
8.1.6	Load Case V	66

8.2	The C_2 -factor	67
8.2.1	Comments	67
8.2.2	Load Case II	68
8.2.3	Load Case III	69
8.2.4	Load Case IV	70
8.2.5	Load Case V	71
9	ANALYSIS OF RESULTS	72
9.1	Observations concerning C_1	72
9.1.1	The influence of lateral boundary conditions	72
9.1.2	COLBEAM tables and “Advanced calculation of C_1 ”	73
9.1.3	Accuracy of finite element software	75
9.2	Observations concerning C_2	75
10	DISCUSSION	76
10.1	Evaluation of elastic critical moments	76
10.2	The parametric study	77
10.2.1	Validity and reliability of the results	78
11	CONCLUDING REMARKS	80
11.1	Further studies	80
12	REFERENCES	81
APPENDICES		
A	Boundary conditions for common beam connections	
B	Serna et al. (2005) and table values from Access Steel (2005) and ECCS (2006)	
C	Derivation of the elastic critical moment	
D	Examples of .in-files used for the parametric study in ADINA	
E	Results from the parametric study	

Preface

This Master's thesis was initiated by Reinertsen Sweden AB and was conducted between January 2013 and June 2013 at the Division of Structural Engineering, Steel and Timber Structures, Chalmers University of Technology, Sweden. Associate Professor Mohammad Al-Emrani from the Division of Structural Engineering was examiner of the thesis.

We would like to thank our supervisors at Reinertsen, Martin Gustafsson and Emanuel Trolin. Their support and guidance have been greatly appreciated.

We are also thankful for the feedback and the thoroughly proofreading of the thesis by our opponents Annelie Dahlgren and Louise Svensson.

Lastly, we would like to thank Lisa Lee Källman and Stina Lundqvist for the helpful discussions during our coffee breaks concerning the formatting of the report. We also appreciate your generosity in lending us your computers when we suffered from compatibility problems between Mac and PC.

Göteborg June 2013

Martin Ahnlén & Jonas Westlund

Notations

Abbreviations

<i>CTICM</i>	Centre Technique Industriel de la Construction Métallique
<i>ECCS</i>	European Convention for Constructional Steelwork
<i>Eurocode 3</i>	EN-1993-1-1:2005
<i>FEM</i>	Finite Element Method
<i>GC</i>	Centre of Gravity
<i>LDC</i>	Load-Displacement Control
<i>NCCI</i>	Non-Contradictory Complementary Information
<i>PLA</i>	Point of Load Application
<i>SC</i>	Shear Centre
<i>SBI</i>	Stålbyggnadsinstitutet (Swedish Institute of Steel Construction)
<i>TC</i>	Centre of Twist

Roman upper case letters

C_1	Moment gradient factor or equivalent uniform moment factor; Correction factor in the <i>3-factor formula</i> primarily accounting for the moment distribution
C_2	Correction factor in the <i>3-factor formula</i> primarily accounting for the point of load application
C_3	Correction factor in the <i>3-factor formula</i> primarily accounting for cross-section asymmetry with respect to y-axis
E	Young's modulus [Pa]
EI	Bending stiffness [$\text{Pa} \cdot \text{m}^4$]
F	Force [N]
G	Shear modulus [Pa]
GI_t	Torsional stiffness [$\text{Pa} \cdot \text{m}^4$]
H	Potential energy [J]
H_e	External potential energy of a system [J]
H_i	Internal potential energy of a system [J]
H_{straight}	The potential energy in a straight state of equilibrium (before buckling) [J]
I_t	Saint Venant's torsion constant [m^4]
I_z	Second moment of inertia in bending about z-axis [m^4]
I_w	The warping constant [m^6]
$\underline{\underline{K}}$	Stiffness matrix
$\underline{\underline{K}}_E$	Elastic linear part of the stiffness matrix
$\underline{\underline{K}}_G$	Geometric non-linear load dependent part of the stiffness matrix
$\underline{\underline{K}}^{t_0}$	Stiffness matrix before start of the analysis
$\underline{\underline{K}}^{t_1}$	Stiffness matrix at the time of the first load-step
L	Beam length between bracings [m]
L_b	Critical buckling length [m]
L_{cr}	Critical buckling length [m]
M	Moment [Nm]
M_{cr}	Elastic critical moment [Nm]
$M_{cr,ref}$	Elastic critical reference moment [Nm]

$M_{cr,0}$	Special case of $M_{cr,ref}$ (when $k=1.0$) [Nm]
M_y	Bending moment about y-axis [Nm]
N	Normal force [N]
N_{cr}	Critical normal force [N]
\underline{P}	Load vector
P	Force [N]
P_{cr}	Critical force [N]
W_y	Bending resistance about y-axis [m ³]

Roman lower case letters

h_{f1}	Width of top flange [m]
h_{f2}	Width of bottom flange [m]
h_w	Height of web [m]
k	Effective length factor
k_w	Effective length factor in the <i>3-factor formula</i> accounting for warping boundary conditions
k_z	Effective length factor in the <i>3-factor formula</i> accounting for lateral bending boundary conditions
\underline{p}	Displacement vector
q_{cr}	Critical distributed load [N/m]
t_{f1}	Thickness of top flange [m]
t_{f2}	Thickness of bottom flange [m]
t_w	Thickness of web [m]
u_t	Displacement due to twisting [m]
u_w	Displacement due to warping [m]
u_x	Displacement in x-direction [m]
u_y	Displacement in y-direction [m]
u_z	Displacement in z-direction [m]
z_g	Distance between the point of load application and the shear centre [m]
z_j	Distance related to the effects of asymmetry about y-axis [m]
z_s	Distance between the shear centre and the centre of gravity [m]

Greek upper case letters

θ	Rotation about x-axis in LTBeam
θ'	Warping degree of freedom in LTBeam
χ	Buckling factor
χ_{LT}	Buckling factor with regard to lateral torsional buckling
Ψ	End-moment ratio

Greek lower case letters

γ_{MI}	Partial safety factor
$d\varphi$	Twisting angle of an infinite small beam element subjected to torsion
λ_{cr}	Critical load factor (eigenvalue)
λ_{LT}	Slenderness parameter with regard to lateral torsional buckling
μ	Ratio that C_I depends on according to Fruchtengarten (2006), Access Steel (2005), and ECCS (2006)
v	Lateral deflection in LTBeam
v'	Lateral rotation in LTBeam
φ	Twisting angle
ϕ_i	Buckling mode

1 Introduction

1.1 Background

Structural stability is an essential part in the design process for steel structures. In *EN-1993-1-1:2005*, hereinafter referred to as *Eurocode 3*, the capacity of a member with regard to buckling and instability is taken into account by a reduction factor χ . This reduction factor is strongly dependent on the member slenderness parameter, $\bar{\lambda}$, which in turn is inversely proportional to the square root of the elastic critical moment, M_{cr} . When considering lateral torsional buckling, the buckling factor can be determined according to equations (1.1), (1.2) and (1.3).

$$\chi_{LT} = \frac{1}{\Phi_{LT} + \sqrt{\Phi_{LT}^2 - \bar{\lambda}_{LT}^2}}, \quad \chi_{LT} \leq 1.0 \quad (1.1)$$

$$\Phi_{LT} = 0.5 \left(1 + \alpha_{LT} (\bar{\lambda}_{LT} - 0.2) + \bar{\lambda}_{LT}^2 \right) \quad (1.2)$$

$$\bar{\lambda}_{LT} = \sqrt{\frac{W_y \cdot f_y}{M_{cr}}} \quad (1.3)$$

Therefore, evaluation of the design capacity with regard to stability is dependent on M_{cr} , and requires that M_{cr} can be computed for the actual load case.

However, there are no guides in *Eurocode 3* on how to determine M_{cr} . It is simply stated that the real section properties, moment distribution and possible lateral restraints should be taken into account. Early editions of *Eurocode* included an analytical expression of M_{cr} known as the *3-factor formula*. However, the expression was later removed without replacement. The formula can still be found in handbooks and additional guides for steel construction. In a few standard load cases where the parameters included in the *3-factor formula* are known, it can provide more or less exact solutions of M_{cr} . For other load cases where the parameters are unknown, they can be estimated by closed-form expressions based on curve fitting techniques. In these cases the accuracy of M_{cr} depends on the accuracy of the approximated parameters.

Commonly M_{cr} is determined with commercial software. If a finite element model with shell elements is established carefully, accurate and reliable results can be provided. Generally, conducting such analysis on every member in a structure is too time consuming and not economically justified, why often task specific software are used instead. These programs can either be based on analytical expressions such as the *3-factor formula*, or based on finite elements.

At Reinertsen Sweden AB it has been noticed that the magnitude of M_{cr} in specific load cases differs depending on which software is used. The divergence can be seen not only in complex load cases but also in simple cases. Sometimes the magnitude is big enough to raise questions on the reliability of the results. In design, a most important aspect is that approximate results are conservative.

Some of the programs used at Reinertsen Sweden AB are ADINA, COLBEAM, LTBeam and SAP2000. ADINA and LTBeam use finite elements in calculations,

while COLBEAM implements analytical expressions. In SAP2000 it is possible to use either finite elements or analytical expressions.

1.2 Aim and objectives

The aim of this Master's thesis was to examine how different design software calculate the elastic critical moment and to explain potential differences in the results.

Two objectives could be formulated.

- (1) The theory behind lateral torsional buckling should be presented, providing a thorough understanding of the mechanisms involved, the design procedures and the evaluation of M_{cr} .
- (2) Prerequisites, assumptions and calculation methods in different design software should be compared and the accuracy of M_{cr} should be evaluated for common load cases.

1.3 Method

A literature review was carried out where the lateral torsional buckling phenomena and the evaluation of elastic critical moments were studied.

Furthermore, a parametric study was conducted where the evaluation of elastic critical moments in ADINA, COLBEAM, LTBeam and SAP2000 was investigated. The differences in sectional constants and material properties implemented in the programs were small. Thus, comparisons could be made directly by studying the C -factors in the *3-factor formula*. In finite element programs equivalent C -factors could be refracted from the expression of the critical moment.

The study was divided into two parts; one concerning the C_1 -factor and one concerning the C_2 -factor. Load cases and beam geometry were chosen so that comparisons could be made between the programs and with reference values from Serna et al. (2005). Therefore, the study was limited to singled-spanned IPE500 beams. When studying C_2 , two points of load application were considered; on the top flange, and on the bottom flange.

1.3.1 Motivation and discussion of chosen methodology

The thesis work was conducted during 20 weeks at Reinertsen Sweden AB in Gothenburg. Here access was granted to the licenced software ADINA, COLBEAM, SAP2000 and the free software LTBeam. Therefore the choice of methodology had to be adjusted to fit this time limit and to the restrictions in available tools.

Generally when a causal relationship is investigated, an experimental strategy is to be preferred. Methods like interviews and surveys are good tools in studies where in-depth or representative views are sought respectively, but when cause and effects of a certain phenomenon is investigated these methods are not effective (Biggum 2008, p. 130 & p. 139). On the basis of this reasoning a parametric study was conducted in order to evaluate the differences of the computer programs. A big advantage by using parametric studies is also that full control is gained over the affecting parameters of

the test. The same beam measurements, loads, material properties and boundary conditions can be applied and varied in numerous ways. This result in high validity and make sure that the results of the comparison are reliable.

The sample population used in an experimental research project should be chosen carefully, so that a sufficient representation of the population is achieved allowing generalizations to be made (Biggham 2008, p. 126). A lot of knowledge regarding instability is based on extensive testing of real beams. However, using such methods can be time-consuming and also leave room for errors due to poor construction of the test samples. The elastic critical moment is a theoretical moment with respect to a perfect beam with no imperfections. Modelling such a beam is both easier and faster using computer based techniques. In a program it is also easy to test a big sample population by changing properties of the same start model between the tests. This is however not possible to the same extent when testing real beams, where changes in the test set-up are very time-consuming.

In order to perform a rewarding computer based investigation, a solid foundation of knowledge on the theory of lateral torsional buckling was needed. A great many research groups have studied the subject, writing numerous books and papers that explain the instability phenomena, and the mechanisms involved. Using this already existing knowledge by conducting a literature review was an effective way to compile the information. In addition to books and reports about lateral torsional buckling, the European and American design codes, calculation handbooks and user manuals provided information on how computer based software determines the elastic critical moment.

It can be argued that also other methods than the chosen ones are beneficial. General information about the software can be gathered through interviews and surveys with the program creators and program users. However, since the study had narrow and profound aims concerning specific models of beams, not focusing on the software in general, such quantitative or qualitative methods were not suitable. An additional problem with interviews is guaranteeing the objectivity of the results. Since the program developers and users have interests of their own, they may consciously or unconsciously avoid highlighting interesting problems concerning the software.

An observation on how engineers treat instability problems could also provide an interesting angle. However, because of the narrow time limit, such studies were left out of the scope of this thesis.

1.4 Limitations

The parametric study was limited to 8- and 16-meter single-spanned IPE500 steel beams, using the software ADINA, COLBEAM, LTBeam and SAP2000.

Since the study was limited to IPE500 beams (with double-symmetric cross-sections), the $C_3 \cdot z_j$ -factor is zero, and C_3 was therefore left out of the study.

In ADINA, warping beam elements are used in a linearized buckling analysis. In SAP2000 the elastic critical moments are calculated analytically in a “design module”. In both these programs more advanced methods could be used. However, these methods are not evaluated since they are generally too time-consuming to use in design.

2 Lateral torsional buckling

2.1 Definitions and description of concepts

2.1.1 Orientation of coordinate system

The beams in this report are orientated according to the coordinate system presented in Figure 2.1. The span is directed along the x -axis while the y - and z -axis are in the plane of the cross-section.

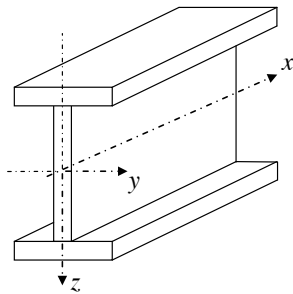


Figure 2.1 Orientation of beam coordinates.

When a beam is subjected to *major axis bending*, i.e. bending about the y -axis, it will deflect in the z -direction. This type of bending is sometimes referred to as *bending about the strong axis*. Analogous, *minor axis bending* is when a beam is bent about the z -axis, deflecting in the y -direction. This is sometimes called *lateral bending* or *bending about the weak axis*. See Figure 2.2.

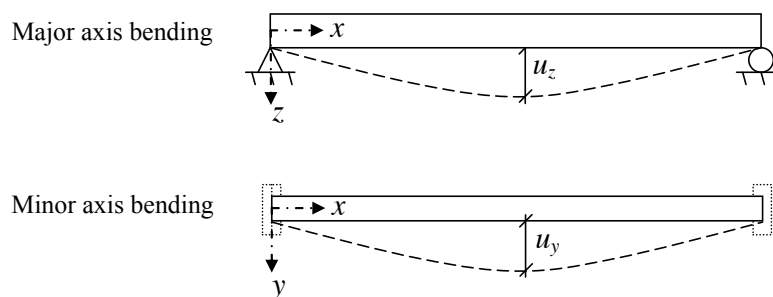
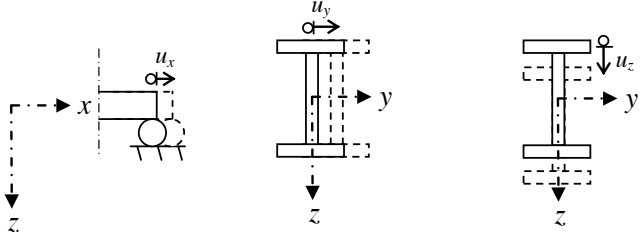
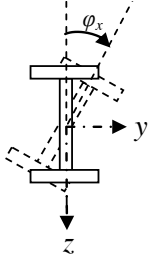
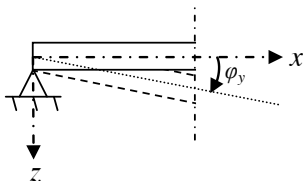
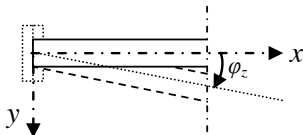
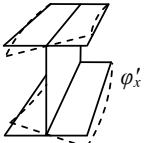


Figure 2.2 Beams subjected to major and minor axis bending.

2.1.2 Degrees of freedom

A beam element can be considered to have seven degrees of freedom in each node. These are *translation* in x -, y -, and z -direction, *rotation* about x -, y -, and z -axis and *warping*, see Table 2.1. The warping degree of freedom is explained further in chapter 2.1.10.

Table 2.1 *Degrees of freedom for a beam element.*

Translation in x , y and z	
Rotation about x -axis	
Rotation about y -axis (Major axis bending)	
Rotation about z -axis (Minor axis bending, lateral bending)	
Warping (see chapter 2.1.10)	

2.1.3 Boundary conditions

At the boundary, some degrees of freedom must always be restrained in order to have equilibrium. When considering ordinary beams on two supports, translation in y - and z -direction are always restrained. Translation in x is normally considered free at one side and fixed at the other. Rotation about the x -axis must be restrained since the beam otherwise would rotate about its own axis. Since these degrees of freedom are given, the remaining are of extra interest when studying beams on two supports.

- (1) Rotation about the y -axis (major axis bending)
- (2) Rotation about the z -axis (minor axis bending, lateral bending, k_z)
- (3) Warping (k_w)

An important and often mentioned support condition is the fork support, see Figure 2.3. A fork support is defined to have the following boundary conditions.

- (1) Translation in x , y and z (Fixed)
- (2) Rotation about x -axis (Fixed)
- (3) Rotation about y -axis (Free)
- (4) Rotation about z -axis (Free)
- (5) Warping (Free)

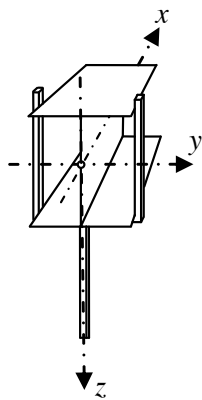


Figure 2.3 A principal sketch of a fork support. Translation in x , y , z and rotation about the x -axis is fixed. The other degrees of freedom are free.

2.1.4 Cross-section geometry

If nothing else stated, the following labelling of cross-section dimensions are used in the thesis.

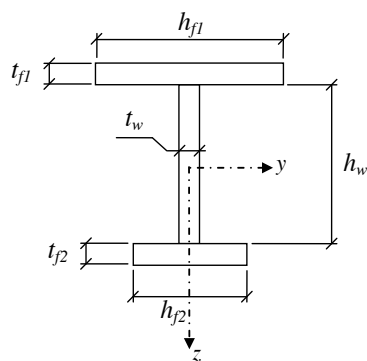


Figure 2.4 Cross-section labelling in the thesis.

2.1.5 Centre of gravity, GC

The *centre of gravity*, GC , is the point in a body of mass where the total weight of the body can be thought to be concentrated for convenience in calculations. The sum of the gravitational moment created from the mass of the body, i.e. the static moment, is zero in this point (Lundh 2007, p. 78).

GC coincides with the centroid (geometric centre) if the material is homogenous. In a double-symmetric homogenous I-section, GC is located at the intersection of the two symmetry lines (see Figure 2.5).

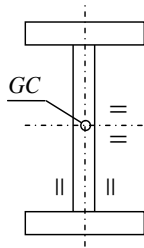


Figure 2.5 In a double-symmetric I-section of homogenous material the centre of gravity is located at the intersection of the two section symmetry lines.

2.1.6 Shear centre, SC

By definition the *shear centre*, SC , is the point through which the line of action of the shear force must act in order to cause pure in-plane bending. For beams with double-symmetric cross-sections, such as an I-section, the centre of gravity and the shear centre coincide (Lundh 2007, p. 322).

However, considering single-symmetric or non-symmetric sections there are cases where GC and SC do not coincide. Figure 2.6 shows a loaded u-section with sectional forces and resultants marked out. If the section is loaded in the plane of the web, the moment from the forces in the flanges will twist the section. Hence, SC is located to the left of the web where moment equilibrium is achieved (ibid.).

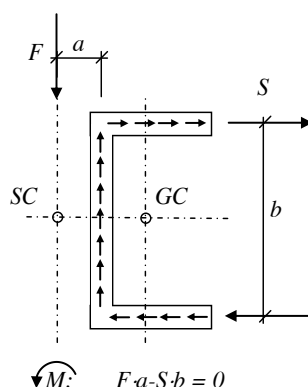


Figure 2.6 The shear centre and the centre of gravity in an U-section. A force acting in the shear centre will not cause any twisting of the section (Adapted from Lundh 2007, p. 322).

2.1.7 Centre of twist, TC

The *centre of twist*, TC , is the point a cross-section will twist about when subjected to a twisting moment. Since the definitions of TC and the *shear centre*, SC , are different, they are derived in different ways. However, as seen in Barretta (2012) and Ecsedi (2000) they basically always coincide.

In double-symmetric sections GC , SC and TC all coincide, and are located where the two symmetry lines of the cross-section intersect (Lundh 2007, p. 322).

2.1.8 Point of load application, PLA

The *point of load application*, PLA , is the point in a cross-section where the acting load is applied. It is common to assume that PLA is located in the *shear centre*. When considering lateral torsional buckling, PLA has a considerable effect on the buckling capacity. An assumption that the load acts in TC will therefore yield wrong results if it in reality acts on the top or the bottom flange.

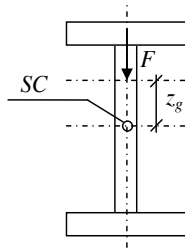


Figure 2.7 A force (F) is applied at a distance (z_g) from the shear centre.

2.1.9 Saint Venant torsion

When an infinitesimal beam element is subjected to torsion as in Figure 2.8, the element will twist by an angle $d\phi$ (Höglund 2006, p. 29).

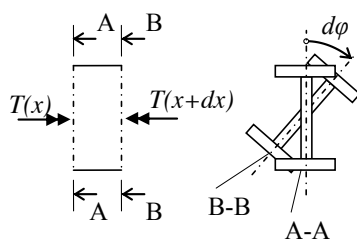


Figure 2.8 Twisting of an infinitesimal beam element (adapted from Höglund 2006, p. 29).

In I-beams subjected to torsion, the sections will not remain plane. This means that both twisting and local warping occur. These effects are resisted by shear forces in the sections and depend on the torsional stiffness, GI_t .

$$T = GI_t \frac{d\phi}{dx} \quad (2.1)$$

Where G = Shear modulus
 I_t = Saint Venant's torsion constant

For an I-section the torsion constant can be approximated as (Lundh 2006, p. 339)

$$I_t = \sum_{i=1}^n \frac{t_i^3 h_i}{3} \quad (2.2)$$

Where t_i = Thickness of the plates in the cross-section
 h_i = Height of the plates in the cross-section

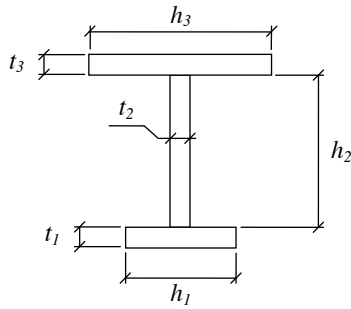


Figure 2.9 The section dimensions needed to approximate Saint Venant's torsion constant for an I-section.

2.1.10 Warping

The torsion constant, I_t , of an I-section depends on both twisting and warping. These are local effects that act in each section. Warping also has a global effect that will be discussed below.

Elements in a circular-symmetric section subjected to a torque, will twist to a new location within the same plane. Hence, the twisted section will consist of the same material as before the torque was applied (Höglund 2006, p. 29).

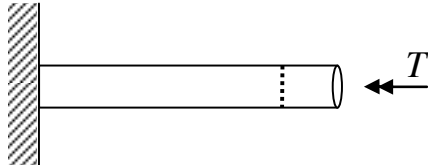


Figure 2.10 Circular-symmetric cantilever member subjected to a twisting moment. Any section in the member remains in-plane after the moment is applied.

However, when non-circular-symmetric sections are subjected to torsion, sectional elements will not remain in their initial planes. The reason for this is that the twisting moment will cause parts of the member to bend, moving elements along the member and out of their initial planes. This type of deformation is called warping (Höglund 2006, p. 29). Figure 2.11 shows a cantilever I-beam subjected to a twisting moment resulting in warping due to lateral bending of the flanges. When the flanges deflect in different directions, sections are no longer in their initial planes. At the support, the flanges are restrained and consequently warping is prevented.

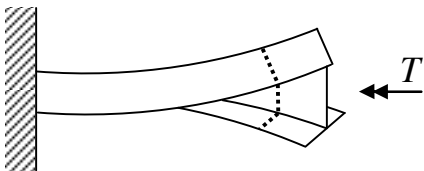


Figure 2.11 A cantilever I-beam is subjected to a twisting moment resulting in warping. Observing the beam-end it is clear that the section has not remained in its initial plane, the material movement along the beam can be seen clearly. At the support, the flanges cannot move and thus warping is prevented.

Due to the warping, stresses are created in the flanges as shown in Figure 2.12.

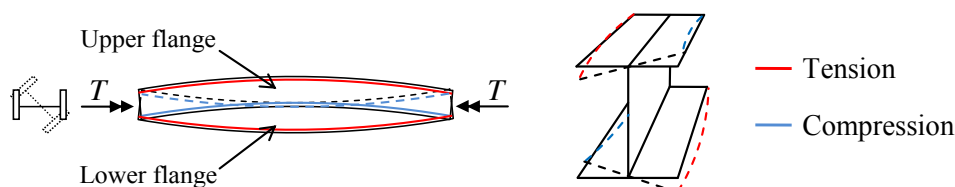


Figure 2.12 Tension and compression stresses are created along the flanges as a result of lateral bending. (Adapted from Höglund 2006, p. 29).

If one of the flanges is studied (see Figure 2.12), it can be observed that the deformation resembles the behaviour of a beam in bending. Hence, bending moments and shear forces will arise, contributing to the resisting moment.

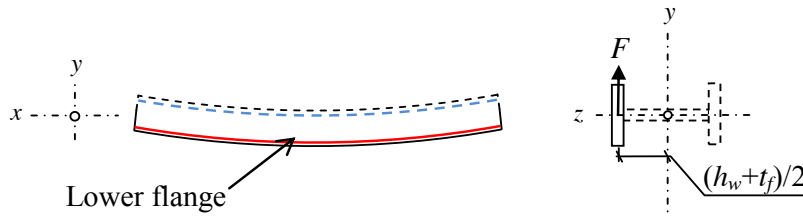


Figure 2.13 A shear force F is induced by lateral bending of the lower flange, contributing to the resisting moment of the section (Adapted from Höglund 2006, p. 29).

Sections resistance to warping is described by the warping constant, I_w . For a single-symmetric I-section, where the contribution from the web is neglected, the warping constant can be approximated as (Atsuta & Chen 2008, p. 84)

$$I_w = \frac{\alpha \cdot h_{f1}^3 \cdot t_{f1} \left(h_w + \frac{t_{f1}}{2} + \frac{t_{f2}}{2} \right)^2}{12} \quad (2.3)$$

Where

$$\alpha = \frac{1}{1 + \left(\frac{h_{f1}}{h_{f2}} \right)^3 \left(\frac{t_{f1}}{t_{f2}} \right)}$$

For a double-symmetric section, the expression for I_w is reduced to

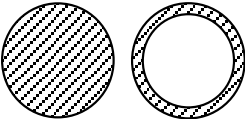
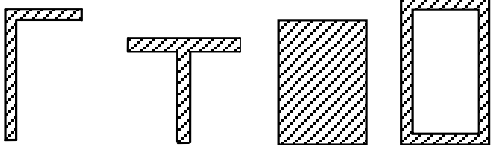
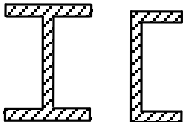
$$I_w = \frac{h_f^3 \cdot t_f (h_w + t_f)^2}{24} \quad (2.4)$$

$$I_w = \frac{I_{z, flanges} (h_w + t_f)^2}{4} \quad (2.5)$$

A derivation of the warping constant is shown in Appendix C.

According to Höglund (2006), it can be distinguished between three different section categories with regard to warping; *warping free sections* where no warping occurs, *semi warping free sections* where warping can be neglected in calculations, and *warping sections* where warping must be taken into account.

Table 2.2 Classification of section shapes with regard to warping sensitivity.

(1) Warping free sections	
(2) Semi warping free sections	
(3) Warping sections	

2.2 Classical theory of instability

In classical theory of instability, it is possible to distinguish between three different equilibrium states; *stable*, *indifferent* and *instable*. These states are often illustrated principally as a ball placed on different shaped surfaces (Höglund 2006, p. 2).

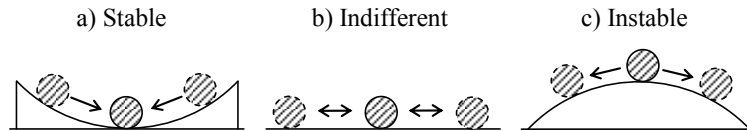


Figure 2.14 The states of equilibrium from the left; a) stable, b) indifferent c) instable (Höglund 2006, p. 3).

- a) A structural system is considered to be in stable equilibrium if it returns to its initial state of equilibrium after a small disturbance. This is a fundamental principle in the field of structural engineering, which if not satisfied would lead to collapse of the system.
- b) At an indifferent equilibrium, a disturbance will move the system. After the disturbance is removed, the system will stay in the displaced position.
- c) When a system in instable equilibrium is disturbed, forces will arise that move the system further and further away from the initial condition (Höglund 2006, pp. 2-3).

Consider an ideal column with no imperfections fixed at one end and free at the other. The column is subjected to a normal force, N , and an eventual lateral deflection is denoted δ , see Figure 2.15.



Figure 2.15 Ideal column without imperfections subjected to a normal force N .

The behaviour of such a system under an increasing normal force N can be described by small deformation theory or large deformation theory (Höglund 2006, p. 11).

In small deformation theory the column will be in stable equilibrium until N reaches a critical load, N_{cr} . At N_{cr} the system becomes instable and the column buckles. With this theory, it is not possible to determine the magnitude of the deflection (ibid.).

With large deformation theory it is possible to track the whole equilibrium path for the ideal elastic column. When N_{cr} is reached the column deflects rapidly, but the deformation will not be infinitely large. It can be shown that for every $N > N_{cr}$, there exists a deflected state of equilibrium as long as the material is elastic. The magnitude of the deflection after buckling is mostly of theoretical interest, since the member has failed from a structural point of view.

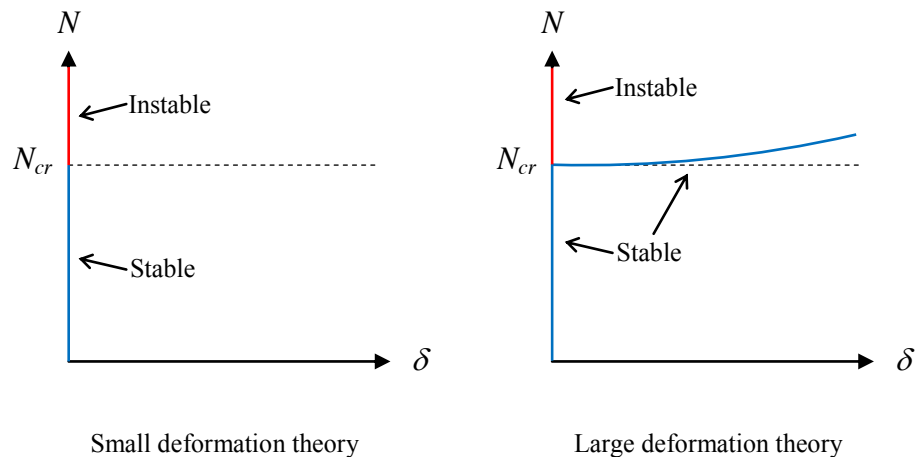


Figure 2.16 Equilibrium paths for a column under increasing normal force.

When considering structural systems it is usually not necessary to differ between indifferent and instable states of equilibrium. In the example above the system could be considered indifferent when N is exactly N_{cr} , since almost no disturbance is needed to bring the column to a deflected state.

2.2.1 Global buckling and buckling modes of loaded members

A member can fail in different types of buckling modes. These modes are defined by the type of loading and the deformation shape of the member. In a general case, a member can be subjected to several types of deformations simultaneously, e.g. bending, torsion, warping etc. The resisting forces in the member will be dependent on the stiffness coupled to the different deformations. Hence, the flexural, torsional and warping stiffness of a cross section are important when evaluating the resistance to buckling (Höglund 2006).

It can be distinguished between *flexural buckling* (1), *torsional buckling* (2) and *lateral torsional buckling* (3), see Table 2.3.

- (1) When a member in compression buckles in one plane only, it is called flexural buckling (Serna et al. 2005). The resisting sectional forces that arise in the member are directly dependent on the flexural stiffness EI (Höglund 2006, p. 12).

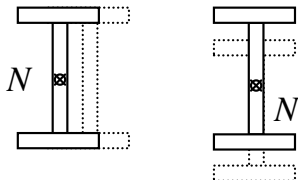
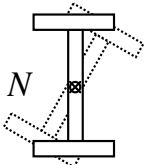
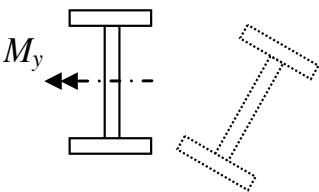
$$\begin{aligned} E &= \text{Young's modulus} \\ I &= \text{Second moment of inertia} \end{aligned}$$

- (2) When buckling due to compression only twists the member it is called torsional buckling. The sectional resistance is dependent on the torsional stiffness GI_t and the warping stiffness EI_w (Höglund 2006, p. 29).

G	=	Shear modulus
I_t	=	Saint-Venant's torsion constant
E	=	Young's modulus
I_w	=	Warping constant

- (3) When a member loaded in bending deflects laterally and twists at the same time, it is called lateral torsional buckling. The resistance to this buckling mode is governed by the flexural, torsional and warping stiffness (Serna et al. 2005). Lateral torsional buckling is explained in the next chapter.

Table 2.3 Deformations due to flexural, torsional and lateral torsional buckling (Höglund 2006, p. 37).

(1) Flexural buckling	
(2) Torsional buckling	
(3) Lateral torsional buckling	

2.3 Mechanisms behind lateral torsional buckling

Consider a beam in major axis bending subjected to increasing loading. If the beam is slender, it may buckle before the sectional capacity is reached. This kind of buckling involves both lateral deflection and twisting, and is called lateral torsional buckling. See Figure 2.17 (Serna et al. 2005).

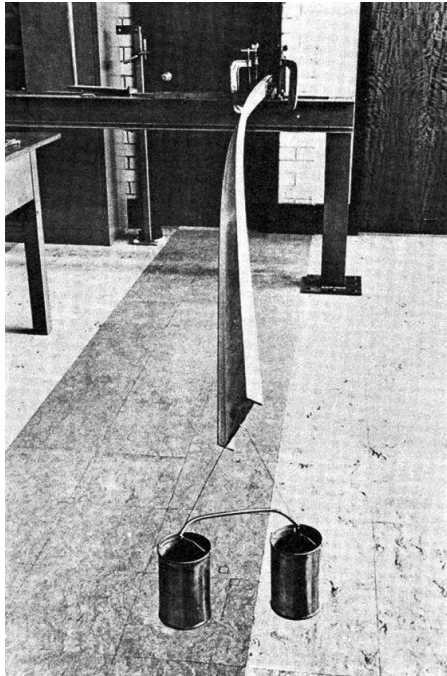


Figure 2.17 *Lateral torsional buckling of a cantilever beam (N.S Trahair cited in Atsuta & Chen 2008, p. 72)*



Figure 2.18 *Lateral torsional buckling of beam with fork supports subjected to a concentrated load - test set-up (Adapted from Camotim et al. 2011, p. 2058).*

Longer beams become instable at smaller loads compared to shorter beams. Also, if beams with the same length but different cross-sections are tested, beams with slender cross-sections buckle at smaller loads than beams with stubby sections. However, not only the length of the beam and the cross-section shape is of importance. Many other factors also affect beams sensitivity to lateral torsional buckling, see Table 2.4.

Table 2.4 Lateral torsional buckling is affected by material-, cross-section- and geometric properties, boundary conditions, and loading (Lopez et al. 2006).

Factors that affect lateral torsional buckling	
Material properties	Shear modulus (G) Youngs's modulus (E)
Cross-section properties	Torsion constant (I_t) Warping constant (I_w) Second moment of inertia about weak axis (I_z)
Geometric properties	Length of the beam (L)
Boundary conditions	Bending about major axis Bending about minor axis Warping
Load	Type of loading (distributed, concentrated etc.) Point of load application (top flange, in shear centre, bottom flange etc.)

By considering the factors in Table 2.4 and choosing a beam with the right properties, lateral torsional buckling can be avoided. The risk of lateral torsional buckling is high for beams with the below listed properties (Höglund 2006, p. 78)

- Low flexural stiffness about the weak axis (EI_z)
- Low torsional stiffness (GI_t)
- Low warping stiffness (EI_w)
- High point of load application
- Long unrestrained spans (L)

2.4 Measurements against lateral torsional buckling

To avoid lateral torsional buckling the affecting factors presented in Table 2.4 can be manipulated in different ways. Choosing a stable cross-section with high flexural stiffness about the weak axis is one method. If the geometric and material properties are already determined, a low point of load application or restraints can be used.

2.4.1 Influence of the cross-section

Lateral torsional buckling is only possible in major axis bending. If the flexural stiffness is high enough about the weak axis or if the stiffness is equal about both axes, lateral torsional buckling will not occur. Figure 2.19 show sections that are safe with regard to lateral torsional buckling (Höglund 2006, p. 54 & p. 78).

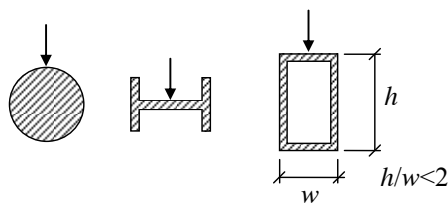


Figure 2.19 Sections with little or no risk of lateral torsional buckling (Höglund 2006, p. 54 & p. 78).

2.4.2 Influence of the point of load application

A low point of load application reduces the risk of lateral torsional buckling. Hence, a load placed on the bottom flange makes a beam considerably more stable than a load on the top flange. This is provided that the load does not contribute with any restraining effects (Höglund 2006, p. 54 & p. 78).

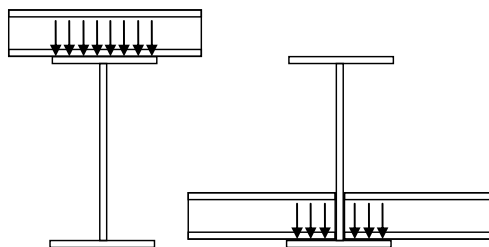


Figure 2.20 A beam loaded by a concentrated load from a secondary girder. If a low point of load application is used the load helps to stabilize the beam. A high point of load application contributes to twisting moments and makes the beam less stable.

When a beam deflects due to lateral torsional buckling, loads above the centre of twist will contribute with a twisting moment. Loads below the centre of twist counteract rotations of the sections and stabilizes the beam (Höglund 2006, p. 54).

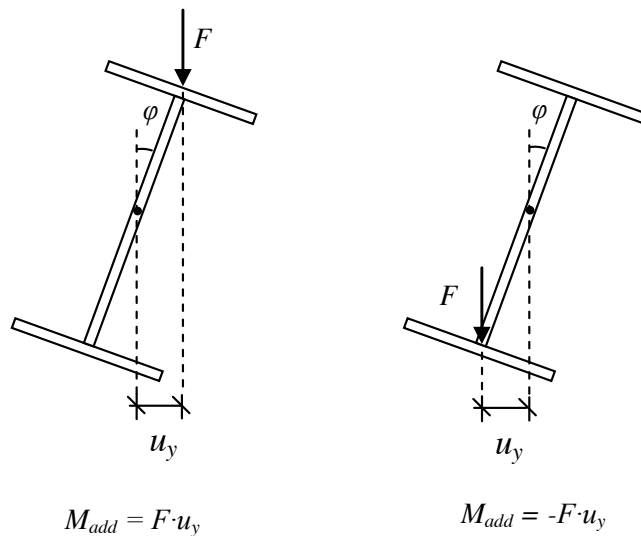


Figure 2.21 A load, F , acting above the centre of twist contributes to the rotation of the section with an additional moment. When placed under the centre of twist, the load stabilizes the section.

2.4.3 Influence of lateral restraints

If the flange in compression is restrained from lateral bending, lateral torsional buckling can be fully prevented. The spacing of the restraints must be small enough so that buckling cannot occur between them.

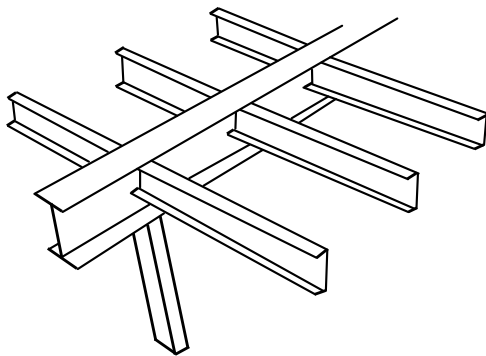


Figure 2.22 Provided that the top flange is in compression, the beam can be restrained from lateral torsional buckling by secondary girders.

2.4.3.1 Restrained flange in compression

As in Figure 2.22, restraints can often be provided from secondary members in a construction. If a simply supported beam is loaded directly by an evenly distributed load from a slab, the beam can be fully prevented from lateral torsional buckling provided that the slab is part of a stable system. The upper flange of the beam is in compression in the whole span, and restrained at all points. A twist of such a beam will be counteracted by the slab. See Figure 2.23 (Höglund 2006, p. 78).

Even if the slab is part of a stable system in the finished structure, other conditions may apply during the erection of the building. Hence, commonly the beam is attached to the slab by some kind of connection to assure that it is restrained also during assembly.

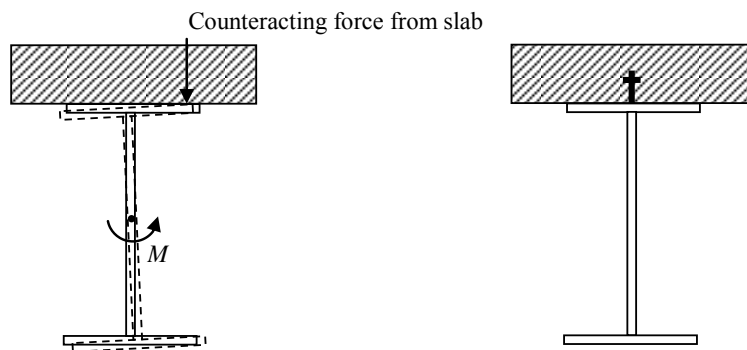


Figure 2.23 A beam subjected to a twisting moment is restrained on the compression flange by a floor slab. A counteracting moment is created from the reaction force from the slab, holding the beam in place (left). Often the beam is attached to the slab to make sure that system is stable (right).

2.4.3.2 Restrained flange in tension

If the beam instead is made continuous, the top flange will be in tension close to the mid-supports. Restraining the tension flange will also increase the stability of the beam, but in some cases this is not enough to prevent the compression flange from buckling. This type of buckling is called *distortional buckling* and can be prevented by restraining the compression flange, i.e. restraining the bottom-flange, close to the mid-supports (Höglund 2006, p. 78).

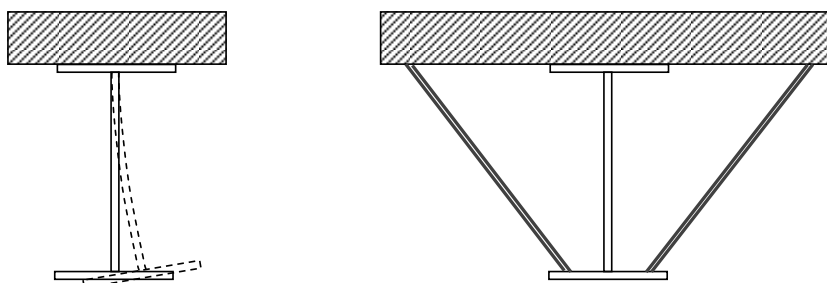


Figure 2.24 If a beam is restrained on the tension flange, the unrestrained compression flange may buckle laterally due to distortional buckling (to the left). This can be prevented by placing restraints onto the compression flange (to the right).

2.4.3.3 Unrestrained beams with slender webs and rigid flanges

Unrestrained beams sometimes buckle in a mix between lateral torsional buckling and distortional buckling. This buckling mode is possible for beams with slender flexible webs and rigid flanges, and is called *lateral distortional buckling*, see Figure 2.25 (Kurniawan & Mahendran 2011).

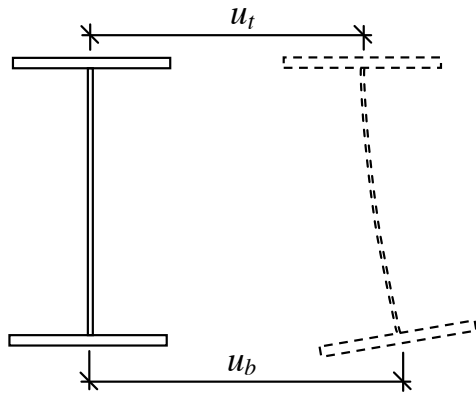
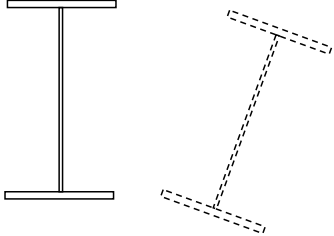
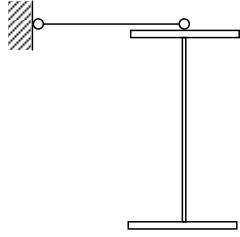
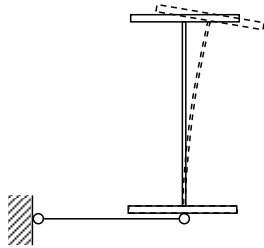
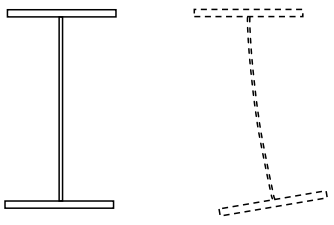


Figure 2.25 *Lateral distortional buckling is possible for beams with slender webs and rigid flanges.*

2.4.3.4 Buckling modes of restrained and unrestrained beams

Table 2.5 Buckling modes and corresponding restraints (Adapted from Höglund 2006, p. 78).

<p>No restraints</p> <p>- Free to buckle due to lateral torsional buckling</p>	
<p>Compression flange restrained</p> <p>- No lateral torsional buckling is possible</p>	
<p>Flange in tension restrained</p> <p>- Distortional buckling is possible</p>	
<p>No restraints</p> <p>- Lateral distortional buckling is possible for beams with slender flexible webs and rigid flanges</p>	

2.5 Behaviour of real beams

The theory of lateral torsional buckling is valid under ideal elastic conditions for beams with perfect geometry and no initial imperfections. In reality however, no beams are perfect why real beams will behave different than ideal ones, see Figure 2.26.

An ideal beam is laterally un-deformed until the load reaches the elastic critical moment. At this point an indifferent state of instability is reached and a large instantaneous deflection occurs laterally. Since the material is ideal elastic, infinitely large deformations can take place and a new state of equilibrium can be found in the deflected position. Each small further increase of the load will result in large additional deflection. See Figure 2.26 (Höglund 2006, p. 77).

A real beam has a decreased capacity compared to an ideal beam due to imperfections, residual stresses etc. When a load is applied to a real beam, a lateral imperfection already exists. This initial deformation increases when the load increases. Close to the critical load the deflection starts to increase more dramatically, but the theoretical value of M_{cr} is never reached. This failure is governed by plastic material response, non-linear geometry and by possible local buckling (ibid.)

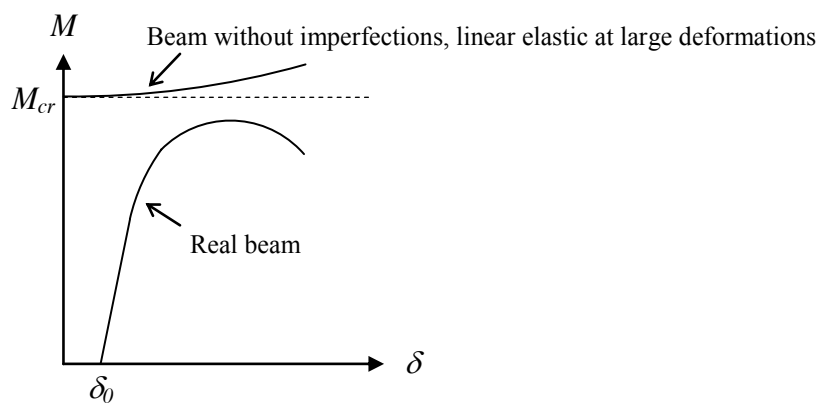


Figure 2.26 Increasing moment plotted against lateral deflection. An ideal beam shows no deflection until the elastic critical moment is reached, where a large instantaneous deflection occurs. A real beam has imperfections and residual stresses, and deflects as the load is increased. The failure of the real beam is governed by its imperfections and non-linear response (Adapted from Höglund 2006, p. 77).

2.5.1.1 Factors that decrease the capacity of real beams

- Non-linear material response, i.e. plastic material behaviour.
- Initial lateral imperfections; the beam is not perfectly straight.
- Residual stresses from manufacturing.
- Local buckling of beam sections in section class 4.
- Piercings, asymmetry and defects (Höglund 2006, p. 79).

These effects can be taken into account in design through design buckling curves, which simulate real beam behaviour, see chapter 3.1.

3 Design with regard to lateral torsional buckling

In *Eurocode 3* the general procedure when designing against buckling is to introduce a buckling factor, $\chi \leq 1$, that reduces the capacity of the member. In the case of lateral torsional buckling, this factor is denoted χ_{LT} and accounts for all the effects that decrease the capacity due to buckling. The moment capacity according to *Eurocode 3* can be written as

$$M_{b,Rd} = \chi_{LT} \frac{W_y f_y}{\gamma_{M1}} \quad (3.1)$$

Where	W_y	=	Bending resistance corresponding to the cross-section classification of the member
	f_y	=	Yield strength of the steel
	γ_{M1}	=	Partial safety factor

The buckling factor χ_{LT} is defined as

$$\chi_{LT} = \frac{1}{\Phi_{LT} + \sqrt{\Phi_{LT}^2 - \bar{\lambda}_{LT}^2}}, \quad \chi_{LT} \leq 1.0 \quad (3.2)$$

$$\Phi_{LT} = 0.5 \left(1 + \alpha_{LT} (\bar{\lambda}_{LT} - 0.2) + \bar{\lambda}_{LT}^2 \right) \quad (3.3)$$

Where	α_{LT}	=	Imperfection factor
-------	---------------	---	---------------------

From equation (3.2) and (3.3) it is clear that the buckling behaviour is strongly dependent on the slenderness parameter, $\bar{\lambda}_{LT}$.

$$\bar{\lambda}_{LT} = \sqrt{\frac{W_y \cdot f_y}{M_{cr}}} \quad (3.4)$$

M_{cr} in equation (3.4) is the elastic critical moment in classical buckling theory, i.e. the theoretical critical moment without regard to initial imperfections or residual stresses.

Eurocode 3 does not provide any information on how to determine M_{cr} , but simply states that it should be based on the gross cross-section, the loading conditions, the real moment distribution and the lateral restraints.

3.1 Buckling curves

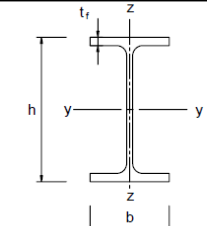
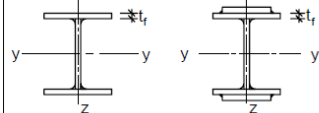

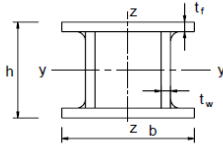
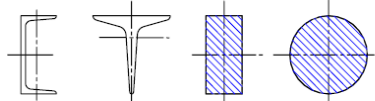
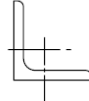
Even when considering theoretical beams without imperfections, buckling will occur before failure in bending if the member is slender. From the definition of the slenderness, it can be shown that this reduction in capacity corresponds to a theoretical buckling factor, $\chi_{LT} = 1/\bar{\lambda}_{LT}^2$. See equation below.

$$\bar{\lambda}_{LT} = \sqrt{\frac{W_y f_y}{M_{cr}}} \leftrightarrow \bar{\lambda}_{LT}^2 = \frac{W_y f_y}{M_{cr}} \leftrightarrow M_{cr} = \frac{1}{\bar{\lambda}_{LT}^2} W_y f_y \quad (3.5)$$

If the theoretical buckling factor $1/\bar{\lambda}_{LT}^2$ is plotted for different values of $\bar{\lambda}_{LT}$, the relationship between the slenderness and the buckling factor can be described with an *ideal buckling curve*. This curve corresponds to a perfect beam and is plotted as the dashed line in Figure 3.1.

In reality, imperfections and residual stresses decrease the moment capacity even more. *Eurocode 3* take these effects into account by using design buckling curves, determined from extensive testing. These curves correspond to different residual stresses and imperfections of the members (see Table 3.1 and Figure 3.1).

Table 3.1 Choice of buckling curves on the basis of cross-section layout, steel quality and manufacturing method (EN-1993-1-1:2005, table 6.2).

Cross section		Limits	Buckling about axis	Buckling curve	
				S 235 S 275 S 355 S 420	S 460
Rolled sections 	$h/b > 1.2$	$t_f \leq 40 \text{ mm}$	y-y z-z	a b	a ₀ a ₀
		$40 \text{ mm} < t_f \leq 100$	y-y z-z	b c	a a
	$h/b \leq 1.2$	$t_f \leq 100 \text{ mm}$	y-y z-z	b c	a a
		$t_f > 100 \text{ mm}$	y-y z-z	d d	c c
Welded I-sections 	$t_f \leq 40 \text{ mm}$		y-y z-z	b c	b c
	$t_f > 40 \text{ mm}$		y-y z-z	c d	c d
Hollow sections 	hot finished		any	a	a ₀
	cold formed		any	c	c
Welded box sections 	generally (except as below)		any	b	b
	thick welds: $a > 0.5t_f$ $b/t_f < 30$ $h/t_w < 30$		any	c	c
U-, T- and solid sections 			any	c	c
L-sections 			any	b	b

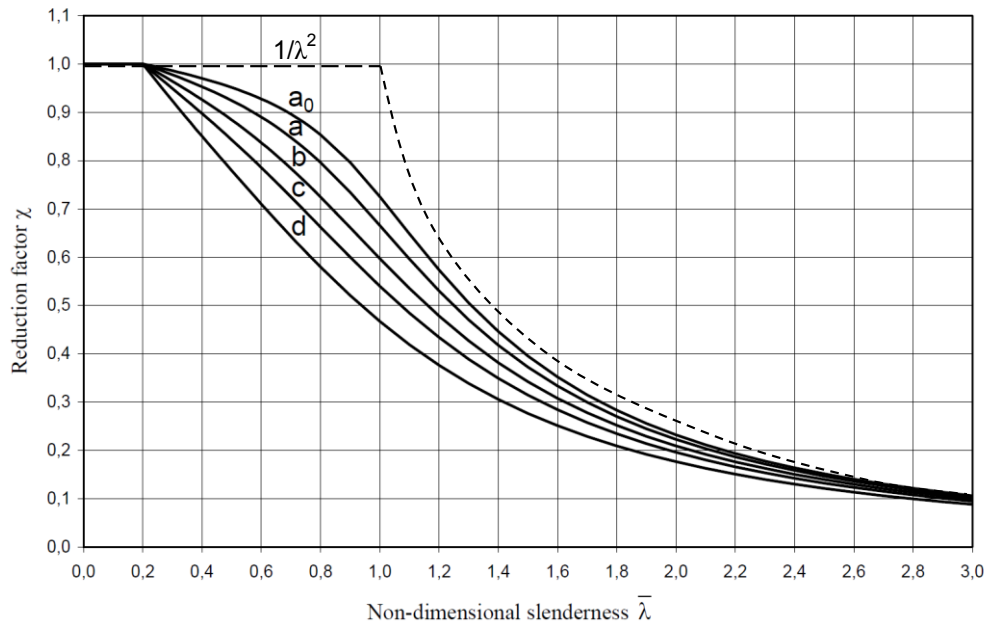


Figure 3.1 Buckling curves (adapted from EN-1993-1-1:2005, Figure 6.4).

If Figure 3.1 is studied, some general conclusions can be drawn about members' behaviour with regard to buckling. When the slenderness is low, most of the sectional capacity can be utilized, and the buckling factor is close to, or equal to 1.0. When the slenderness is high, the resistance approaches that of a perfect beam, and the influence of imperfections and residual stresses are small. At intermediate slenderness, the influence of initial imperfections and residual stresses are high and the design buckling factors are considerable lower than the ideal buckling factor.

3.2 Comment

The briefly presented procedures in this chapter are general. Also the buckling curves are general. In some situations, other methods and other buckling curves may be used instead. For details, see EN-1993-1-1:2005.

4 Analytical evaluation of M_{cr}

At the critical load, M_{cr} , the beam will change from a straight state of equilibrium to a deflected state of equilibrium. To determine the critical load analytically it is therefore necessary to investigate if such a change of equilibrium state is possible. This can be done in two ways, either by an *equilibrium study* of a small element of the deflected member, or by a study of the *potential energy of the system*. The potential of the system can be used because of the theorem that states that the potential will have a minimum at the equilibrium (Höglund 2006).

In complex situations, where several types of buckling are present (e.g. lateral torsional buckling), it is common to derive the theoretical critical load on the basis of energy methods.

4.1 Energy methods

M_{cr} can be derived for specific load cases, using the method of potential energy. This method is based on two important conditions (Höglund 2006, p. 33)

- (1) The total potential of a system has always a minimum at the state of equilibrium. Hence, a loaded beam will adjust itself to a deflected shape that corresponds to the lowest potential energy.
- (2) At the critical load, no energy is needed to deform a beam into a deflected state of equilibrium. Hence, the potential will not change.

If the straight state of equilibrium is considered as the zero-level, e.g. $H_{Straight} = 0$ the total potential in the deflected state must be equal to zero according to (2) and is denoted H .

It can also be concluded that the mechanical work done by the external loads during buckling is equal to the internal work done by the sectional forces, i.e. the work done by the external loads is stored as elastic energy in the structure. Hence, it is possible to divide the total potential H into two parts, *internal potential energy* which is equal to the work done by the sectional forces and *external potential energy* which is equal to the work done by the external loads.

Consequently, instability can only arise if the following two conditions are satisfied

$$(1) H = H_i + H_e = 0 \quad (4.1)$$

$$(2) H = H_i + H_e = \min \quad (4.2)$$

The elastic critical moment can be derived by solving these two equations with calculus of variations. Exact solutions can only be derived in simple cases. In complex cases, an approximate deflective shape is generally assumed that can be varied until the potential is sufficiently small (Höglund 2006, p. 38).

The drawback with this method is that the solution only is valid for the specific load case it was derived for. If the load is moved, or the boundary conditions are changed in any way, a new expression of M_{cr} must be derived. These derivations can bring

great difficulties in more complicated load cases, involving complex coupled differential equations (Höglund 2006, p. 58).

Clearly the method of potential energy is not practical to use in design. However, it has been used successfully multiple times, providing solutions for simple and common load cases presented in books such as (Lopez et al. 2006)

- *Theory of Elastic Stability* by Timoshenko S.P. and Gere J, 1961
- *Principles of Structural Stability* by Chajes A, 1974
- *Flexural-Torsional Buckling of Structures* by Trahair N.S, 1993

4.2 The 3-factor formula

In practical design M_{cr} can be estimated by task-specific software or from hand calculations. Early *ENV*-editions of *Eurocode 3* included an expression of M_{cr} . However, it was later removed without replacement. This expression is known as the *3-factor formula* and is one of the most used analytic formulas to estimate the elastic critical moment (Andrade et al. 2006). Today it can be found in *NCCI*-guides by Access Steel (2005) and in other handbooks.

The *3-factor formula* is based on a reference load case, to which correction factors are added in order to make the equation fit other cases. The reference case comprises a *beam on two fork supports with double-symmetric cross-section with constant moment distribution*. The critical moment related to this reference case is denoted $M_{cr,0}$ and is derived in Appendix C. See equation (4.3) below.

$$M_{cr,0} = \frac{\pi^2 \cdot EI_z}{L^2} \sqrt{\frac{I_w}{I_z} + \frac{L^2 \cdot GI_t}{\pi^2 \cdot EI_z}} \quad (4.3)$$

The *3-factor formula* expands the expression of $M_{cr,0}$ to be valid for single-symmetric cross sections with arbitrary moment distributions. This is done by introducing three correction factors, C_1 , C_2 and C_3 that account for these conditions. The factors can either be found in tables and figures, or estimated from approximate closed-form expressions. To account for warping degrees of freedom and lateral rotation at the supports, the expression is also expanded with the factors, k_z and k_w . The *3-factor formula* is presented below in equation (4.4).

$$M_{cr} = C_1 \frac{\pi^2 \cdot EI_z}{(k_z \cdot L)^2} \left(\sqrt{\left(\frac{k_z}{k_w} \right) \frac{I_w}{I_z} + \frac{(k_z \cdot L)^2 GI_t}{\pi^2 \cdot EI_z} + (C_2 \cdot z_g)^2} - (C_2 \cdot z_g - C_3 \cdot z_j) \right) \quad (4.4)$$

Where	E	=	Young's modulus
	G	=	Shear modulus
	I_z	=	Second moment of inertia about weak axis
	I_t	=	Torsion constant
	I_w	=	Warping constant
	L	=	Length between lateral restraints

k_z	=	Effective length factor which is related to the restrain against lateral bending at the boundaries
k_w	=	Effective length factor which is related to the restrain against warping at the boundaries
z_g	=	Distance between the point of load application and the shear centre
z_j	=	Distance related to the effects of asymmetry about y-axis
C_1	=	Factor that account for the shape of the moment diagram
C_2	=	Factor that account for the point of load application in relation to the shear centre
C_3	=	Factor that account for asymmetry about y-axis

4.2.1 Comment

The *3-factor formula* is only valid under the following conditions.

- Uniform cross-section with symmetry about weak axis
- Bending about major axis

4.2.2 The equivalent uniform moment factor, C_1

In literature, the C_1 -factor is referred to as the *equivalent uniform moment factor* or the *moment gradient factor*.

As explained in chapter 4.1, the critical buckling load can be derived for different load cases through methods of potential energy. Examples are given below for a double-symmetric beam on fork supports, subjected to a concentrated load (1) and a uniformly distributed load (2) (Yoo & Lee 2011).

- (1) Critical load for a concentrated load in mid-span, fork supports

$$P_{cr} = \frac{4 \cdot \pi^3}{L^3} \sqrt{\frac{3}{\pi^2 + 6} EI_z \left(GI_t + \frac{EI_w \cdot \pi^2}{L^2} \right)} \quad [N] \quad (4.5)$$

- (2) Critical load for a uniformly distributed load, fork supports

$$q_{cr} = \frac{2 \cdot \pi^3}{L^3} \sqrt{\frac{30}{\pi^4 + 45} EI_z \left(GI_t + \frac{EI_w \pi^2}{L^2} \right)} \quad \left[\frac{N}{m} \right] \quad (4.6)$$

When equation (4.5) and (4.6) are rewritten as expressions of the elastic critical moment, a comparison can be made with $M_{cr,0}$ as reference. The influence of the different loading conditions can now be studied.

- (1) Critical load for a concentrated load in mid-span, fork supports

$$M_{cr} = \frac{P_{cr} \cdot L}{4} = 1.36 \frac{\pi^2 \cdot EI_z}{L^2} \sqrt{\frac{I_w}{I_z} + \frac{L^2 \cdot GI_t}{\pi^2 \cdot EI_z}} \quad [Nm] \quad (4.7)$$

- (2) Critical load for a uniformly distributed load, fork supports

$$M_{cr} = \frac{q_{cr} \cdot L^2}{8} = 1.13 \frac{\pi^2 \cdot EI_z}{L^2} \sqrt{\frac{I_w}{I_z} + \frac{L^2 \cdot GI_t}{\pi^2 \cdot EI_z}} \quad [Nm] \quad (4.8)$$

If equation (4.7) and (4.8) are compared to the reference equation (4.3), the only difference is a factor 1.36 and 1.13 respectively. Hence, it is expected that the elastic critical moment for a general load case can be written as

$$M_{cr} = C_1 \frac{\pi^2 \cdot EI_z}{L^2} \sqrt{\frac{I_w}{I_z} + \frac{L^2 \cdot GI_t}{\pi^2 \cdot EI_z}} \quad (4.9)$$

Where C_1 take the following values

- A concentrated load in mid-span, fork supports, $C_1 = 1.36$
- A uniformly distributed load, fork supports, $C_1 = 1.13$
- Reference load case, $M_{cr,0}$, $C_1 = 1.0$

The moment diagrams in the three different load cases above take the shapes of a rectangle, a parabola and a triangle respectively. Thus, the factor C_1 seems to be related to the shape of the moment diagram, where big areas under the curve yield small values of C_1 (Yoo & Lee 2011). Since the boundary conditions affect the moment diagram, it is expected that they also will influence the values of C_1 and M_{cr} .

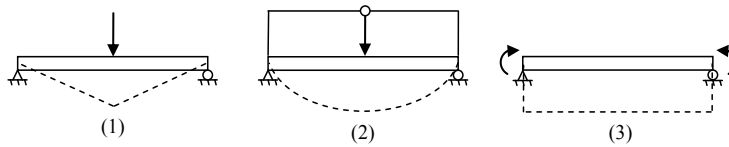


Figure 4.1 The moment diagrams in the different load cases.

4.2.2.1 Values from tables and figures

Values of C_1 for standard load cases can be found in tables and figures given in handbooks. Two examples are given below.

- “NCCI: Elastic critical moment for lateral torsional buckling” by Access Steel (2005) provides information on how to treat instability of steel members and gives tabled values of the C -factors in the 3-factor formula.
Access Steel is a project with the purpose to provide guidance and “thorough understanding of how the Eurocodes should be used” (Access Steel 2013). Contributors to the project are some of the leading research institutions in Europe (e.g. CTICM, SBI, SCI) and some of the largest steel producers (e.g. ArcelorMittal, Ruukki, SSAB) (Access Steel 2013).
NCCI stands for Non-Contradictory, Complementary Information, and refers to guides who give useful information that is not stated in the Eurocodes themselves.
- “Rules for Member Stability in EN 1993-1-1” by ECCS (2006) presents solutions to M_{cr} in some common cases. ECCS (European Convention for Constructional Steelwork) is an “organisation which brings together the Steel Industry, the Fabrication and Contracting specialists, and the Academic world through an international network of representatives, steel producers, and technical centres” (ECCS 2013).

In Appendix B, the table values of ECCS (2006) and Access Steel (2005) are compared to reference values from Serna et al. (2005).

4.2.2.2 Closed-form expressions

In cases where table values are not available, C_1 can be calculated with closed-form expressions. By using curve fitting-techniques, several researchers have presented approximate expressions of C_1 , generally constructed to give lower-bound solutions. Exact expressions are difficult to construct since C_1 is dependent on more factors than the shape of the moment diagram. See further discussion in chapter 4.2.2.3.

4.2.2.2.1 Closed-form expression by M.G. Salvadori

One of the first closed-form expressions for estimating C_1 was presented by M.G. Salvadori in 1955 (Serna et al. 2005). The expression gives reasonable results when considering linear moment distributions.

$$C_1 = 1.75 - 1.05\Psi + 0.3\Psi^2 \leq 2.3 \quad (4.10)$$

Where Ψ = Ratio of end-moments, M_1/M_2

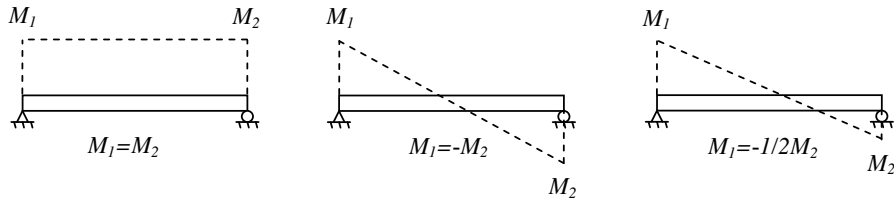


Figure 4.2 Linear moment distributions.

4.2.2.2.2 Closed-form expression by P.A. Kirby and D.A. Nethercot

Kirby & Nethercot (1979) formulated an expression of C_l that applies to both linear and non-linear moment diagrams. See equation (4.11).

$$C_l = \frac{12M_{\max}}{3M_A + 4M_B + 3M_C + 2M_{\max}} \quad (4.11)$$

Where M_{\max} = Maximum moment
 M_A, M_B, M_C = Absolute values of the moments at $L/4$, $L/2$ and $3L/4$ respectively, see Figure 4.3

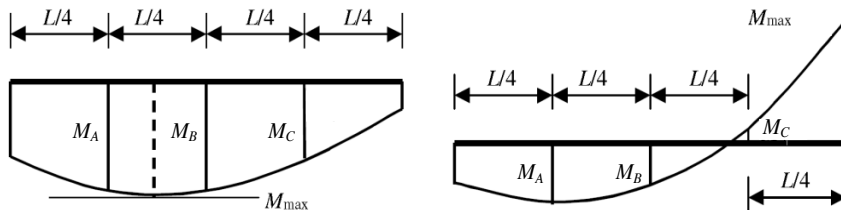


Figure 4.3 The moments M_A, M_B, M_C in equation (4.11) are the absolute values of the bending moment along the length of the beam, L , at the positions $L/4$, $L/2$ and $3L/4$ respectively. M_{\max} is the absolute value of the maximum moment (Adapted from Serna et al. 2005).

With a slight modification this expression is used in the design code of the *American Institute of Steel Construction, AISC LRFD* (Serna et al. 2005). Compare with equation (4.23).

According to Serna et al. (2005) and Lopez et al. (2006), equation (4.23) from *AISC LRFD* provides good approximations for most of the common load cases. Nonetheless, their studies show that C_l is not purely dependent on the moment distribution, as was assumed by Kirby & Nethercot (1979), but also coupled to the lateral boundary conditions of warping and lateral bending. Serna et al. (2005) points out that for some moment distributions equation (4.11) gives highly conservative results. In the cases of beams prevented from lateral bending and warping, the results are sometimes non-conservative (Serna et al. 2005).

4.2.2.2.3 Closed form expression by Serna et al. (2005) and Lopez et al. (2006)

As mentioned above Serna et al. (2005) showed that C_I is coupled to the warping and lateral bending conditions at the supports. This means that it is not possible to derive an exact closed-form expression for C_I that does not contain a factor related to these boundary conditions. A new proposition of a closed-form expression of C_I was presented in their report where two factors, k_z and k_w , were added to account for lateral bending and warping at the boundaries. In 2006 the expression was improved by Lopez et al. (2006) and is presented below in equations (4.12)-(4.15).

$$C_I = \frac{\sqrt{\sqrt{k} \cdot A_1 + \left(\frac{1-\sqrt{k}}{2} A_2\right)^2} + \left(\frac{1-\sqrt{k}}{2}\right) A_2}{A_1} \quad (4.12)$$

$$k = \sqrt{k_z \cdot k_w} \quad (4.13)$$

$$A_1 = \frac{M_{\max}^2 + \alpha_1 \cdot k \cdot M_1^2 + \alpha_2 \cdot k \cdot M_2^2 + \alpha_3 \cdot k \cdot M_3^2 + \alpha_4 \cdot k \cdot M_4^2 + \alpha_5 \cdot k \cdot M_5^2}{(1 + \alpha_1 + \alpha_2 + \alpha_3 + \alpha_4 + \alpha_5) M_{\max}^2} \quad (4.14)$$

$$A_2 = \left| \frac{M_1 + 2M_2 + 3M_3 + 2M_4 + M_5}{9M_{\max}} \right| \quad (4.15)$$

Where $\alpha_1 = (1 - k_w)$

$$\alpha_2 = 5 \frac{k_z^3}{k_w^2}$$

$$\alpha_3 = 5 \left(\frac{1}{k_z} + \frac{1}{k_w} \right)$$

$$\alpha_4 = 5 \frac{k_w^3}{k_z^2}$$

$$\alpha_5 = (1 - k_z)$$

k_z = Effective length factor related to lateral bending at the boundaries

k_w = Effective length factor related to warping at the boundaries

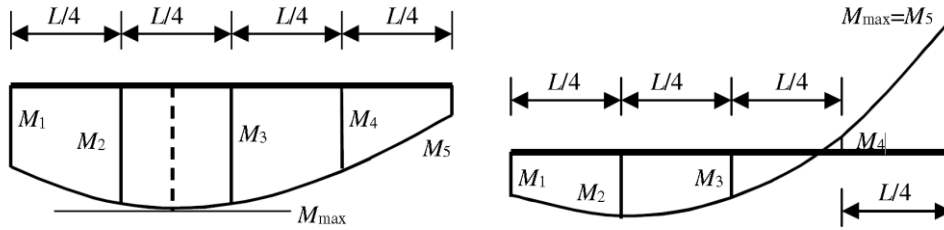


Figure 4.4 The moments M_1, M_2, M_3, M_4 and M_5 are the absolute values of the bending moment along the length of the beam, L , at the positions $0, L/4, L/2, 3L/4$ and L respectively. M_{max} is the absolute value of the maximum moment (Serna et al. 2005).

4.2.2.3 The μ -ratio and its effect on C_I

As seen in chapter 0, Serna et al. (2005) and Lopez et al. (2006) showed that the C_I -factor is not only dependent on the moment diagram but also coupled to the effective length factors k_z and k_w . According to Fruchtengarten (2006), Access Steel (2005), and ECCS (2006) C_I is also dependent on the ratio

$$\mu = \frac{GI_t \cdot L^2}{EI_w} \quad (4.16)$$

This means that in addition to moment distribution and lateral boundary conditions, also section parameters, material parameters and beam-length affect the C_I -factor. An interesting consequence is that it is not possible to give an exact value of C_I without knowing the length of the beam.

In Figure 4.5 C_I -values for two different lateral support conditions are plotted against the ratio μ . The results are valid for beams simply supported about major axis, subjected to concentrated loads in the mid-span. In the plot, $k = 1.0$ implies that both k_z and k_w are equal to 1.0.

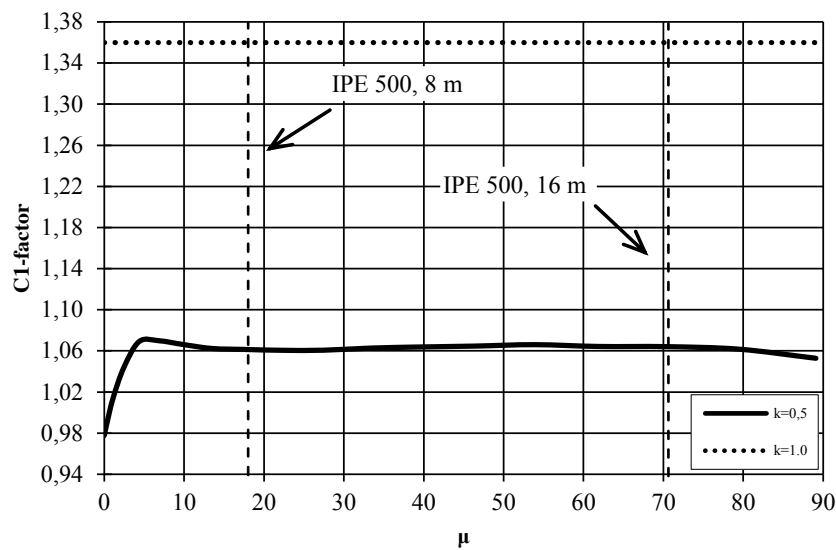


Figure 4.5 C_1 -values for a beam subjected to a concentrated load in the mid-span (Fruchtengarten 2006).

It can be concluded from the figure, that smaller values of μ yield lower values of C_1 for $k = 0.5$. According to Fruchtengarten (2006) this is mainly due to the influence of shear effects. In situations where $k = 1.0$, the influence of μ is very small. Graphs for distributed loads and end-moments show the same characteristics as Figure 4.5.

Assuming $\mu = \infty$ is generally a conservative assumption and the values of C_1 given in Access Steel (2005) and ECCS (2006) are based on this assumption.

In chapter 7, IPE500-beams with lengths 8 and 16 meters are studied. The lengths correspond to μ -values of 17.6 and 70.4 respectively. As seen in Figure 4.5, small deviations in C_1 between these two beams are expected.

4.2.3 Correction factor for the point of load application, C_2

Equation (4.9), with the C_1 -factor added, is only valid when the load acts in the shear centre. In reality, beams are often loaded on the top or bottom flange, and not in the shear centre. Thus a second correction factor, C_2 , has been added to account for the effects of the point of load application, PLA .

When PLA is separated from SC , the load contributes with an additional twisting moment that is added to the potential energy of the system. Therefore, a load applied under SC helps to stabilize the beam and a load above SC destabilize the beam (See Figure 4.6).

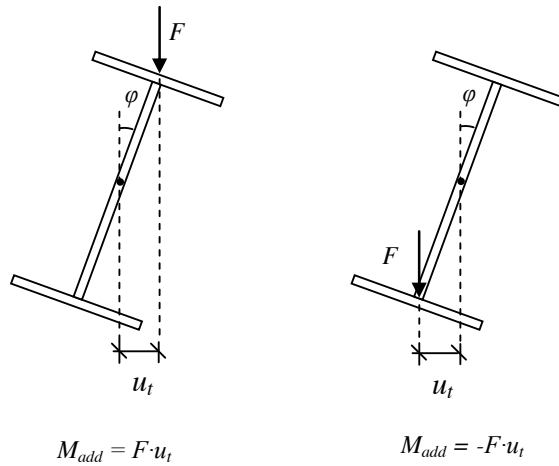


Figure 4.6 The additional moment due to the point of load application contributes to the potential energy of the system.

With the C_2 -factor added to the formula, equation (4.17) below is obtained.

$$M_{cr} = C_1 \frac{\pi^2 \cdot EI_z}{L^2} \left(\left(\sqrt{\frac{I_w}{I_z} + \frac{L^2 \cdot GI_t}{\pi^2 \cdot EI_z} + (C_2 \cdot z_g)^2} \right) - (C_2 \cdot z_g) \right) \quad (4.17)$$

Where C_2 = Correction factor for the point of load application
 z_g = Distance between the point of load application and the shear centre, measured positive above SC . See Figure 4.7

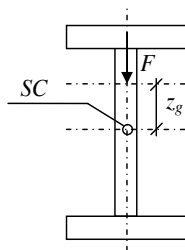


Figure 4.7 The distance z_g is the distance between the point of load application and the shear centre measured positive above SC .

4.2.3.1 Values from tables and figures

As for C_1 , values of the C_2 -factor for standard load cases can be found in tables and figures given in handbooks such as Access Steel (2005) and ECCS (2006). See chapter 4.2.2.1.

4.2.4 Correction factor for cross-section asymmetry, C_3

With the C_1 - and C_2 -factors, the *3-factor formula* can be used for calculation of M_{cr} for double-symmetric beams with various loads and points of load application. Still, the equation is only valid for double-symmetric sections, i.e. sections where both the major and minor axis are symmetry lines of the section. In order to analytically estimate M_{cr} for sections with symmetry only about the minor axis, a third correction factor C_3 must be introduced.

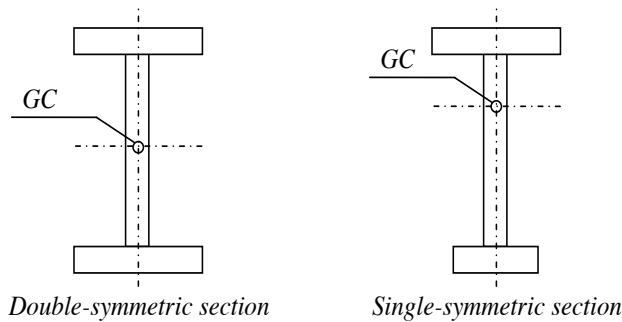


Figure 4.8 Examples of a double- and a single-symmetric cross-section.

With C_3 added, the expression takes the following form.

$$M_{cr} = C_1 \frac{\pi^2 \cdot EI_z}{L^2} \left(\left(\sqrt{\frac{I_w}{I_z} + \frac{L^2 \cdot GI_t}{\pi^2 \cdot EI_z} + (C_2 \cdot z_g)^2} \right) - (C_2 \cdot z_g - C_3 \cdot z_j) \right) \quad (4.18)$$

Where C_3 = Correction factor for asymmetry about y-axis
 z_j = Distance related to the effects of asymmetry about y-axis. See equation (4.19) below

$$z_j = z_s - \frac{0.5 \int (y^2 + z^2) z \, dA}{I_y} \quad (4.19)$$

Where z_s = Distance between the shear centre and the centre of gravity. For a more detailed definition, see ECCS (2006)

4.2.4.1 Comment

The C_3 -factor is not studied further since the thesis is limited to double-symmetric sections.

4.2.5 Effective length factors k_z and k_w

With the three C -factors implemented, M_{cr} can be evaluated for different load cases, sections and points of load application. However, different boundary conditions cannot be considered without some further expansion of the expression. Research by Salvadori, Lee and Vlasov in the 1950s and 60s showed that such an expansion can be done by introducing effective length-factors analogues with those of column-buckling (Yoo & Lee 2011, p. 364).

The effective length-factors relate the length between lateral restraints, L , to the buckling length corresponding to the boundary conditions, L_b .

$$L_b = kL \quad (4.20)$$

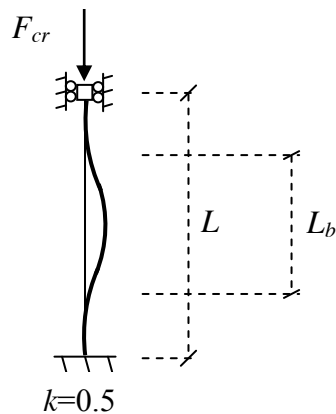


Figure 4.9 The effective length factor, k , relates the length of the member, L , to the buckling length corresponding to the boundary conditions, L_b .

Since both the warping and the lateral bending resistance of the boundary are of interest, two effective length factors can be defined; k_z (lateral bending) and k_w (warping).

$$M_{cr} = C_1 \frac{\pi^2 \cdot EI_z}{(k_z \cdot L)^2} \left(\sqrt{\left(\frac{k_z}{k_w} \right) \frac{I_w}{I_z} + \frac{(k_z \cdot L)^2 GI_t}{\pi^2 \cdot EI_z}} + (C_2 \cdot z_g)^2 \right) - (C_2 \cdot z_g - C_3 \cdot z_j) \quad (4.21)$$

Where k_z = Effective length factor which is related to the restraint against lateral bending at the boundaries
 k_w = Effective length factor which is related to the restraint against warping at the boundaries

The effective length factors are equal to 1.0 if the boundaries are free, 0.5 if the boundaries are fixed and 0.7 if the boundaries are free at one side and fixed at the other. See Table 4.1 below.

Table 4.1 Effective length factors for lateral torsional buckling

Boundary conditions	k_z and k_w
Free at both sides	1.0
One end fixed, one end free	0.7
Fixed at both sides	0.5

In situations where $k_z = k_w$, the effective length factors are often just denoted k . The values of k_z and k_w are analogues to case 2, 3 and 4 of classical Euler buckling. See Figure 4.10.

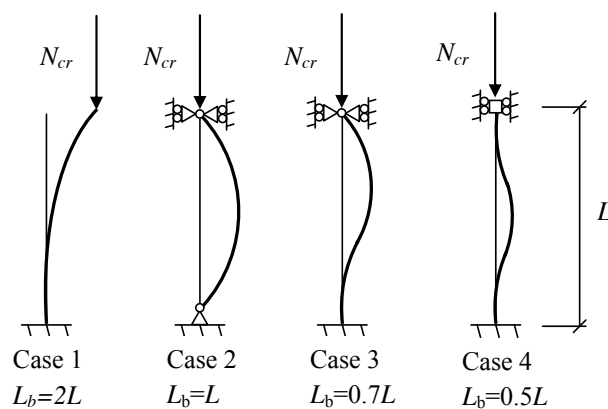


Figure 4.10 Euler buckling cases showing the effective buckling length, L_b , for axially loaded columns with different boundary conditions.

In Appendix A, choices of boundary conditions (k_z and k_w) are discussed for common beam connections.

4.3 American Institute of Steel Construction, *AISC LRFD*

In papers on lateral torsional buckling and the elastic critical moment, many references are given to the design code of the *American Institute of Steel Construction, AISC LRFD*. This chapter gives a short presentation on how this code treats calculations of the elastic critical moment.

4.3.1 Evaluation of M_{cr}

The formula for elastic critical moment presented in *AISC LRFD* is a variation of the *3-factor formula*. For double-symmetric sections with the point of load application in the shear centre, M_{cr} can be calculated with the expression below (AISC LRFD 1999, p. 34).

$$M_{cr} = C_b \frac{\pi}{L_b} \sqrt{EI_y \cdot GJ + \left(\frac{\pi \cdot E}{L_b} \right)^2 I_y \cdot C_w} \quad (4.22)$$

$$\text{Where} \quad L_b = k \cdot L$$

Equation (4.22) is analogous with the *3-factor formula* (4.4) if the following assumptions and changes in notations are made.

$$\begin{aligned} C_b &= C_1 \\ C_w &= I_w \\ J &= I_t \\ I_y &= I_z \\ k &= k_z = k_w \\ C_2 &= C_3 = 0 \end{aligned}$$

No distinction is made between lateral bending and warping in AISC (2005), i.e. k_z and k_w must take the same value. Also, it is not possible to use equation (4.22) for other than double-symmetric sections with the load applied in the shear centre.

4.3.2 Equivalent Uniform Moment Factor, C_b

Between 1961 and 1993 equation (4.10) by Salvadori was used in *AISC LRFD* to calculate C_b . In 1993 it was replaced by equation (4.23) below (Yoo & Lee 2011).

$$C_b = \frac{12.5M_{\max}}{3M_A + 4M_B + 3M_C + 2.5M_{\max}} \quad (4.23)$$

$$\begin{aligned} \text{Where} \quad M_{\max} &= \text{Maximum moment} \\ M_A, M_B, M_C &= \text{Absolute values of the moments at } L/4, \\ &\quad L/2 \text{ and } 3L/4 \text{ respectively (Figure 4.11)} \end{aligned}$$

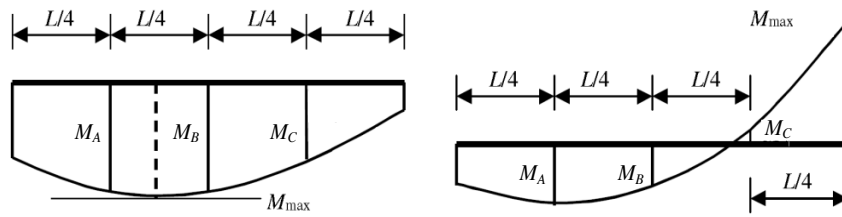


Figure 4.11 The moments M_A , M_B , M_C in equation (4.23) are the absolute values of the bending moment along the length of the beam, L , at the positions $L/4$, $L/2$ and $3L/4$ respectively. M_{\max} is the absolute value of the maximum moment (Adapted from Serna et al. 2005).

Equation (4.23) is very similar to Kirby's and Nethercot's expression (4.11). The only difference is the weighting of the moments along the beam. Compared to the previously used equation by Salvadori, it provides similar results for linear moment distributions between bracings, but better solutions for beams with fixed ends (AISC 2005).

5 Evaluation of M_{cr} with finite element methods

With computer-based techniques such as finite element and finite difference methods, it is possible to determine M_{cr} in complex situations. In this chapter, two techniques of determining M_{cr} in finite element software are presented briefly; *linearized buckling analysis* and buckling analysis by *load-displacement control*, *LDC*.

5.1 Linearized buckling analysis

Finite element software often provide the possibility of stability analysis by the implementation of an eigenvalue-problem to the global stiffness matrix of the system. Such analyses can be referred to as *eigenvalue buckling*, *linearized buckling* or just *buckling analysis* (Earls 2006).

Linearized buckling analysis is a powerful tool for determining approximate critical loads since it is relatively fast. The solution corresponds to the theoretical critical load of an ideal-elastic structure without imperfections. If a structure's pre- or post-buckling behaviour is of interest, more detailed incremental analyses are often necessary, see chapter 5.2 (Earls 2006).

5.1.1 Eigenvectors and eigenvalues

An eigenvector of a matrix is a nonzero vector that only undergoes a scalar transformation when multiplied with the matrix. The corresponding scalar to the eigenvector is called an eigenvalue, if a nontrivial solution exists.

$$\underline{A}\underline{x} = \lambda\underline{x} \quad (5.1)$$

$$(\underline{A} - \lambda\underline{I})\underline{x} = \underline{0} \quad (5.2)$$

Where \underline{x} = Eigenvector
 λ = Eigenvalue

According to the *Invertible Matrix Theorem* solving λ in equation (5.2) is equivalent of finding λ such that the matrix $(\underline{A} - \lambda\underline{I})$ is singular (not invertible). When a matrix is singular, its determinant is equal to zero. Hence, the eigenvalues of a matrix A can be solved from the following equation.

$$\det(\underline{A} - \lambda\underline{I}) = 0 \quad (5.3)$$

5.1.2 Eigenvalue problems applied on structural stability

The stiffness matrix of a beam relates the applied load to the resulting deformation, and can be divided into an elastic part and a load-dependent geometric part. In a situation where the stiffness matrix, $\underline{\underline{K}}$, is singular, no load is needed to move the structure into a displaced configuration, i.e. buckling occurs.

$$\underline{\underline{K}}\underline{p} = \underline{P} \quad (5.4)$$

$$\underline{\underline{K}} = \underline{\underline{K}}_E + \underline{\underline{K}}_G \quad (5.5)$$

Where	$\underline{\underline{K}}$	=	Stiffness matrix
	\underline{p}	=	Displacement vector
	\underline{P}	=	Load vector
	$\underline{\underline{K}}_E$	=	Elastic, linear part of the stiffness matrix
	$\underline{\underline{K}}_G$	=	Geometric, nonlinear, load-dependent part of the stiffness matrix

Since the geometric part of the stiffness matrix, $\underline{\underline{K}}_G$, is nonlinear dependent on the applied load, it is necessary to linearize the problem. This is done differently depending on how the stability problem is implemented in the finite element software. Commonly, the classical and the secant formulation can be chosen.

5.1.2.1 The classical formulation

In the classical formulation, the load dependent part of the stiffness matrix, $\underline{\underline{K}}_G$, is assumed to be linearly dependent on the load factor, λ .

$$\underline{\underline{K}} = \underline{\underline{K}}_E + \lambda \underline{\underline{K}}_G \quad (5.6)$$

Now critical load factors are sought, so that $\underline{\underline{K}}$ becomes singular. As mentioned in chapter 5.1.1, a matrix is singular when its determinant is zero. Thus, the load factors, λ_{cr} , can be found by solving

$$\det(\underline{\underline{K}}_E + \lambda_{cr} \underline{\underline{K}}_G) = 0 \quad (5.7)$$

Where λ_{cr} = Critical load factor (eigenvalue)

5.1.2.2 The secant formulation

In the secant formulation the stiffness matrix is formulated according to equation (5.8). Here, t_0 represents the “time” before the start of the current analysis, and t_1 represents the “time” of the first load step.

$$\underline{\underline{K}} = \underline{\underline{K}}^{t_0} + \lambda(\underline{\underline{K}}^{t_1} - \underline{\underline{K}}^{t_0}) \quad (5.8)$$

By solving the determinant of the stiffness matrix, $\underline{\underline{K}}^t$, the critical load factors, λ_{cr} , can be found.

$$\det(\underline{\underline{K}}^{t_0} + \lambda_{cr}(\underline{\underline{K}}^{t_1} - \underline{\underline{K}}^{t_0})) = 0 \quad (5.9)$$

Where λ_{cr} = Critical load factor (eigenvalue)

5.1.3 The influence of the base load

The base load is the load that is applied to the structure before running the linearized buckling analysis. In the finite element program ABAQUS the base load do not influence the buckling load, while in ADINA it can have a significant impact. The reason is how the classical and the secant formulation are implemented in the software, or in other words how the geometric stiffness matrix is approximated. In ADINA, the stiffness matrix is an approximate tangent matrix with an accuracy influenced by the load level (Earls 2006).

Figure 5.1 shows an eigenvalue plot of how the base load affects the buckling load for a given load case. The load calculated in LTBeam is used as reference, and both axes are normalized against it.

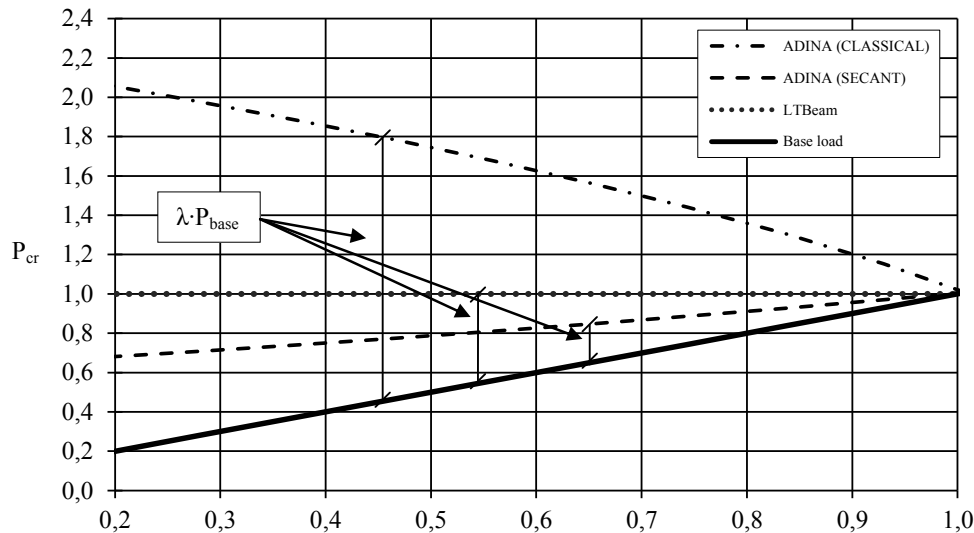


Figure 5.1 Eigenvalue plot of how the base load influences P_{cr} for a fixed 8 meter IPE500 beam. The lateral boundary condition is $k=1.0$ and the beam is subjected to a concentrated load in the mid-span on the top-flange.

It can be seen that the base load has a big impact on the solution and that the accuracy improve when the base load is increased, independent on which formulation that is used. The reason for this can be seen in the problem implementation. The eigenvalue problem solved by ADINA using the classical formulation is

$$\underline{\underline{K}}\phi_i = \gamma_i(\underline{\underline{K}} - \underline{\underline{K}}_G)\phi_i \quad (5.10)$$

Where $\gamma_i = \frac{\lambda_{cr} - 1}{\lambda_{cr}}$

$$\phi_i = \text{Buckling mode}$$

This means that if the base-load is chosen so that the critical load factor, $\lambda_{cr} \approx 1$, then $\gamma_i \approx 0$, which implies that $\det(K) \approx 0$. This in turn means that the load level corresponds to buckling.

5.2 Load-displacement control, *LDC*

LDC is a static analysis where the load is applied in increments and the response of the system is calculated for each load-step. In order to capture the buckling behaviour of a beam, an initial imperfection must be given. A common approach is to first run a linearized buckling analysis to find the shape of the buckling mode and then use this shape as an initial imperfection in the *LDC* analysis. *LDC* gives more detailed information about the behaviour of a structure compared to a linearized buckling analysis, since it also describes pre- and post-buckling behaviour.

6 Presentation of software

This chapter provides some background information on how the commercial software ADINA, COLBEAM, LTBeam and SAP2000 conducts buckling analyses and estimates M_{cr} .

6.1 ADINA Solids & Structures, 900 Nodes Version 8.8

ADINA (Automatic Dynamic Incremental Nonlinear Analysis) is a finite element software with a wide range of applications. Buckling analysis can be conducted either by a linearized buckling analysis or by an incremental static analysis, *LDC*.

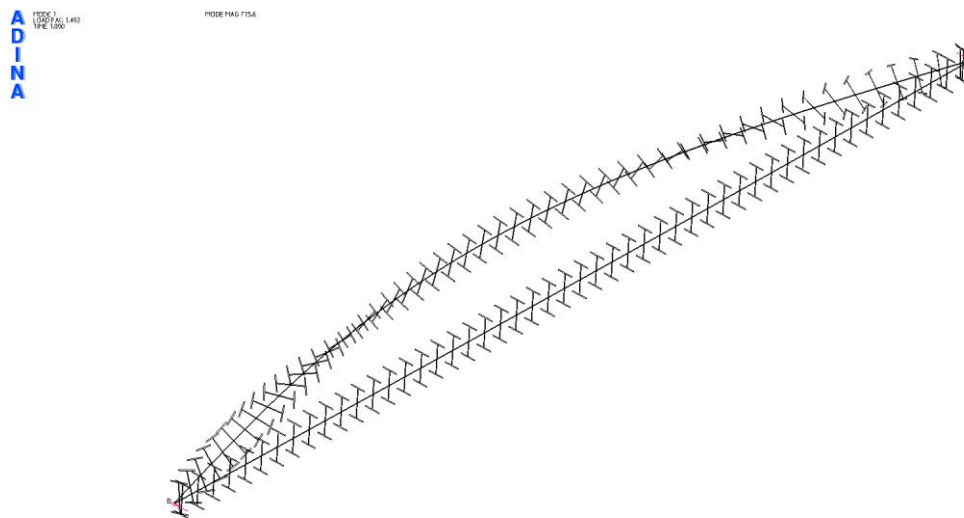


Figure 6.1 Visualisation of the lateral torsional buckling mode of a beam in ADINA.

It is important to consider warping effects in lateral torsional buckling analysis. ADINA distinguishes between beam elements and warping beam elements, where the latter has an additional warping degree of freedom. The ADINA user manual does not recommend the use of warping beam elements in large displacement analysis, since they for some cases yield incorrect results. Therefore, the warping beam element cannot be used in linearized buckling analysis in version 8.8 of ADINA. However, it is possible to override this obstruction and access the 8.7 version of the element formulation from the 8.8 version (ADINA 2011).

Shell elements can be used instead of beam elements in buckling analysis. A model with shell elements is more time consuming to establish, but will take more effects into account than a beam model (e.g. arch action). The boundary conditions must be set very carefully when working with shell elements since they have a significant impact on the results.

When using shell elements, an I-beam is often modelled as three plates neglecting the radiuses of the rolled section. Such a simplification may not be justified in all situations, since it yields a deviation in the results. Before evaluating M_{cr} in chapter 7, a pre-study was carried out in ADINA to determine the magnitude of this deviation. It was found to be about 4% in the studied cases, which was considered non-neglectable.

6.2 COLBEAM, EC3 v1.0.6

COLBEAM is a steel beam/column calculation software developed by StruProg AB, Sweden. The program conducts static analysis for single spanned beams and makes section and buckling controls according to Eurocode 3.

In buckling analysis COLBEAM implements the *3-factor formula* presented in chapter 4.2.

$$M_{cr} = C_1 \frac{\pi^2 \cdot EI_z}{(k_z \cdot L)^2} \left(\left(\sqrt{\left(\frac{k_z}{k_w} \right) \frac{I_w}{I_z} + \frac{(k_z \cdot L)^2 GI_t}{\pi^2 \cdot EI_z} + (C_2 \cdot z_g)^2} \right) - (C_2 \cdot z_g - C_3 \cdot z_j) \right) \quad (6.1)$$

The elastic critical moment is found under the tab “More Results” on COLBEAM’s main screen.

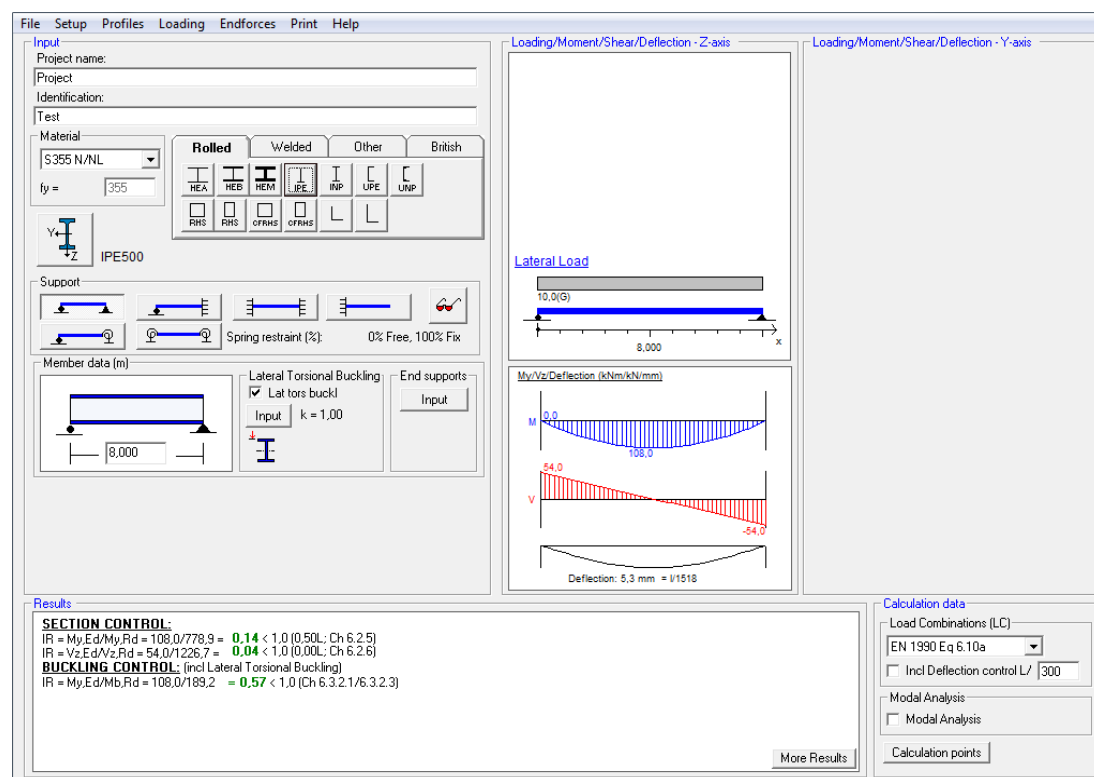


Figure 6.2 Main screen of COLBEAM. The results of the static analysis are displayed in the bottom of the screen. The elastic critical moment can be found under the tab “More Results”.

6.2.1 Implementation of C-factors

By default COLBEAM uses table values to determine the *C*-factors, see Figure 6.3. In cases of a beams simply supported about the major axis, the values come from ECCS (2006). For beams with fixed supports about the major axis, COLBEAM refers to a table in *ENV-1993-1-1:1992*, which is a pre-edition of *Eurocode 3*. In cases of multiple loading, the dominating load determines what table value to be used.

By marking the box “Advanced calculation of C1”, COLBEAM uses the closed-form expression by Lopez et al. (2006) to calculate C_1 (see chapter 0.). This option is not

available for linear moment distributions. In these cases there are no references to the C_1 -values used by COLBEAM, but it can be concluded through comparison that these values are collected from ECCS (2006).

The point of load application controls the term $C_2 \cdot z_g$ in the *3-factor formula*. The load can be applied on the top, centre or bottom of the section by clicking on the corresponding icon. A custom distance from the applied load to the gravity centre can also be set, see *Figure 6.3*.

6.2.2 Implementation of lateral restraints

Lateral boundary conditions are accounted for by the k -factor, which can take the values 0.5 (fixed at both ends), 0.7 (fixed at one end and free at the other) or 1.0 (free at both ends). Note that no distinction can be made between the warping restraint, k_w , and the end rotation restraint, k_z , which implies that the same value of k must be assigned to both these restraints.

Table values of C_1 , C_2 and C_3 are only available for $k=0.5$ and $k=1.0$. When k is chosen as 0.7, COLBEAM makes a linear interpolation between the C -values of $k=0.5$ and $k=1.0$.

In addition to the k -factor, lateral restraints along the compression flange can be added in order to control lateral fixation.

Lateral torsional buckling length

k-factor is related to member length or the length between restraint points

Lateral restraint points along compression flange

0

Loadlevel

This has only influence if you have loading on the beam and that lateral restraint points = 0 (C2-factor)

Lateral torsional bending/buckling capacity

Md/Rb = 189,2 kNm

C1 = 1,120

C2 = 0,450

C3 = N/A

☐ Manual input of C-factors
Only valid for loaded member and no restraints

☐ Advanced calculation of C1

☒ Lateral torsional buckling curves (ref ch 6.3.2.2/6.3.2.3)

☒ General Case (conservative, ch 6.3.2.2)

☐ Rolled or welded I-sections (ch 6.3.2.3)

Loading and support condition	k	C ₁	C ₂	C ₃
1)	1.0 0.5	1.12 0.97	0.45 0.36	0.525 0.478
2)	1.0 0.5	1.285 0.712	1.562 0.652	0.753 1.070
1)	1.0 0.5	1.35 1.05	0.59 0.48	0.411 0.338
2)	1.0 0.5	1.565 0.938	1.267 0.715	2.640 4.800
1)	1.0 0.5	1.04 0.95	0.42 0.31	0.562 0.539

1) Ref: "Rules for Member Stability in EN 1993-1-1", Background Documentation and Design Guidelines, ECCS, 2006, Table 64
2) Ref: ENV 1993.1.1 : 1992, Table F.1.2

OK

Figure 6.3 *Input screen for lateral torsional buckling in COLBEAM. To the right; table values of C_1 , C_2 and C_3 are displayed for standard cases of loading and support conditions. To the left; settings for the point of load application can be adjusted under the heading "Loadlevel". In the left upper corner, the lateral boundary conditions can be chosen to 1.0, 0.7 or 0.5.*

6.3 LTBeam, version 1.0.11

LTBeam is a free software developed by CTICM (Centre Technique Industriel de la Construction Métallique) in France solely for calculation of elastic critical moments. The program performs a buckling analysis with finite elements, treating both single spanned beams and cantilevers.

LTBeam consists of four tabs/windows. In the first three, information can be added about the section, lateral restraints and loading conditions. In the fourth tab, “Critical Moment”, the analysis is performed and the results can be viewed. Figure 6.4 below show the lateral restraints tab.

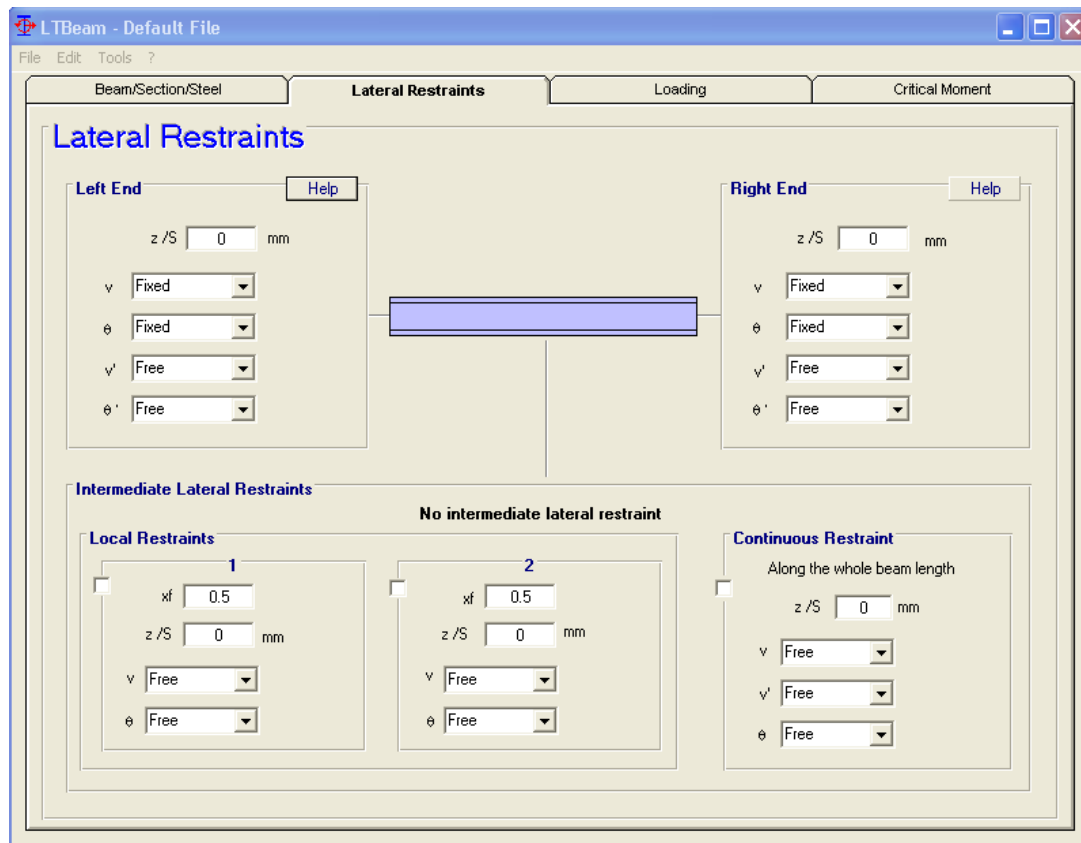


Figure 6.4 The “Lateral Restraints” tab in LTBeam.

6.3.1 Implementation of lateral restraints

In LTBeam it is possible to set end-restraints independently for lateral bending, warping, lateral deflection and rotation about the x -axis. If the restraints are set as free at one side and fixed at the other, the model will represent a cantilever (provided that also the major axis restraints correspond to a cantilever).

ψ'	=	Lateral rotation about the y -axis, if set to free the beam can bend out laterally at the end. This boundary condition corresponds to k_z in the <i>3-factor formula</i>
θ'	=	Warping degree of freedom. This boundary condition corresponds to k_w in the <i>3-factor formula</i> .
v	=	Lateral deflection, if set to free the beam can deflect laterally at the end
θ	=	Rotation about the x -axis, if set to free the beam can rotate around its own axis

Figure 6.5 below shows these boundary conditions and their notations in LTBeam. In addition to the end-restraints, lateral bracings along the beam can also be added to the model.

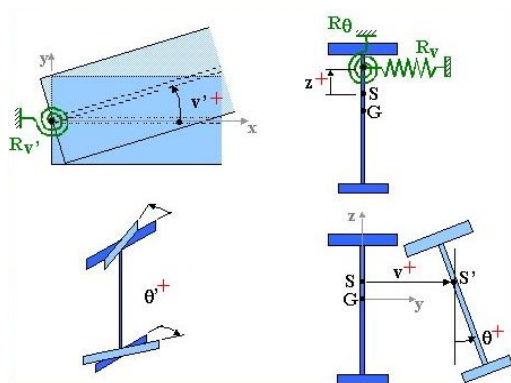


Figure 6.5 Lateral boundary conditions in LTBeam.

According to *CTICM*, LTBeam is only intended for those with enough knowledge to assess the accuracy of the result. The use of the program is entirely under the responsibility of the user. There is little background documentation on LTBeam, which makes it hard to interpret the results (as required by *CTICM*). However, several trusted sources (e.g. Access Steel (2005) and ECCS (2006)) make references to LTBeam as a useful program.

LTBeam can be downloaded from <<http://www.steelbizfrance.com>>.

6.4 SAP2000, Ultimate 15.1.0, “design module”

SAP2000 is a 3D-object based modelling program often used to analyse multi-element structures. It can also be used to analyse separate members and beams. The elastic critical moment can be calculated in SAP2000 from finite element analysis with shell elements, or from a “design module” that implements analytical expressions. In the “design module”, several design codes can be chosen. This thesis focuses on the “design module” with section analysis according to *Eurocode 3*.

A structure can be modelled in SAP2000 by using the “drawing tool”, but there are also many templates of beams and plates etc. Figure 6.6 shows the main window in SAP2000. Load patterns, load cases and load combinations are created under the “Define” tab. Boundary conditions and loads are applied under the “Assign” tab.

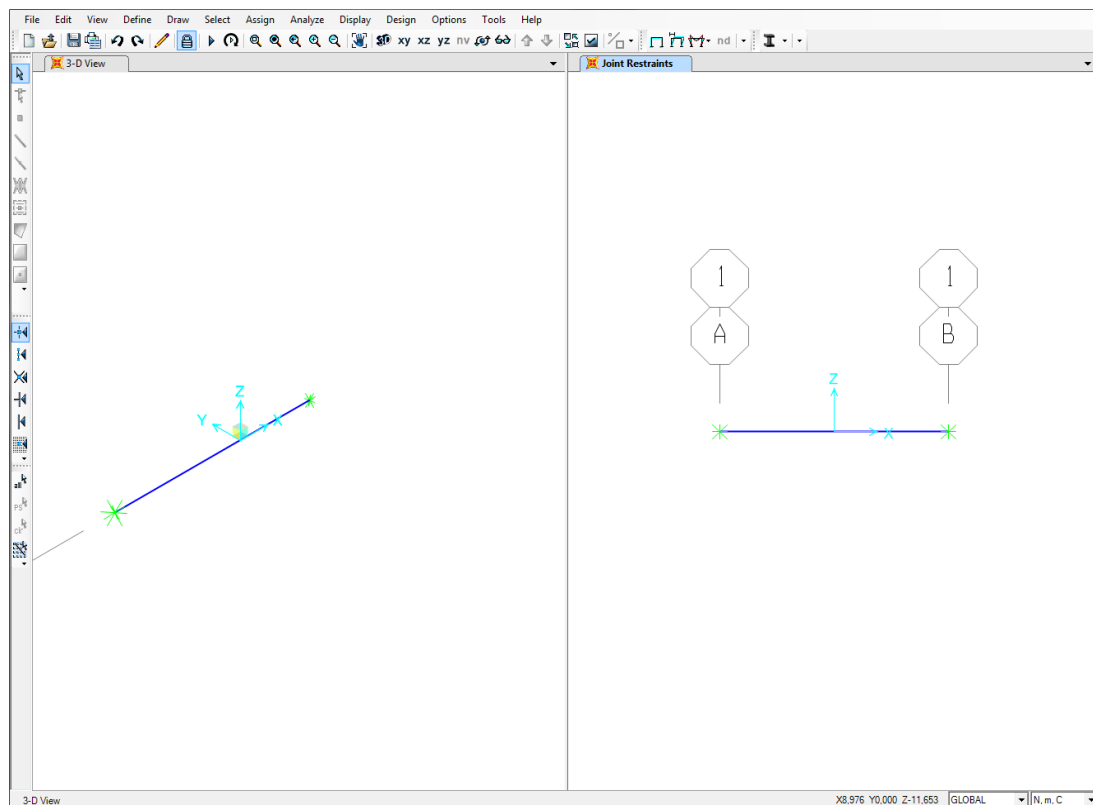


Figure 6.6 The main window in SAP2000. Loads are defined under the “Define” tab and boundary conditions are applied under the “Assign” tab.

When designing according to *Eurocode 3*, SAP2000 implements equation (6.2) in the “design module”. This expression is analogous with the expression used in *AISC LRFD* (CSI 2011). See equation (4.22).

$$M_{cr} = C_1 \frac{\pi^2 \cdot EI_z}{L_{cr}^2} \sqrt{\frac{I_w}{I_z} + \frac{L_{cr}^2 \cdot GI_t}{\pi^2 \cdot EI_z}} \quad (6.2)$$

$$\text{Where} \quad L_{cr} = k \cdot L$$

This form of the 3-factor formula is valid when

$$\begin{aligned} C_2 \cdot z_g &= 0 \\ C_3 \cdot z_j &= 0 \\ k &= k_z = k_w \end{aligned}$$

This means that this expression does not take the point of load application into account and can only be used for double-symmetric sections. Both lateral bending and warping restraints must be assigned the same value.

6.4.1 Implementation of C-factors

According to CSI (2011), SAP2000 calculates C_1 with equation (6.3) when using the *Eurocode 3* setting.

$$C_1 = 1.88 - 1.40\psi + 0.52\psi^2 \quad (6.3)$$

Where ψ = Ratio of the end-moments

However, it is obvious that SAP2000 actually uses equation (6.4) from *AISC LRFD* (see Table 6.1).

$$C_1 = \frac{12.5M_{\max}}{3M_A + 4M_B + 3M_C + 2.5M_{\max}} \quad (6.4)$$

Table 6.1 Comparison of C_1 -values from SAP2000 with equations (6.3) and (6.4) for an 8 meter IPE500 beam ($k=1.0$).

		SAP2000, <i>Eurocode 3</i>	AISC LRFD, equation (6.4)	CSI (2011), equation (6.3)
End-moments		1.000	1.000	1.000
Simply supported (major axis)	Concentrated load	1.316	1.316	1.000
	Distributed load	1.136	1.136	1.000
Fixed (major axis)	Concentrated load	1.923	1.923	1.000
	Distributed load	2.381	2.381	1.000

6.4.2 Implementation of lateral restraints

When evaluating the elastic critical moment, lateral boundary conditions can be applied in three different ways.

- (1) As boundary conditions in the model
- (2) As lateral bracings in the model
- (3) By overwriting values on the effective length factor, k , in the “design module”

6.5 Summary of software properties

Table 6.2 Summary of the properties in ADINA, COLBEAM, LTBeam and SAP2000.

	ADINA “Warping beam elements”	COLBEAM	LTBEAM	SAP2000 “Design module” <i>Eurocode 3</i>
*	FE-analysis Linearized buckling analysis, or <i>LDC</i>	Analytical expression, see equation (6.1)	FE-analysis	Analytical expression, see equation (6.2)
C₁	Implicitly implemented in FE-analysis	Table values from ECCS (2006) & ENV-1993-1-1 If “Advanced calculation of C ₁ ” is used, C ₁ is estimated by the closed- form expression by Lopez et al. (2006), see chapter 0	Implicitly implemented in FE-analysis	$C_1 = \frac{12.5M_{\max}}{3M_2 + 4M_3 + 3M_4 + 2.5M_{\max}}$ This expression does not take lateral boundary conditions into account in calculation of C ₁
C₂	Implicitly implemented in FE-analysis	The point of load application can be varied between the top, centre and bottom of the section, or set manually	Implicitly implemented in FE-analysis	Does not implement C ₂
C₃	Implicitly implemented in FE-analysis	Implemented when single-symmetric sections are analysed	Implicitly implemented in FE-analysis	Does not implement C ₃
k_z, k_w	Implicitly implemented in FE-analysis	The lateral boundary conditions can be set to 1.0, 0.7 or 0.5 No distinction can be made between lateral bending and warping conditions, k _z and k _w	Warping, θ' , and lateral bending, v' , are controlled with separate degrees of freedom and can be chosen as free or fixed individually Lateral deflection, v , and rotations about the x-axis, θ , can also be set to free or fixed	Lateral boundary conditions can be applied as boundary conditions, lateral restraints or by overwriting the effective buckling length factor, k , in the “design module” No distinction can be made between lateral bending and warping conditions, k _z and k _w

* Calculation method

7 Parametric study

7.1 Background

The main aim of this Master's thesis was to examine how ADINA, COLBEAM, LTBeam and SAP2000 calculate the elastic critical moment, and to explain potential differences in the results. In order to achieve this, a parametric study was carried out where M_{cr} was calculated for selected situations in the programs.

There are small differences in the sectional data implemented by the programs, see Table 7.1. It was therefore expected that the differences in computed critical moments should be primarily dependent on the C -factors of the *3-factor formula*. This was also confirmed in a pre-study where the biggest deviation in M_{cr} due to sectional data was about 6 ‰.

The study was divided into two parts, one concerning C_1 , and the other concerning C_2 . Serna et al. (2005) have presented exact finite difference values of the C_1 -factor for 8 and 16 meter IPE500 beams subjected to different loading conditions. Since exact reference values are needed to make evaluations of the accuracy, the same beams and loading conditions have been used as in the research by Serna et al. (2005). No reference values were available for C_2 . The study of C_2 should therefore be seen as a comparison between the programs, rather than an evaluation of the accuracy.

7.2 Prerequisites and assumptions

7.2.1 Software

The following programs are investigated in the study.

- ADINA Solids & Structures, 900 nodes version 8.8
- COLBEAM, EC3 v1.0.6
- LTBEAM version 1.0.11
- SAP2000, Ultimate 15.1.0, “design module” for *Eurocode 3*

ADINA and LTBEAM are FEM-software. COLBEAM and SAP2000 implement analytical expressions. See chapter 6.

7.2.2 Material

The modelled steel beams are assumed to be isotropic with a linear elastic material response. Pure elastic material behaviour is a reasonable assumption since the elastic moment is of interest.

- Steel S355
- Young's modulus, $E = 210$ [GPa]
- Poisson's ratio, $\nu = 0.3$
- Shear modulus, $G = E / 2(1 + \nu)$ [GPa]

7.2.3 Geometry

Two IPE-beams with different lengths are investigated.

- IPE500, 8 meter
- IPE500, 16 meter

In COLBEAM, LTBeam and SAP2000 the sectional properties are accessed from databases in the programs. In ADINA the section is defined manually by the “general cross-section” command, and the properties are taken from ArcelorMittal’s product catalogue (ArcelorMittal 2013).

Table 7.1 Section properties of studied IPE500 beams.

	ADINA (general section)	COLBEAM	LTBeam	SAP2000
h_w [mm]	-	468	468	468
h_f [mm]	-	200	200	200
t_f [mm]	-	16.0	16.0	16.0
t_w [mm]	-	10.2	10.2	10.2
r [mm]	-	21	21	-
A [mm ²]	11600	11550	11552	11600
I_y [mm ⁴]	4.82e8	4.82e8	4.819855e8	4.82e8
I_z [mm ⁴]	2.142e7	2.142e7	2.14169e7	2.142e7
I_t [mm ⁴]	8.93e5	*	8.901e5	8.91e5
I_w [mm ⁶]	1.249e12	1.25e12	1.254258e12	*

* Calculated implicitly by the program

7.2.4 Point of load application, PLA

In the study concerning the C_1 -factor, all loads are assumed to act in the shear centre. When studying C_2 , the loads are applied either on top of the upper flange or under the lower flange. All three points are located on the symmetry line along the z -axis.

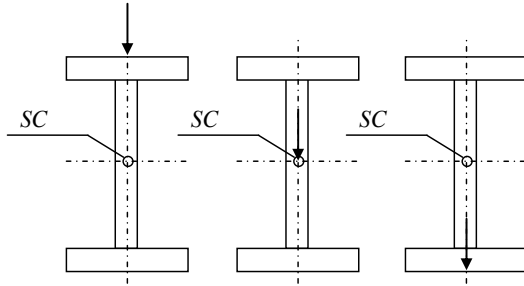


Figure 7.1 Three different PLA used in the study; on top of the upper flange, in the shear centre and under the lower flange.

7.2.5 Lateral boundary conditions

In the 3-factor formula, the lateral boundary conditions are controlled by the factors k_z (lateral bending) and k_w (warping). Since COLBEAM and SAP2000 cannot treat these degrees of freedom separately, the studies are limited to situations where $k_z=k_w$. In such situations, the factors are just denoted k .

Three different cases of lateral boundary conditions are investigated.

- (1) Both ends free, $k=1.0$
- (2) One end free and one end fixed, $k=0.7$
- (3) Both ends fixed, $k=0.5$

7.2.6 Studied load cases

7.2.6.1 Load Case I - End-moments

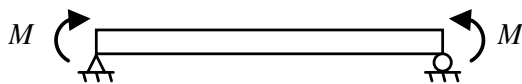


Figure 7.2 Load Case I; The beam is subjected to end-moment loading.

7.2.6.2 Load Case II - Simply supported, concentrated load

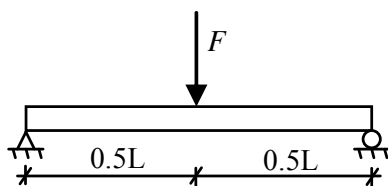


Figure 7.3 Load Case II; The beam is simply supported about major axis and subjected to a concentrated load in the mid-span.

7.2.6.3 Load Case III - Simply supported, distributed load

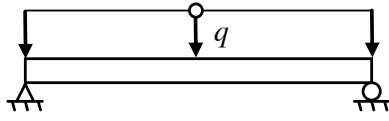


Figure 7.4 Load Case III; The beam is simply supported about major axis and subjected to an evenly distributed load.

7.2.6.4 Load Case IV – Fixed, concentrated load

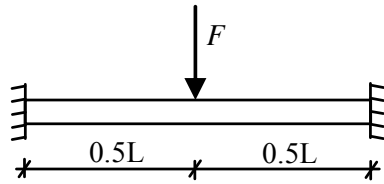


Figure 7.5 Load Case IV; The beam is fixed about major axis and subjected to a concentrated load in the mid-span.

7.2.6.5 Load Case V – Fixed, distributed load

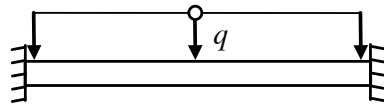


Figure 7.6 Load Case V; The beam is fixed about major axis and subjected to an evenly distributed load.

7.3 Procedure

7.3.1 The reference moment, $M_{cr,ref}$

In finite element software, the critical moment is evaluated directly, without the use of the 3-factor formula. As described below, it is possible to extract equivalent C_1 - and C_2 -factors in such programs when M_{cr} is known.

Consider the 3-factor formula when $C_2=0$ and $C_3=0$

$$M_{cr} = C_1 \frac{\pi^2 \cdot EI_z}{(k_z \cdot L)^2} \sqrt{\left(\frac{k_z}{k_w} \right) \frac{I_w}{I_z} + \frac{(k_z \cdot L)^2 GI_t}{\pi^2 \cdot EI_z}} \quad (7.1)$$

Define a reference moment $M_{cr,ref}$

$$M_{cr,ref} = \frac{\pi^2 \cdot EI_z}{(k_z \cdot L)^2} \sqrt{\left(\frac{k_z}{k_w} \right) \frac{I_w}{I_z} + \frac{(k_z \cdot L)^2 GI_t}{\pi^2 \cdot EI_z}} \quad (7.2)$$

In cases where $C_2=0$, $C_3=0$ and M_{cr} is known, C_1 can be calculated from

$$C_1 = \frac{M_{cr}}{M_{cr,ref}} \quad (7.3)$$

In cases where $C_3=0$ and M_{cr} and C_1 are known, C_2 can be refracted from

$$M_{cr} = C_1 \frac{\pi^2 \cdot EI_z}{(k_z \cdot L)^2} \left(\sqrt{\left(\frac{k_z}{k_w} \right) \frac{I_w}{I_z} + \frac{(k_z \cdot L)^2 GI_t}{\pi^2 \cdot EI_z}} + (C_2 \cdot z_g)^2 \right) - C_2 \cdot z_g \quad (7.4)$$

7.3.2 Parametric study of the C_1 -factor

The procedure for the parametric study of the C_1 -factor is outlined below.

- (1) Establish 8 and 16 meter beam models valid for the given load cases with points of load application in the centre of gravity.
- (2) Calculate M_{cr} in the 5 load cases for the 3 lateral boundary conditions and the 2 beam lengths.
- (3) Extract C_1 -factors corresponding to the calculated values of M_{cr} .

The procedure is followed for all 4 programs considered, making $5 \cdot 3 \cdot 2 \cdot 4 = 120$ the total number of calculated critical moments.

7.3.2.1 ADINA - Comments

- Models are established using warping beam elements.
- In all load cases, including the fixed load cases IV and V, the x-translation is assumed free at one side of the beam.
- M_{cr} is calculated by running a linearized buckling analysis under increasing base load until $\lambda \approx 1$.
- The classical formulation of the eigenvalue problem is used in the buckling analysis.
- Version 8.7 of the element formulation is used.

- The C_I -factor is extracted by dividing the critical moment calculated in ADINA with the reference moment $M_{cr,ref}$.
- Details on how the modelling is made in ADINA can be seen in Appendix D.

7.3.2.2 LTBeam - Comments

- LTBeam is a finite element program and calculates M_{cr} directly. Thus, the C_I -factor is extracted by dividing the critical moment by the reference moment, $M_{cr,ref}$, in the same way as for ADINA.

7.3.2.3 COLBEAM - Comments

- COLBEAM uses analytical expressions to calculate M_{cr} . The C_I -factor can be found directly in the program.

7.3.2.4 SAP2000 - Comments

- Models are established using beam elements.
- A static analysis is conducted to obtain sectional forces.
- In the “design module”, the effective length factors are overwritten in order to match the different boundary conditions.
- The *Eurocode 3* setting is used in the “design module”.
- Similar to COLBEAM, the “design module” in SAP2000 uses analytical expressions to calculate M_{cr} . The C_I -factor can be found directly in the results tab.

7.3.3 Parametric study of the C_2 -factor

The study concerning C_2 follows a procedure similar to that of C_I .

- (1) Establish 8 meter beam models with points of load application on top of the upper flange and under the bottom flange.
- (2) Calculate M_{cr} in load cases II-V for the 3 lateral boundary conditions and the 2 points of load application.
- (3) Extract C_2 -factors corresponding to the calculated values of M_{cr} .

7.3.3.1 Comments

In ADINA and LTBeam, the critical moments are given directly. C_1 -factors are known for all cases, and thus, the C_2 -factor can be solved from the *3-factor formula*. In COLBEAM, the C_2 -factor is given directly. SAP2000 does not implement C_2 and is left out of the study.

- Only 8-meter beams are considered.
- Load Case I is left out since it would make no sense to try to vary the point of load application for end-moments.
- No reference values are available.
- In ADINA the point of load application is modelled as a rigid link from the beam node to the applied load.

Details on how the modelling is made in ADINA can be seen in Appendix D.

8 Results

All results from the parametric study can be found in Appendix E.

8.1 The C_I -factor

In this chapter values of C_I from ADINA, COLBEAM, LTBeam and SAP2000 are compared to reference values from Serna et al. (2005). The results are presented in graphs showing how C_I depend on the lateral boundary conditions k . Column charts are also presented where the deviation in C_I with regard to the reference values is shown. Reference values are only available for $k=1.0$ and $k=0.5$.

8.1.1 Comments

- When comparing the results of the two beam lengths 8 and 16 meters, it could be seen that the maximum deviation in C_I was about 5 %. Since other effects than the beam length have much greater impact on the C_I -factor, results are only presented for the 8 meter beam. The results of the 16 meter beam are presented in Appendix E.
- COLBEAM values using the option “Advanced calculation of C1” are denoted “COLBEAM ‘Advanced’” in the figures.

8.1.2 Load Case I

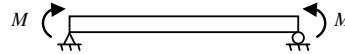


Figure 8.1 presents the C_1 -values of Load Case I. Figure 8.2 shows the deviation of the C_1 -values in relation to the reference values of Serna et al. (2005). The option “Advanced calculation of C_1 ” is not available in COLBEAM for linear moment distributions.

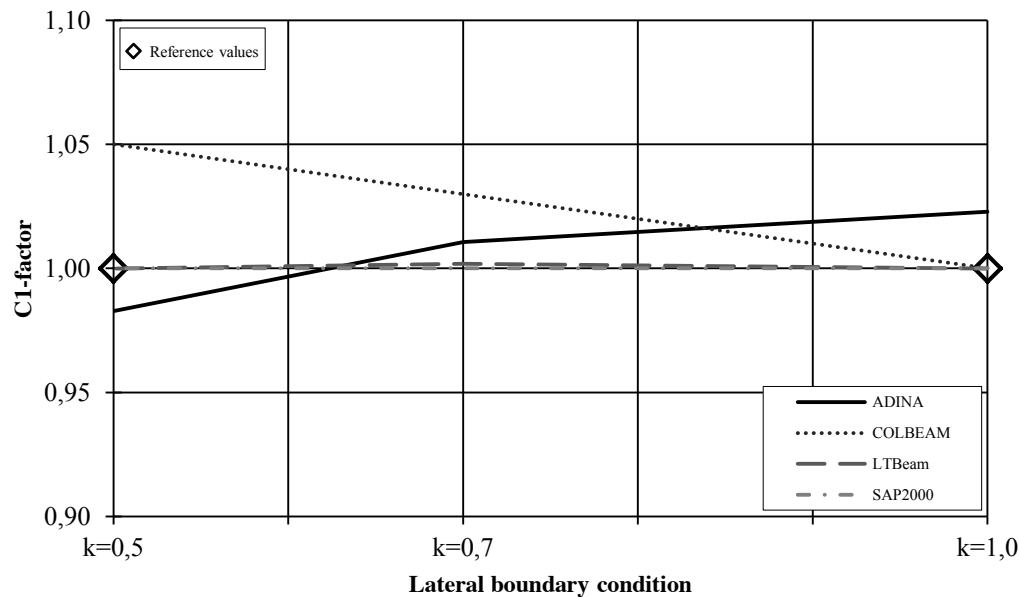


Figure 8.1 Load Case I; The C_1 -factor of software ADINA, COLBEAM, LTBeam and SAP2000 plotted for the lateral boundary conditions $k=0.5$, $k=0.7$ and $k=1.0$.

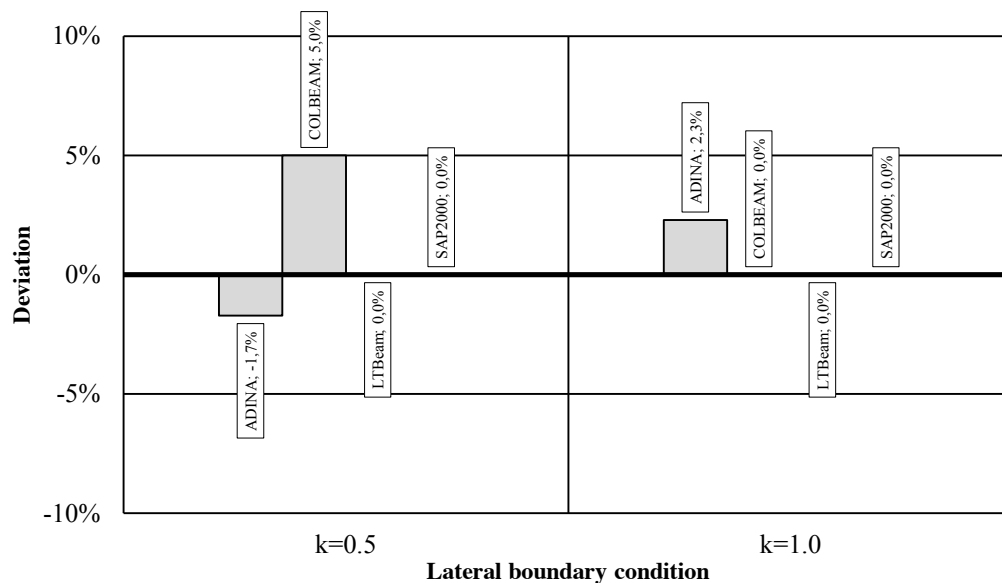


Figure 8.2 Deviation of the C_1 -factor for each program in Load Case I. The results are compared to reference values obtained by Serna et al. (2005) for the lateral boundary conditions $k=0.5$ and $k=1.0$. The values are presented so that conservative values are negative.

8.1.3 Load Case II

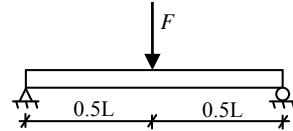


Figure 8.3 presents the C_I -values of Load Case II. Figure 8.4 shows the deviation of the C_I -values in relation to the reference values of Serna et al. (2005).

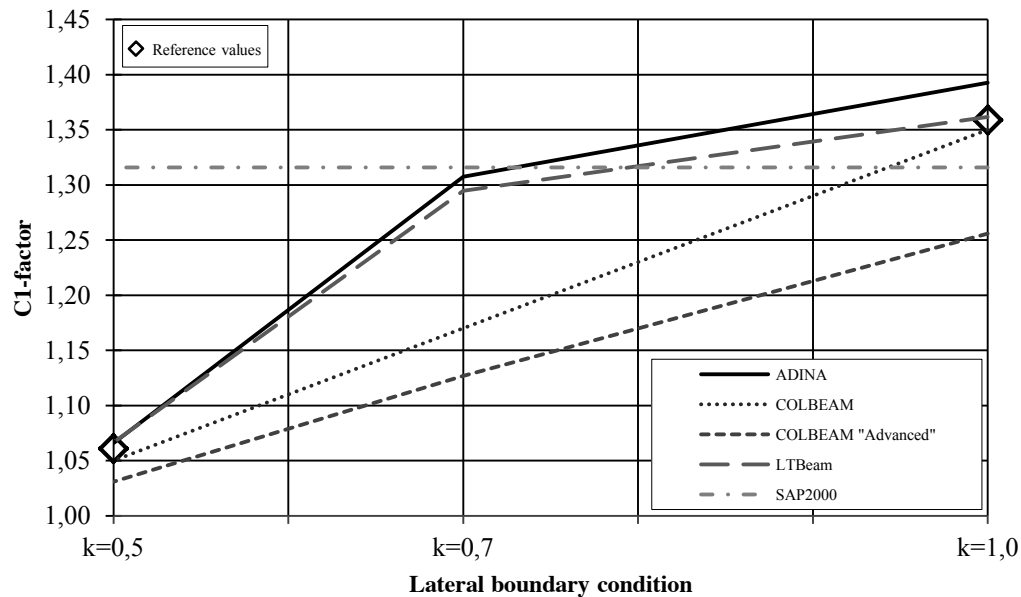


Figure 8.3 Load Case II; The C_I -factor of software ADINA, COLBEAM, LTBeam and SAP2000 plotted for the lateral boundary conditions $k=0.5$, $k=0.7$ and $k=1.0$.

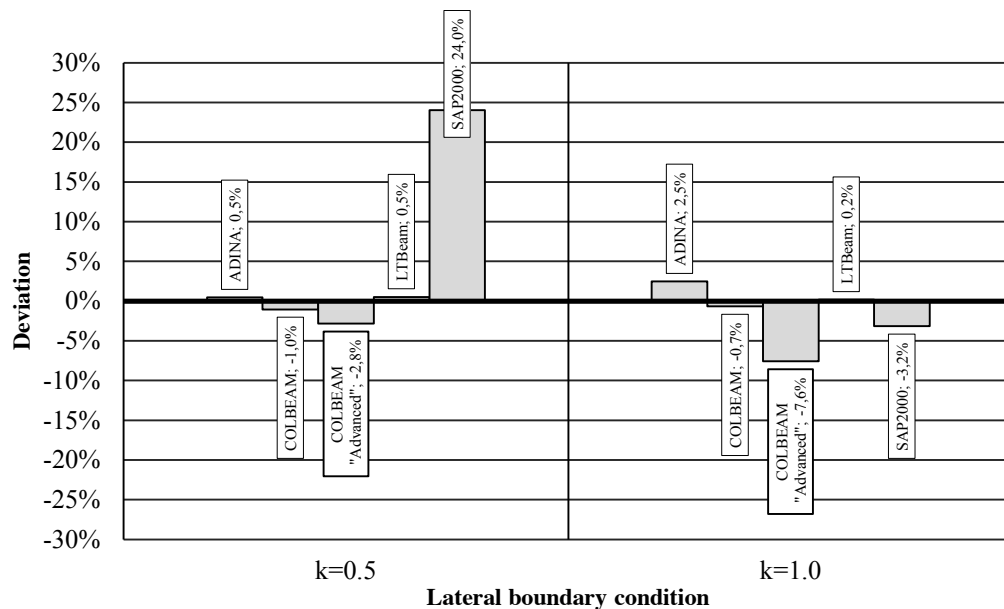


Figure 8.4 Deviation of the C_I -factor for each program in Load Case II. The results are compared to reference values obtained by Serna et al. (2005) for the lateral boundary conditions $k=0.5$ and $k=1.0$. The values are presented so that conservative values are negative.

8.1.4 Load Case III

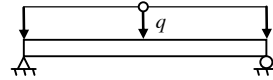


Figure 8.5 presents the C_I -values of Load Case III. Figure 8.6 shows the deviation of the C_I -values in relation to the reference values of Serna et al. (2005).

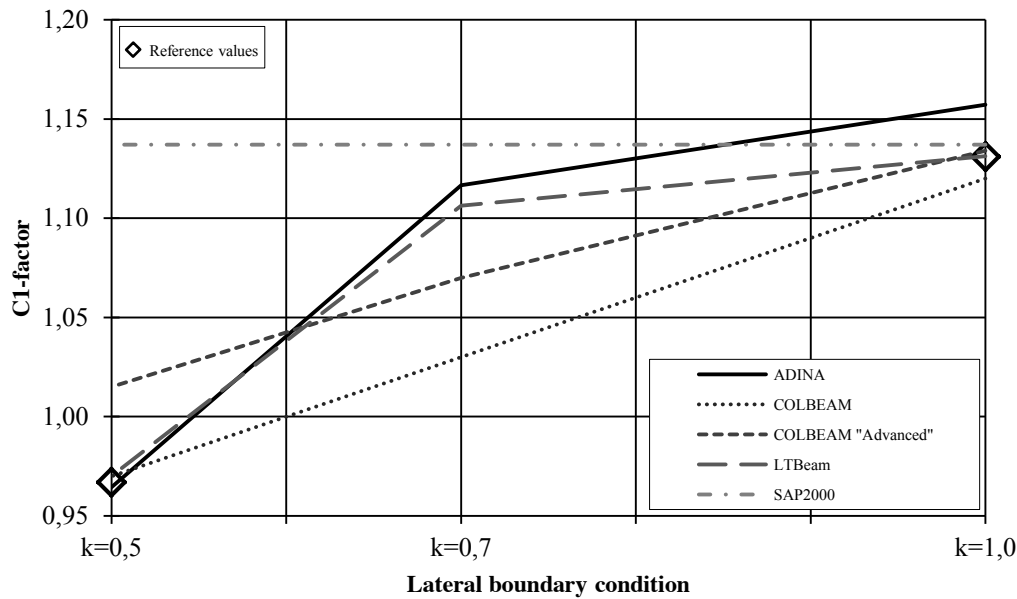


Figure 8.5 Case III; The C_I -factor of software ADINA, COLBEAM, LTBeam and SAP2000 plotted for the lateral boundary conditions $k=0.5$, $k=0.7$ and $k=1.0$.

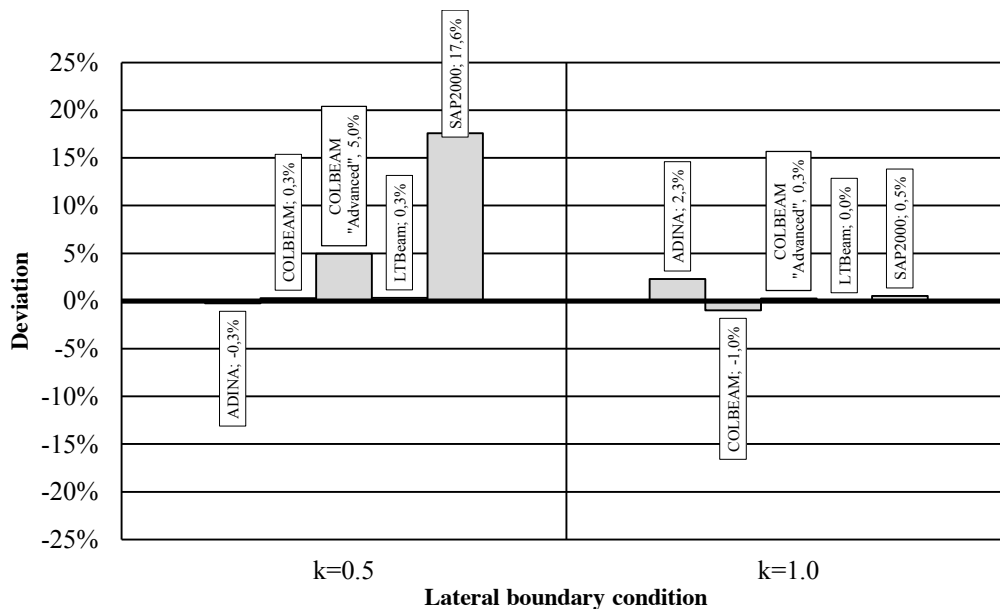


Figure 8.6 Deviation of the C_I -factor for each program in Case III. The results are compared to reference values obtained by Serna et al. (2005) for the lateral boundary conditions $k=0.5$ and $k=1.0$. The values are presented so that conservative values are negative.

8.1.5 Load Case IV

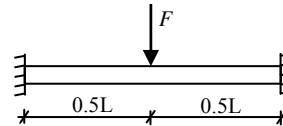


Figure 8.7 presents the C_I -values of Load Case IV. Figure 8.8 shows the deviation of the C_I -values in relation to the reference values of Serna et al. (2005).

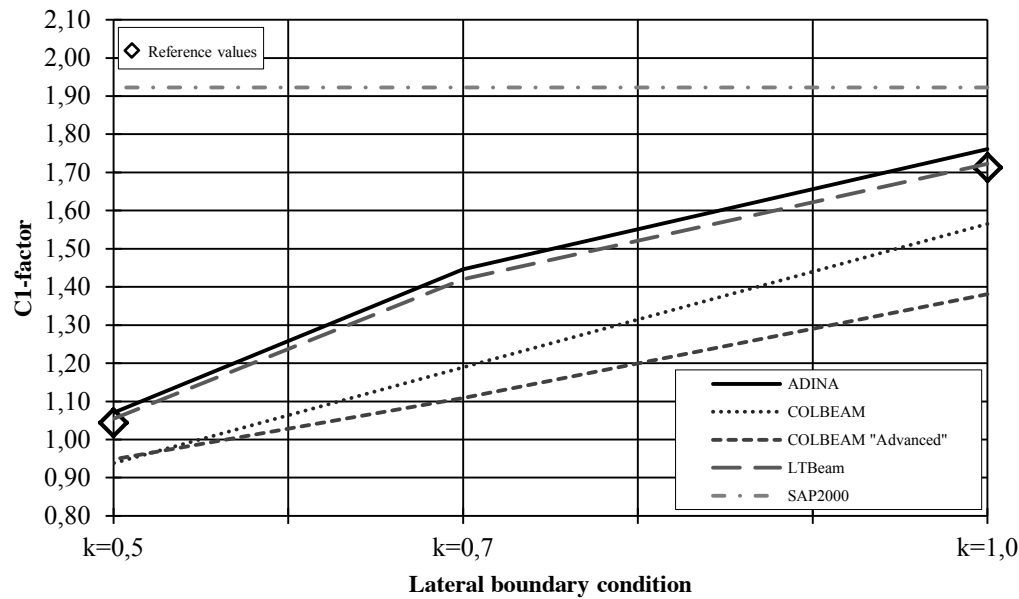


Figure 8.7 Load Case VI; The C_I -factor of software ADINA, COLBEAM, LTBeam and SAP2000 plotted for the lateral boundary conditions $k=0.5$, $k=0.7$ and $k=1.0$.

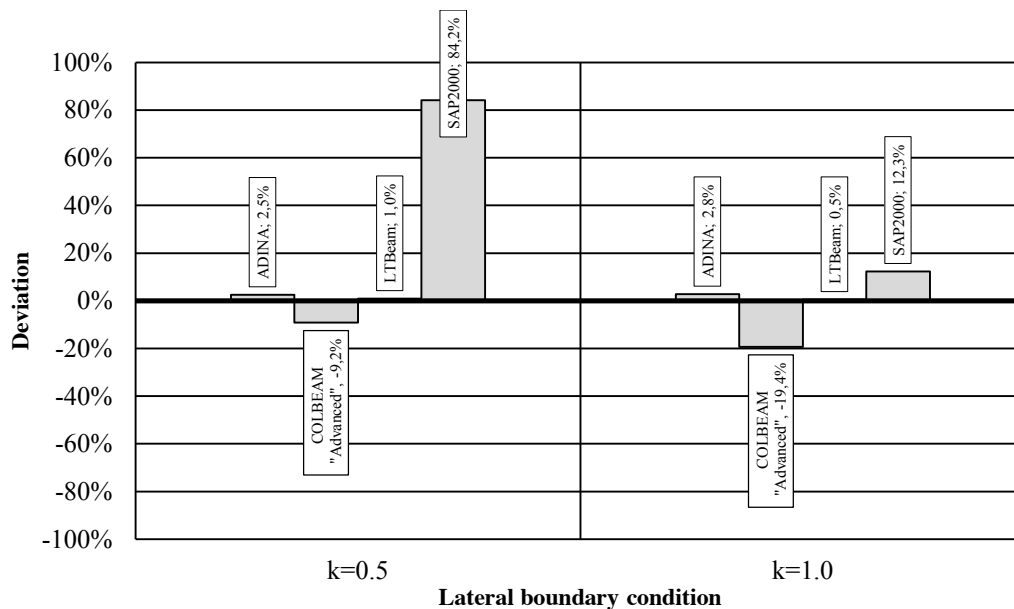


Figure 8.8 Deviation of the C_I -factor for each program in Load Case VI. The results are compared to reference values obtained by Serna et al. (2005) for the lateral boundary conditions $k=0.5$ and $k=1.0$. The values are presented so that conservative values are negative.

8.1.6 Load Case V

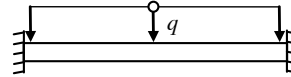


Figure 8.9 presents the C_1 -values of Load Case V. Figure 8.10 shows the deviation of the C_1 -values in relation to the reference values of Serna et al. (2005).

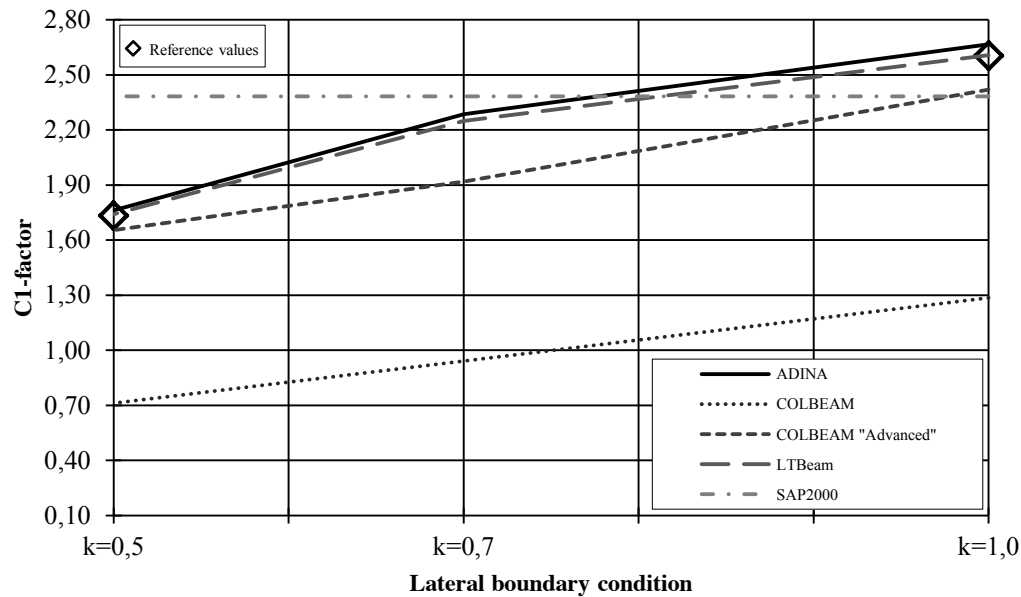


Figure 8.9 Load Case V; The C_1 -factor of software ADINA, COLBEAM, LTBeam and SAP2000 plotted for the lateral boundary conditions $k=0.5$, $k=0.7$ and $k=1.0$.

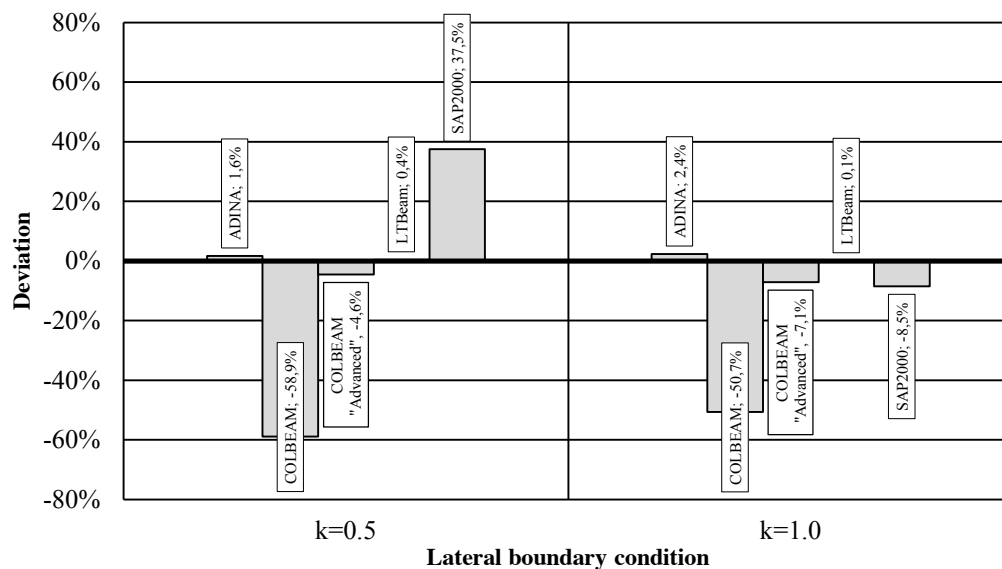


Figure 8.10 Deviation of the C_1 -factor for each program in Load Case V. The results are compared to reference values obtained by Serna et al. (2005) for the lateral boundary conditions $k=0.5$ and $k=1.0$. The values are presented so that conservative values are negative.

8.2 The C_2 -factor

In this chapter, values of C_2 from ADINA, COLBEAM and LTBeam are presented in four load cases with two points of load application.

- Loading on top of the upper flange
- Loading under the lower flange

In addition to the C_2 -plots, normalized graphs of M_{cr} are shown. These graphs are needed since it is hard to draw conclusions on how the point of load application affects M_{cr} just by studying C_2 .

8.2.1 Comments

- When a low point of load application is investigated, the load is placed “hanging” under to bottom flange since this yields the same distance, z_g , to the shear centre, as for a load placed on the top-flange. With regard to the *3-factor formula*, this means that z_g will take the values of 0.25 and -0.25 for an IPE500 beam.
- The graphs of M_{cr} are normalized after the program giving the highest values of M_{cr} .
- SAP2000 is left out of this study since it does not implement the C_2 -factor.

8.2.2 Load Case II

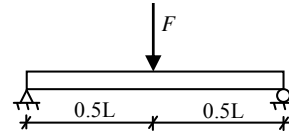


Figure 8.11 presents the C_2 -values of Load Case II. Figure 8.12 shows the elastic critical moment in a graph normalized after the program giving the highest value on M_{cr} .

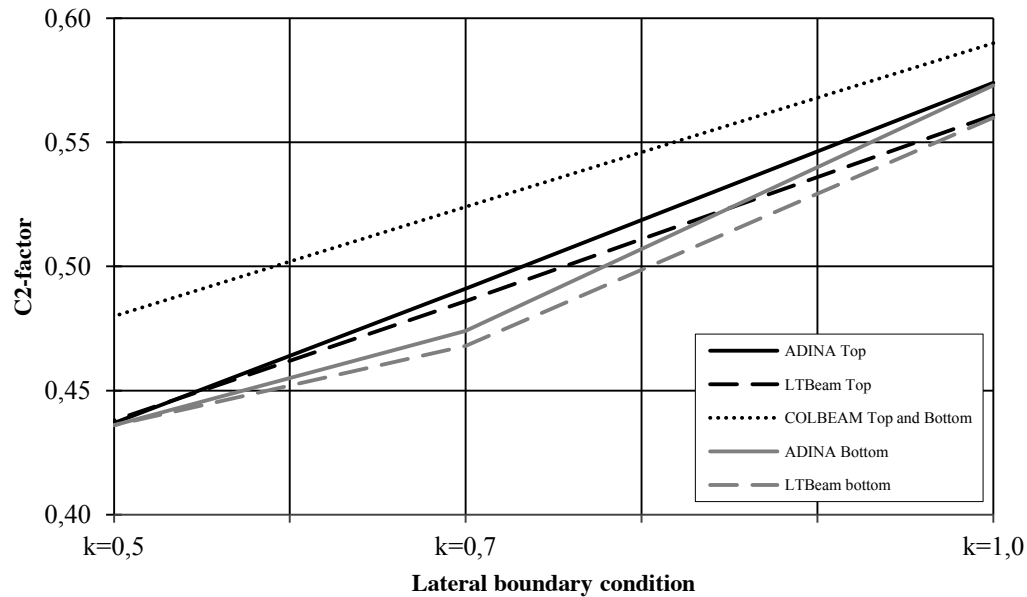


Figure 8.11 Load Case II; The C_2 -factor of software ADINA, COLBEAM, LTBeam and SAP2000 plotted for the lateral boundary conditions of $k=0.5$, $k=0.7$ and $k=1.0$.

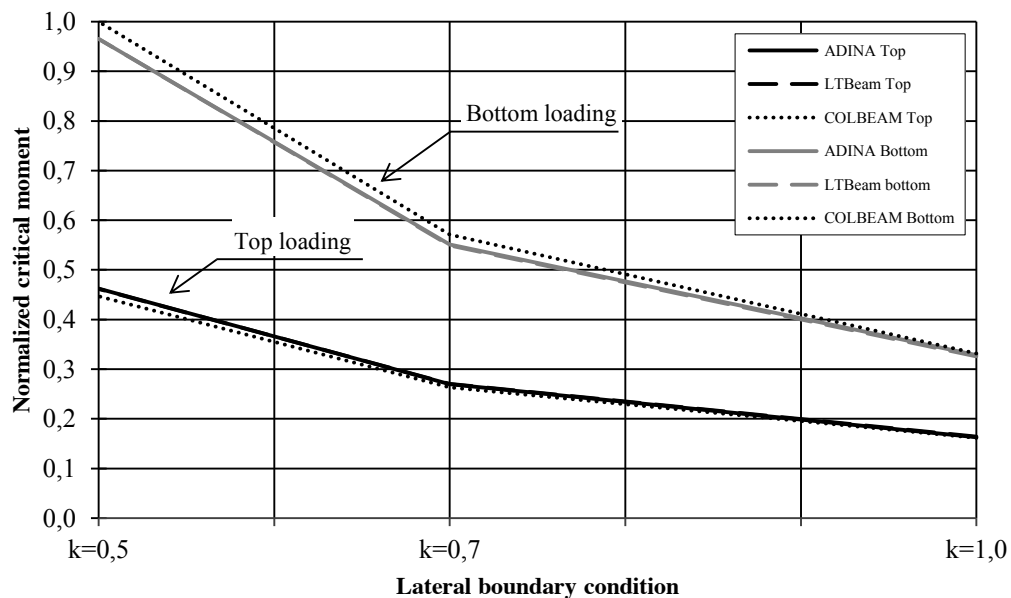


Figure 8.12 Normalized values of the elastic critical moment in Load Case II, plotted for the lateral boundary conditions of $k=0.5$, $k=0.7$ and $k=1.0$. The M_{cr} -values are normalized to bottom loading in COLBEAM.

8.2.3 Load Case III

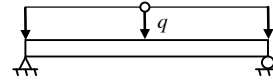


Figure 8.13 presents the C_2 -values of Load Case III. Figure 8.14 shows the elastic critical moment in a graph normalized after the program giving the highest value on M_{cr} .

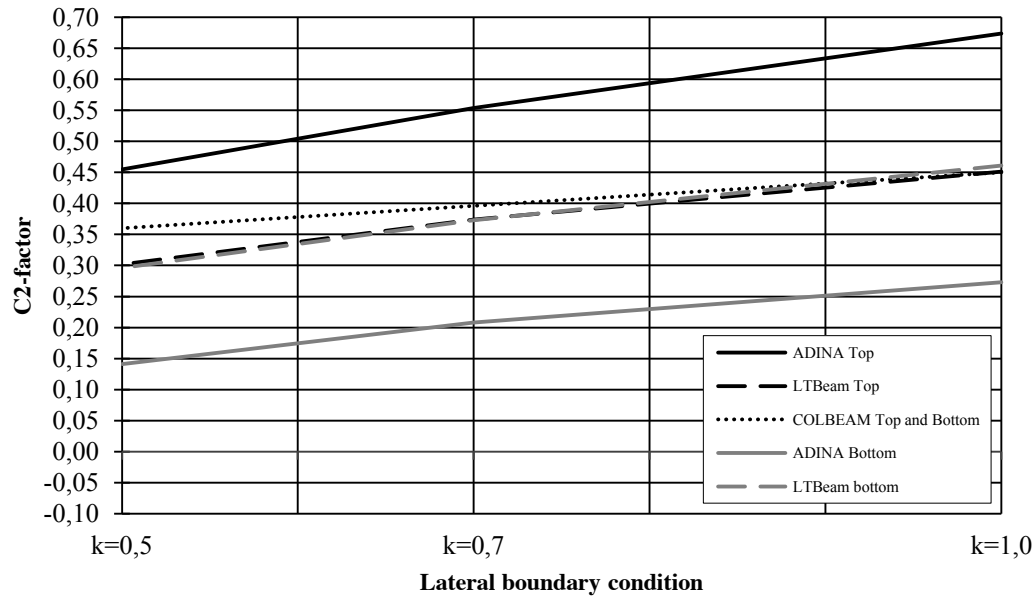


Figure 8.13 Load Case III; The C_2 -factor of software ADINA, COLBEAM, LTBeam and SAP2000 plotted for the lateral boundary conditions of $k=0.5$, $k=0.7$ and $k=1.0$.

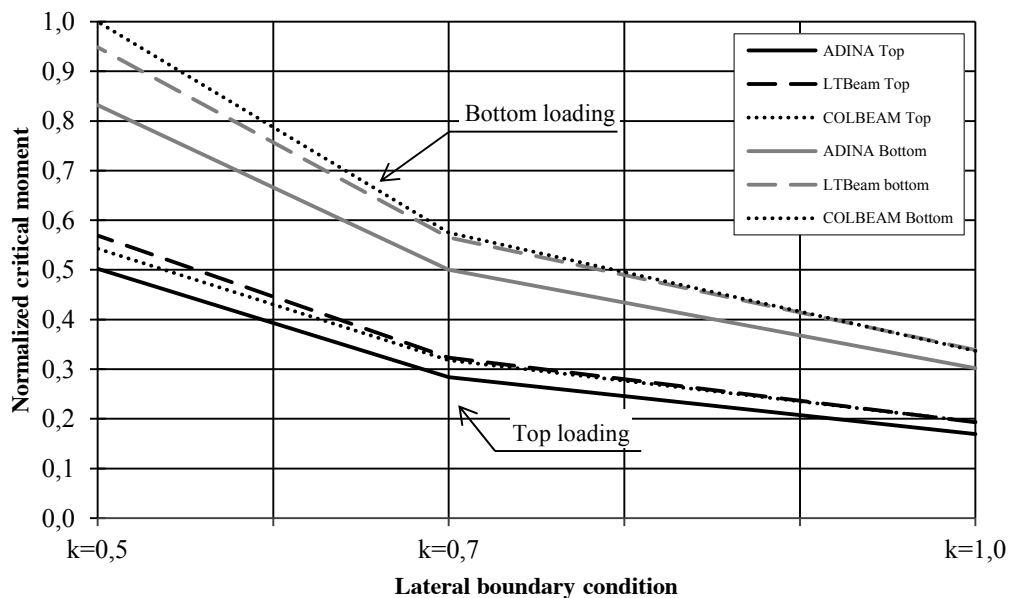


Figure 8.14 Normalized values of the elastic critical moment in Load Case III, plotted for the lateral boundary conditions of $k=0.5$, $k=0.7$ and $k=1.0$. The M_{cr} -values are normalized to bottom loading in COLBEAM.

8.2.4 Load Case IV

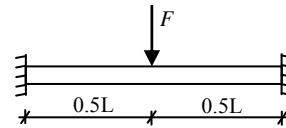


Figure 8.15 presents the C_2 -values of Load Case IV. Figure 8.16 shows the elastic critical moment in a graph normalized after the program giving the highest value on M_{cr} .

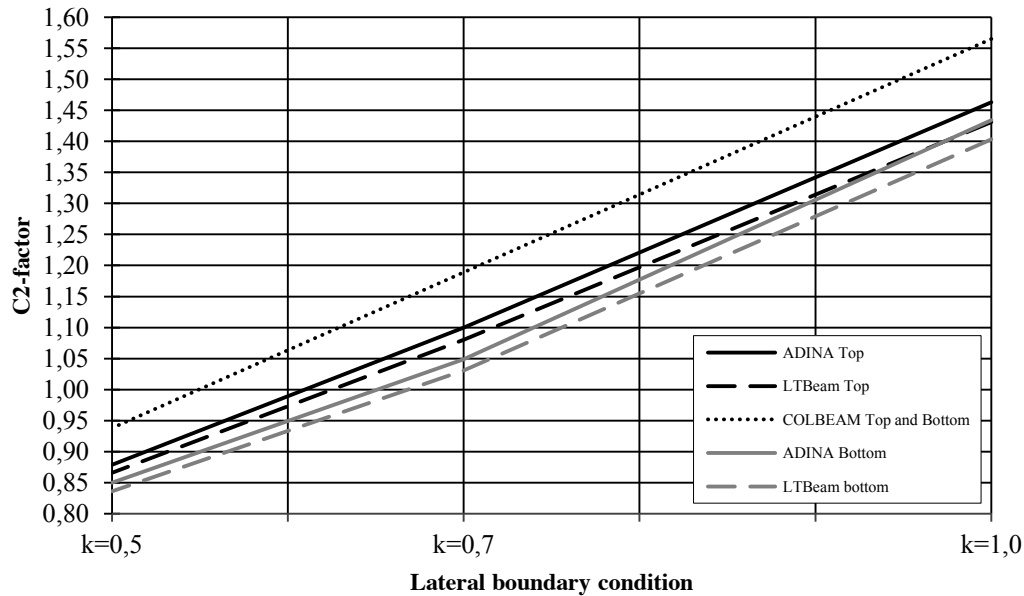


Figure 8.15 Load Case VI; The C_2 -factor of software ADINA, COLBEAM, LTBeam and SAP2000 plotted for the lateral boundary conditions of $k=0.5$, $k=0.7$ and $k=1.0$.

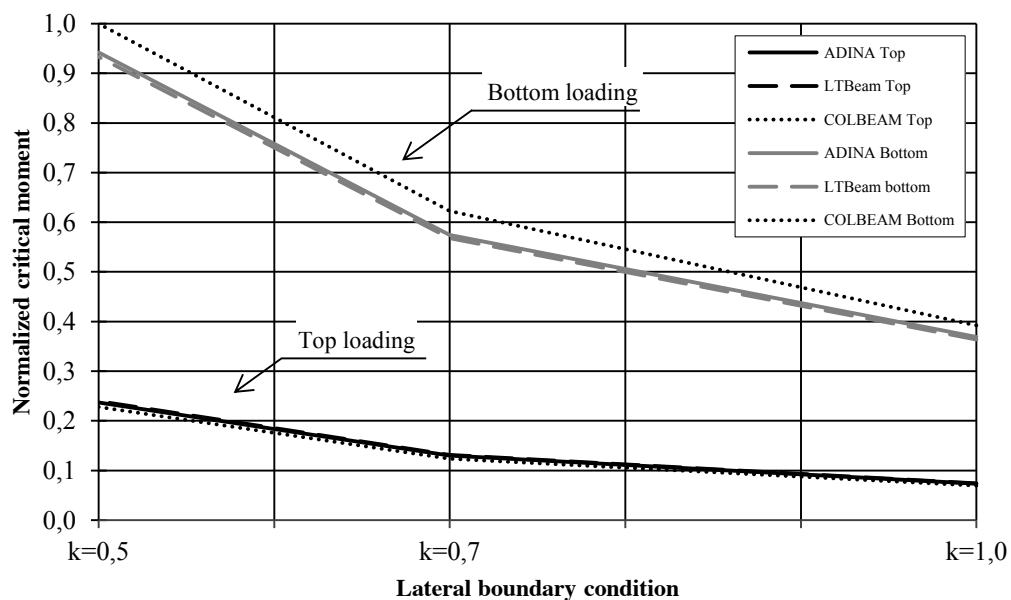


Figure 8.16 Normalized values of the elastic critical moment in Load Case VI, plotted for the lateral boundary conditions of $k=0.5$, $k=0.7$ and $k=1.0$. The M_{cr} -values are normalized to bottom loading in COLBEAM.

8.2.5 Load Case V

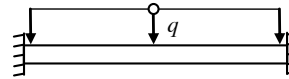


Figure 8.17 presents the C_2 -values of Load Case V. Figure 8.18 shows the elastic critical moment in a graph normalized after the program giving the highest value on M_{cr} .

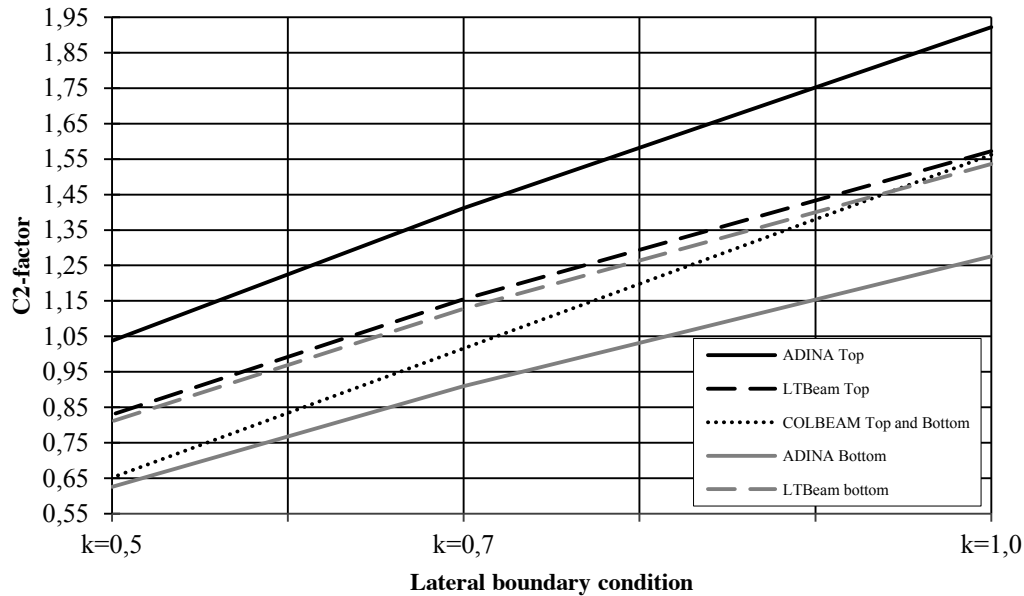


Figure 8.17 Load Case V; The C_2 -factor of software ADINA, COLBEAM, LTBeam and SAP2000 plotted for the lateral boundary conditions of $k=0.5$, $k=0.7$ and $k=1.0$.

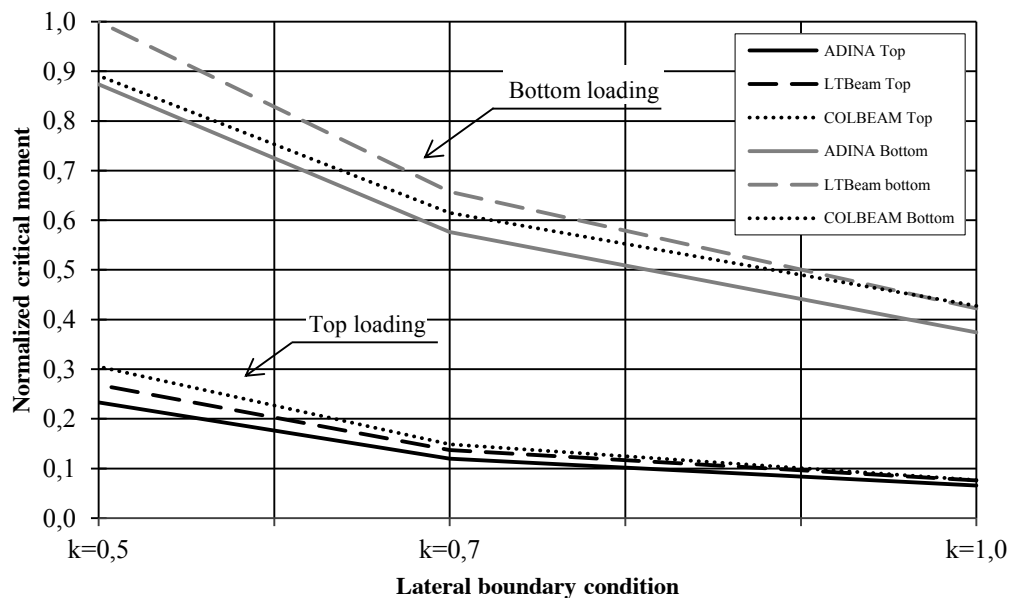


Figure 8.18 Normalized values of the elastic critical moment in Load Case V, plotted for the lateral boundary conditions of $k=0.5$, $k=0.7$ and $k=1.0$. The M_{cr} -values are normalized to bottom loading in LTBeam.

9 Analysis of results

If the figures presented in chapter 8 are studied, some main observations can be pointed out regarding C_I and C_2 . These observations are presented and analysed below in chapter 9.1 and 9.2.

9.1 Observations concerning C_I

9.1.1 The influence of lateral boundary conditions

One main observation that can be seen in the graphs is that the relation between C_I and the lateral boundary conditions, k , differs depending on the programs. The relationship is non-linear in ADINA and LTBeam, linear in COLBEAM and in SAP2000 k does not affect C_I at all.

Generally, SAP2000 gives close and conservative approximations of C_I when the lateral boundary conditions are free, $k=1.0$. When including lateral fixations ($k=0.7$ and $k=0.5$) C_I is unaffected, which yields un-conservative overestimations of C_I . SAP2000 “design module” implements an expression of C_I from the American design code, *AISC LRFD*, see equation (6.4). This expression does not take the effects of lateral boundary conditions into account.

The finite element programs ADINA and LTBeam gives a higher C_I -value for $k=0.7$ compared to the linear interpolated values of COLBEAM. There are no reference values for $k=0.7$, why it is hard to draw sharp conclusions about the accuracy of these values. However, both finite element programs provide close to exact results in the cases with known reference values. They also give almost the same C_I -values for $k=0.7$. Hence it could be argued that the reliability of their results for $k=0.7$ are relatively high. This would mean that COLBEAM makes a conservative approximation when assuming a linear relationship when $k=0.7$.

9.1.1.1 Deviations of SAP2000 results in Load Case IV

In Load Case IV, the C_I -value in SAP2000 is about 84% too high compared to the reference value when $k=0.5$. This is the highest deviation of C_I in SAP2000. In this load case C_I is not only overestimated for $k=0.5$ and $k=0.7$, but also for $k=1.0$ where it is about 12% too high.

The overestimation in this particular load case depends on the implemented expression of C_I (see chapter 4.3). The expression is based solely on the shape of the moment diagram, weighting the moments in three positions along the beam (M_A , M_B , M_C) together with the maximum moment (M_{max}). The weighting has been chosen to give reasonable results in many different situations, but evidently it does not fit this particular load case that well.

By weighting the moments differently, a correct C_I -value could be achieved also in Load Case IV. However, this would be to the cost of less precision in C_I for other load cases.

9.1.2 COLBEAM tables and “Advanced calculation of C_I”

A general conclusion that can be drawn from the parametric study is that the table values in COLBEAM provide better approximations of C_I than the closed-form expression used in the setting “Advanced calculation of C_I”. This could be expected, since the closed-form expression is approximate, while table values are evaluated with greater precision for specific load cases. However, when a load case is not included in the tables, COLBEAM interpolates between known values, and in cases with multiple loads the table value of the dominant load is used. For these more complex load cases the option “Advanced calculation of C_I” could be more suitable to use. Hence, when known table values are available they are to be preferred. For cases where C_I is unknown, the “Advanced calculation of C_I” option can provide a reasonable and in most cases conservative approximations of C_I . All load cases tested in the parametric study are available in COLBEAM tables.

Load Case V is an exception from the argument above. In this load case the table value of COLBEAM is very conservative (less than 50% of the reference value). In this case the option “Advanced calculation of C_I” yields a much more reasonable result. The reason for this is that COLBEAM in cases of beams fixed about major axis uses table values from Table F.1.2 in ENV-1993-1-1:1992 (see Figure 9.1). These table values are valid for maximum span-moments only. Since COLBEAM performs the section analysis for the maximum moment along the whole beam and the maximum moment in Load Case V is located at the support, this table value is not valid.

This can be illuminated further by comparing the ENV-table with a table from Access Steel (2005), see Figure 9.1 and Figure 9.2. The table values from Access Steel (2005) considers the maximum moment along the whole beam and gives $C_I=2.578$ for Load Case V. The corresponding value in the ENV-table is $C_I=1.285$.

The ratio between the support moment and the field moment in Load Case V is 2.0, and as seen below this agrees well with the ratio of the C_I -factors.

$$\frac{C_{I,AccessSteel}}{C_{I,ENV}} = \frac{2.578}{1.285} = 2.006 \quad (9.1)$$

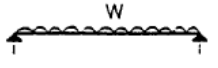

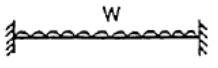
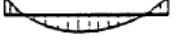
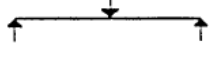

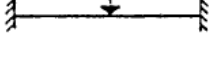

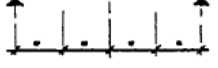
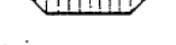
Table F.1.2 Values of factors C_1 , C_2 and C_3 corresponding to values of factor k : Transverse loading cases					
Loading and support conditions	Bending moment diagram	Values of k	Values of factors		
			C_1	C_2	C_3
		1,0 0,5	1,132 0,972	0,459 0,304	0,525 0,980
		1,0 0,5	1,285 0,712	1,562 0,652	0,753 1,070
		1,0 0,5	1,365 1,070	0,553 0,432	1,730 3,050
		1,0 0,5	1,565 0,938	1,267 0,715	2,640 4,800
		1,0 0,5	1,046 1,010	0,430 0,410	1,120 1,890

Figure 9.1 Table F.1.2, ENV-1993-1-1:1992. The C_1 -factor for Load Case V is marked in the table.

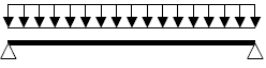





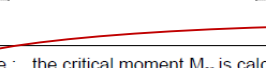
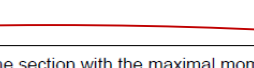
Table 3.2 Values of factors C_1 and C_2 for cases with transverse loading (for $k = 1$)			
Loading and support conditions	Bending moment diagram	C_1	C_2
		1,127	0,454
		2,578	1,554
		1,348	0,630
		1,683	1,645
Note : the critical moment M_{cr} is calculated for the section with the maximal moment along the member			

Figure 9.2 Table from Access Steel (2005). The C_1 -factor for Load Case V is marked in the table.

9.1.3 Accuracy of finite element software

The finite element software ADINA and LTBeam yield close approximations of C_1 in all tested load cases. ADINA tend to give a small un-conservative deviation when $k=1.0$. This deviation is 2.8% in Load Case III. LTBeam has almost no deviation from the reference values; the biggest is about 0.5% in Load Case IV when $k=0.5$.

It can be noted that the deviation from the reference values in ADINA is slightly larger when the ends are fixed about the major axis. This was true for all the tested load cases for $k=0.5$ and $k=1.0$, and coincide with the information in the ADINA (2011) user manual. According to the manual, analysis with warping beam elements sometimes yields in-correct answers, particularly when clamped boundary conditions are used (ADINA 2011).

9.2 Observations concerning C_2

COLBEAM uses the same C_2 -values for both top and bottom loading. In ADINA and LTBeam however, there are differences in the equivalent C_2 -values between top and bottom loading. These differences are small in LTBeam, but bigger in ADINA for load cases with distributed loads (Load Case III and V). The reason is that the modelling of distributed loads with rigid links and warping beam elements in ADINA proved to be difficult. Due to convergence problems, it was not possible to run the analysis until $\lambda \approx 1.0$.

The point of load application has a big impact on M_{cr} . For simply supported beams the elastic critical moment is about twice as high in loading on the bottom flange compared to the top flange. For fixed beams about major axis, M_{cr} is about three times larger for the beams loaded on the bottom flange. Hence, the point of load application has greater influence for beams with fixed ends compared to simply supported beams.

10 Discussion

10.1 Evaluation of elastic critical moments

The mechanisms behind lateral torsional buckling are complex, which makes the evaluation of the elastic critical moment difficult. The *3-factor formula* contains so many variables that the influence of each variable can be hard to grasp. Since the formula is analytical, solutions of M_{cr} are sometimes incorrectly interpreted as exact solutions. Critical moments calculated by the *3-factor formula* can be exact, but this is definitely not certain. One major reason is that no exact closed-form expression of the C_I -factor exists.

In general, structural engineers know that the C_I -factor depends on the moment diagram. It is true that the shape of the moment diagram plays the major role, but the results of the parametric study show that the influence of lateral boundary conditions also are of great importance. This is in line with previous studies and reports concerning the C_I -factor.

Besides lateral boundary conditions, the C -factors also depend on the ratio μ as stated in Access Steel (2005), ECCS (2006), and Fruchtengarten (2006).

$$\mu = \frac{GI_t \cdot L^2}{EI_w} \quad (10.1)$$

Thus, if an exact closed-form expression of C_I was to be constructed, it must include the factors in the ratio μ . An attempt to construct such an expression would lead to a complex and complicated formula.

Today, the best approximate expression of C_I seems to be the equation by Lopez et al. (2006), see equations (4.12) - (4.15). This expression takes both the shape of the moment diagram and the lateral boundary conditions into account. It therefore contains many parameters and can be difficult to handle in hand calculations. On the other hand, closed-form expressions can easily be implemented in the solve-routine of calculation software, such as COLBEAM. In cases where the errors introduced in closed-form expressions are not acceptable, more advanced analyses can be provided by finite element software.

As seen in chapter 5, finite element methods can also be associated with some problematic issues. Linearized buckling analysis is a powerful tool that can provide almost exact solutions when studying lateral torsional buckling. However, it is important to remember that this kind of analysis is approximate and that the accuracy is dependent on the situation and on how the problem is implemented in the software. As shown in chapter 5.1, the base load can affect the solution drastically. In ADINA, the analysis should be run with increasing base load until $\lambda \approx 1$. If the prerequisites for the linearized buckling analysis in a FE-software are unknown, careful validation of the results must be undertaken, for example by more detailed incremental analysis (*LDC*). See chapter 5.2.

10.2 The parametric study

One of the reasons for the initiation of this project was that it had been noticed at Reinertsen Sweden AB that the magnitude of M_{cr} varied depending on which software was used in calculation. To illuminate the reasons for these deviations, a parametric study was conducted with the aim to explain the methods of calculation used in ADINA, COLBEAM, LTBeam and SAP2000. As seen in chapter 9.1.1, these deviations mainly depend on the closed-form expressions and tables that are implemented in the programs.

SAP2000 and COLBEAM uses different analytical expressions for C_I , and in COLBEAM values from tables can also be used. Both programs give strongly deviating results for some of the load cases.

The reason for this is that the expressions and table values are not valid under those conditions. This illuminates the importance of knowing the prerequisites of the chosen method of analysis. As an example, the closed-form expression used to calculate C_I in SAP2000 does not include the effects from lateral restraints. This is the same thing as assuming $k=1.0$. Hence, if the lateral boundary conditions are assumed to be $k=0.7$ and $k=0.5$, SAP2000 will yield un-conservative results.

In some cases it can be reasonable to use coarse approximations and in other cases more accuracy are needed. Accordingly, the assumptions and methods implemented in a program decide if it can be used in a certain situation or not. Unfortunately, it has been noticed that the studied software sometimes lack “easy access” information on how and under what assumptions calculations are made.

ADINA has extensive modelling and theory guides that could serve as role models for other software. However, questions are still raised. In the ADINA theory manual it is clearly written that the large displacement option together with the warping beam element can yield wrong results. Because of this, the element formulation using the large displacement option has been removed in version 8.8, which means that it is not possible to run a linearized buckling analysis with a warping beam element. On the other hand, in an example given in ADINA primer the old element formulation is used without further explanation. In this thesis it was decided to use the old element formulation despite these circumstances, since the results agreed well with the reference values.

COLBEAM has references to the closed-form-expression and table values that are used to calculate C_I , but more information could be added in order to make an assessment of the results easier. The name of the option “Advanced calculation of C1” can be misleading, since the word “advanced” incorrectly could be interpreted as “accurate”, or “precise”. If a table value exists for the situation at hand, it is more accurate to use. Also, as described in chapter 9.1.2, the C_I -value from the ENV-table seems to be wrong for fixed beams with distributed loads. Even without this “error”, it could be reasonable to change the reference since ENV-1993-1-1 is a pre-edition of Eurocode that is no longer used. Finally, it would be convenient with a reference explaining that the table of C -factors used for linear moment distributions comes from ECCS (2006).

The free software LTBeam provide very accurate solutions in the cases studied in this thesis. However, almost no background information could be found on the program. When invoking the program, the developer *CTICM* warns that LTBeam is only intended for those with enough knowledge to assess the accuracy of the results. The

question is how one could assess the accuracy of the results without access to any background information.

In SAP2000, boundary conditions can be applied in different ways as described briefly in chapter 6.4.2. When conducting the parametric study of C_I , the general perception was that different results were obtained when the program calculated C_I directly from the model, compared to when the effective length factor was set manually. This may depend on the authors' limited knowledge on how to apply lateral boundary conditions in the program. From the information given in the program, it can be hard to grasp exactly how the lateral boundary conditions should be applied, especially concerning the effective length factor. Moreover, the SAP2000 Eurocode manual refers to an expression of C_I that is not actually used, as shown in chapter 6.4.1. Because of the limited knowledge on how the "design module" calculates M_{cr} and the questions concerning the manual of the program, the results from the parametric study concerning SAP2000 have less substance compared to the other programs.

A general conclusion from the C_2 -study is that the point of load application has a great influence on M_{cr} for all tested load cases, and omitting these effects will yield large errors in the estimation of M_{cr} . Hence, an assumption that the load acts in the shear centre will yield wrong results on M_{cr} when the load acts on one of the flanges. Especially for beams with fixed ends about major axis.

10.2.1 Validity and reliability of the results

The study of C_I is based on reference values for $k=1.0$ and $k=0.5$ from Serna et al. (2005). These values are given high reliability and were also used to construct the closed-form expression by Lopez et al. (2006). For $k=0.7$ no reference values are known and the accuracy of the results for this case is therefore harder to assess. As discussed in chapter 9.1.1, the finite element programs gave results so close to the reference values for $k=1.0$ and $k=0.5$ that they could be considered reliable also for $k=0.7$. The C_2 -study has no reference values, but shows the effect of the point of load application. It should be seen as a comparison between the programs rather than an evaluation of the actual accuracy.

Considering that the μ -ratio has a relatively low impact on the C_I -factor as explained in chapter 4.2.2.3, it is expected that the C_I -results are valid for other I-sections than IPE500. They should also be valid for other beam lengths, especially for beams with high values of μ .

The parametric study covers several common load cases. However, combined loading is not investigated and only three idealised lateral boundary conditions are considered. The tested load cases and lateral boundary conditions were chosen so that they could be treated by all the programs. COLBEAM and SAP2000 use one combined effective length factor, k . The individual effects of k_z and k_w could therefore not be investigated in the study.

It is hard to draw conclusions on how well the different methods will approximate C_I and M_{cr} in other load cases than the tested. However, since the studied cases describe basic ideal situations often used as examples in literature, it could be argued that the accuracy would be poorer in other situations.

The parametric study presented deviations in M_{cr} . It is important to point out that an error in the critical moment does not cause the same error in the member capacity. The buckling factor, χ_{LT} , is dependent on the slenderness and determines how much the capacity is reduced. As seen in equation (10.2), an error in M_{cr} is reduced by the square root when calculating the slenderness parameter.

$$\bar{\lambda}_{LT} = \sqrt{\frac{W_y \cdot f_y}{M_{cr}}} \quad (10.2)$$

Since the buckling factor is calculated from the slenderness parameter through buckling curves, the accuracy of the buckling curves is also important. This thesis does not cover the buckling curves or their accuracy. However, Höglund (2006, p. 75) mentions that a division into five different curves could be regarded as too fine. The argument for this is the high divergences of the test results on which the buckling curves are based on. Accordingly, the importance of an error in M_{cr} must be put into a bigger context, where many factors affect the accuracy of the capacity.

11 Concluding remarks

The major conclusion drawn in this thesis is that all investigated programs give more or less reasonable results when no lateral restraints are present. For cases with lateral restraints, it is crucial that the designer is well aware of the limitations of the used method. One reason for this is that some common closed-form expressions for C_I , e.g. the expression by Kirby & Nethercot, do not take lateral restraints into account.

The finite element programs ADINA and LTBeam have proven to give results with high accuracy. However, this is not achieved without careful modelling. As an example, the base load affects the buckling analysis in ADINA, which can lead to wrong results if not considered.

It has been pointed out that COLBEAM uses C_I -values from an ENV-table in cases of fixed beams. The value for distributed loads in this table is only valid when the section analysis is made in the mid-span. Since COLBEAM performs the section analysis along the whole beam, this table value will yield very conservative results. This will be checked and if necessary updated by COLBEAM.

The point of load application has a great impact on M_{cr} , especially when the beam is fixed about the major axis. To simplify calculations and modelling, it is sometimes assumed that the load acts in the shear centre instead of on the flanges. This assumption can lead to large errors in the estimation of M_{cr} that are un-conservative if the load in reality acts above the shear centre.

11.1 Further studies

Before the start of this project, the idea was to compare the different programs by establishing a finite element model that could be used as reference. The project would also include a part where lateral boundary conditions of real beam connections were modelled and evaluated. However, since the implementation of different analytical expressions was one of the key reasons for deviations in the critical moment, a lot of focus in this thesis had to be given to the theory behind the *3-factor formula*. Therefore, because of the time limit, the study of real beam connections was left out. Hence, a continuation of the thesis could be to investigate this with a finite element model. The modelling could preferably be done with shell elements and detailed incremental analysis, *LDC*. An example of a research question could be

- When can warping be assumed prevented in beam connections?

Another angle for continuation could be to focus on the design procedures with regard to lateral torsional buckling. Since the error in M_{cr} is not the same as an error in the capacity, the magnitude of errors introduced by buckling curves could be investigated.

12 References

- Access Steel (2005): *NCCI: Elastic critical moment for lateral torsional buckling*. Access Steel, 2005.
- Access Steel (2013): *Content, Contributors*. (Electronic) Available: <http://www.access-steel.com> (Accessed: 2013-03-27).
- ADINA (2011): *Theory and Modelling Guide - Volume I: ADINA Solids & Structures*. ADINA R & D, Inc. 71 Elton Avenue Watertown, MA 02472 USA, December 2011.
- AISC LRFD (1999): *Load and Resistance Factor Design Specification for Structural Steel Buildings*. AMERICAN INSTITUTE OF STEEL CONSTRUCTION, INC. One East Wacker Drive, Suite 3100, Chicago, Illinois 60601-2001, 1999-12-27.
- AISC (2005): *Specification for Structural Steel Buildings*. AMERICAN INSTITUTE OF STEEL CONSTRUCTION, INC. One East Wacker Drive, Suite 700, Chicago, Illinois 60601-1802, 2005-03-09, Commentary, CHAPTER F, DESIGN OF MEMBERS FOR FLEXURE.
- Andrade A.¹, Camotim D.², Providência e Costa P.¹ (2006): *On the evaluation of elastic critical moments in doubly and singly symmetric I-section cantilevers*. Journal of Constructional Steel Research, No. 63, ¹University of Coimbra, Coimbra, Portugal, ²Technical University of Lisbon, Lisbon, Portugal, 2006, pp. 894-908.
- ArcelorMittal (2013): *Steel sections and merchant bars*. (Electronic) Available: http://www.constructalia.com/repository/Products/BeamsSections/SectionRangeFR_EN_DE/IPE.pdf (Accessed: 2013-03-30).
- Atsuta T. & Chen W.F. (2008): *Theory of Beam-Columns - Volume 2 Space Behaviour and Design*. J. Ross Publishing, Fort Lauderdale, Florida, USA, 2008, (ISBN-10: 1-932159-77-0, ISBN-13: 978-1-932159-77-6).
- Barretta R. (2012): *On the relative position of twist and shear centres in the orthotropic and fiberwise homogeneous SAINT-VENANT beam theory*. Department of Structural Engineering, University of Naples Federico II, via Claudio 21, 80125 Naples, Italy, June 2012.
- Biggam J. (2008): *Succeeding With Your Master's Dissertation: A Step-by-step Handbook*. Open University Press, 2008-05-01, chapter 7, (ISBN 978-0335227204).
- Camotim D., Correia J.R., Silva N.M.F., Silvestre N. (2011): *First-order, buckling and post-buckling behaviour of GFRP pulltruded beams. Part 1: Experimental study*. Computers & Structures, Vol. 89, Issues 21-22, November 2011, pp. 2052-2064.
- CSI (2011): *Eurocode 3-2005 with Eurocode 8:2004 Steel Frame Design Manual for SAP2000*. CSI Computers & Structures INC, Version 15, Berkeley, Carleifornia, USA, August, 2011.
- Earls C.J. (2007): *Observations on eigenvalue buckling analysis within a finite element context*. Proceedings of the Structural Stability Research Council, Annual Stability Conference, New Orleans, Louisiana, USA, 2007.

- ECCS (2006): *Rules for Member Stability in EN 1993-1-1, Background documentation and design guidelines*. ECCS, Mem Martins, Portugal, 2006, (ISBN 92-9147-000-84).
- ECCS (2013): *About ECCS*. (Electronic) Available: <http://www.steelconstruct.com> (Accessed: 2013-03-27).
- Ecsedi I. (2000): *A FORMULATION OF THE CENTRE OF TWIST AND SHEAR FOR NONHOMOGENEOUS BEAM*. International Journal of Solids and Structures. Vol 27, No 4, pp. 407-411, March 2000.
- EN-1993-1-1:2005 (2005): *Eurocode 3: Design of steel structures – Part 1-1: General rules and rules for buildings*. CEN, Management Centre; rue de Stassart 36, B-1050 Brussels, Belgium, 2005.
- Fruchtengarten J. & Fruchtengarten J. (2006): *About lateral torsional buckling of steel beams – geometrically exact nonlinear theory results*. Latin American Journal of Solids and Structures, No. 3, North America, 2006, pp. 89-105. Available: <http://www.lajss.org/index.php/LAJSS/article/view/92> (Accessed: 2013-04-16).
- Höglund T. (2006): *Att konstruera med stål, Modul 6 – Stabilitet för balkar och stänger*, Luleå Tekniska Universitet, Kungliga Tekniska Högskolan & Stålbyggnadsinstitutet, Sweden, 2006.
- Kirby P.A. & Nethercot D.A. (1979): *Design for Structural Stability*. John Wiley & Sons Australia, Limited, 1979. (ISBN 13: 9780470266915)
- Kurniawan C.W., Mahendran M. (2011): *Elastic Lateral Buckling of Cantilever LiteSteel Beams Under Transverse Loading*. International Journal of Steel Structures, Vol 11, No 4, December 2011. (DOI 10.1007/s13296-011-4001-z)
- Lopéz A., Yong D.J., Serna M.A. (2006): *LATERAL-TORSIONAL BUCKLING OF STEEL BEAMS: A GENERAL EXPRESSION FOR THE MOMENT GRADIENT FACTOR*. Proceeding of the International Colloquium of Stability and Ductility of Steel Structures, D. Camotin et al. (Eds), Lisbon, Portugal, September 6-8, 2006.
- Lundh H. (2007): *Hållfasthetslära - Grundläggande hållfasthetslära*. Instant Book AB, Stockholm, 2007.
- Serna M.A., Lopéz A., Puente I., Yong D.J. (2005): *Equivalent uniform moment factors for lateral-torsional buckling of steel members*. Journal of Constructional Steel Research, No. 62, University of Navarra, San Sebastian, Spain, 2005, pp. 566-580.
- Treiberg T. (1987): *Balk-balkinfästning*. SBI, Stålbyggnadsinstitutet. Publikation 106, Stockholm, Sweden, September, 1987.
- Treiberg T. (1988): *Balk-pelarinfästning*. SBI, Stålbyggnadsinstitutet. Publikation 103, Stockholm, Sweden, January, 1988.
- Yoo C.H. & Lee S.C. (2011): *Stability of Structures, 1st Editions - Principles and Applications*. Butterworth-Heinemann, Boston, USA, 2011, chapter 7, (ISBN 978-0-12-385122-2).

Appendices

- Appendix A** **Boundary conditions for common beam connections**
- Appendix B** **Serna et al. (2005) and table values from Access steel (2005) and ECCS (2006)**
- Appendix C** **Derivation of the elastic critical moment**
- Appendix D** **Examples of .in-files used for the parametric study in ADINA**
- Appendix E** **Results from the parametric study**

Appendix A

In this appendix, the choices of boundary conditions for common beam connections are discussed.

A1 Boundary conditions for common beam connections

In general, the boundary conditions of a beam can be described by a spring for each degree of freedom. The stiffness's of the springs depends on the stiffness of the connection itself but also on the stiffness's and the lengths of the acting structural members. Thus, even if a certain beam-column connection is very stiff, the beam is close to simply supported if the beam is much stiffer than the column (see Figure 1). The same reasoning holds for lateral boundary conditions.

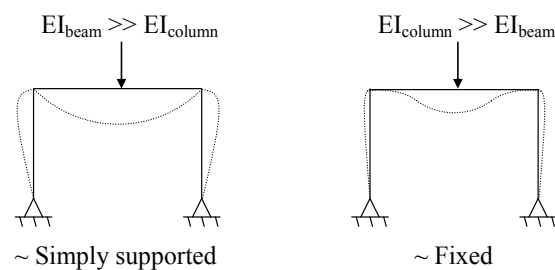


Figure 1 Deformation of frames with rigid connections but different member stiffness's. The beam in the left frame is close to simply supported while the beam in the right frame is close to fixed.

The complexity of the boundary response makes the choice of a suitable boundary model a challenging task. In order to determine the correct degree of fixation, the whole structural system with connections must be modelled and analysed. Since this can be both time consuming and demanding, structural engineers often simplify the boundary to either ideally free or ideally fixed (See Figure 2).

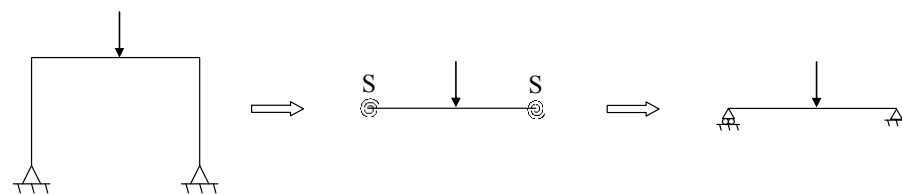


Figure 2 Example of how the major axis boundary of a beam in a frame is simplified in two steps, first to springs, and then to ideally free (simply supported).

If only ideal conditions are considered, the problem is reduced to determining if a certain connection under given conditions can be regarded as free or fixed. A fixed boundary condition is favourable in preventing lateral torsional buckling. Thus, a boundary must be assumed free if fixation cannot be properly justified.

When studying lateral torsional buckling of beams on two supports, 3 degrees of freedom are of interest (see chapter 2.1.3 in the thesis).

- (1) Rotation about the y-axis (major axis bending)
- (2) Rotation about the z-axis (minor axis bending, k_z)
- (3) Warping (k_w)

k_z and k_w are of particular interest since they occur explicitly in the *3-factor formula*.

Below follows a discussion on how these degrees of freedoms are affected in some common beam-beam and beam-column connections. Remember however that the connection itself does not determine the total boundary response, and hence, a rigid connection does not automatically implicate a rigid response.

A1.1 General comments

- Warping can be assumed prevented if the beam end is sufficiently stiffened by the connecting structure, by rigid end plates etc.
- Open steel-sections have low torsional stiffness that seldom can provide fixation. This implicates that major axis bending of beam-beam connections and minor axis bending of beam-column connections often can be assumed free (see Figure 3 and Figure 4) (Treiberg 1987).

A1.2 Beam-beam connections

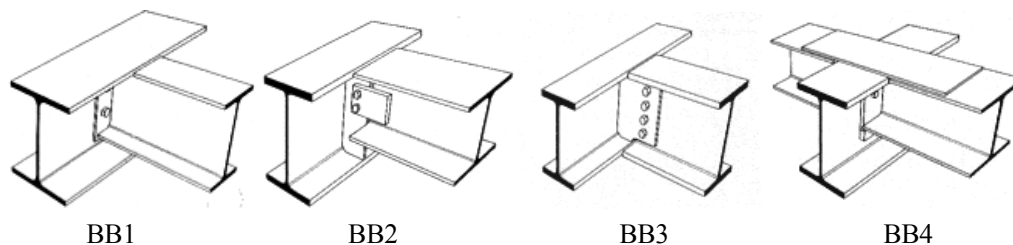


Figure 3 Four common beam-beam connections. BB1-BB3 are considered simply supported. BB4 is an example of how a connection can be made continuous (Adapted from Treiberg 1987).

Beam-beam connections are used in systems of crossing beams. The secondary beam should, if possible, be placed above the main girder since this makes the connection simple. BB1-BB4 are however examples where the secondary beam is connected within the height of the main girder. For connections where the secondary beam is placed above the main girder, see publications by the Swedish Institute of Steel Construction, *SBI* (Treiberg 1987).

BB1-BB3

Single-sided beam-beam connections (BB1-BB3) are generally considered free in major axis bending since the main girder rarely has torsional stiffness enough to provide fixation (ibid.). BB1-BB3 do not have rigid end plates that can prevent warping and are not rigid enough to withstand minor axis bending.

BB4

BB4 can transfer moment about the major axis with help of the splice plate welded to the beams top-flanges. If the welds are strong enough, the splice plates can be design to give the connection a desired moment capacity. Horizontal bracing is achieved by welds between the splice plate and the flange of the main girder (ibid). The bottom flanges of the secondary beams are not fixed to the main girder. The resistance to lateral bending is therefore limited and a conservative assumption of a free minor axis boundary may be reasonable.

For details on the design of the connections, see Treiberg (1987).

Table 1 Rigidity of common beam-beam connections.

Boundary conditions	<i>BB1-BB3</i>	<i>BB4</i>
Major axis bending	Free	Fixed
Minor axis bending (k_z)	Free	Free
Warping (k_w)	Free	Free/Fixed ¹

¹Dependent on the rigidity of the connecting structure and the end plates

A1.3 Beam-column connections

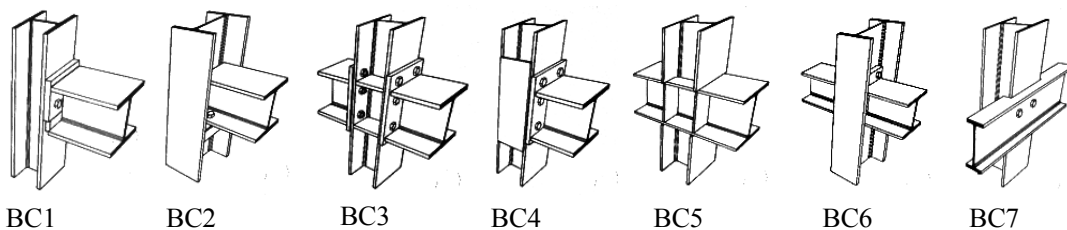


Figure 4 Seven common beam-column connections (adapted from Treiberg 1988).

The beam-column connections presented in this section have columns that continue above the beam. Other types of beam-column connections can be found in publications of the Swedish Institute of Steel Construction, SBI (Treiberg 1988).

Beam-column connections can be divided into moment free, rigid and continuous. BC1 & BC2 are examples of moment free connections, BC3 & BC4 are rigid and BC5-BC7 are continuous (ibid.).

Generally, moment free beam connections are simpler to design and easier to assemble, which makes them cheaper compared to rigid and continuous connections. Rigid and continuous connections allow smaller beams and/or longer spans, but often the reduced material cost does not make up for the more expensive design. Longer spans can however have other economic benefits that justify the use of these connections. Rigid and continuous connections can also be used to stabilize low buildings (ibid.).

The difference in structural behaviour between rigid and continuous connections is that continuous connections do not transfer moments to the column (ibid.).

BC1

BC1 is a connection between an I-section beam and a column. The connection is moment free in both major and minor axis bending. During assembly the beam rests on a console welded to the column. The end plate of the beam is attached to the flange of the column (ibid.).

BC2

BC2 is a connection between a beam and a column with I-sections. The connection is moment free in both major and minor axis bending. The beam is resting on a console welded to the column and attached with two bolts. If the beam is placed close to the web of the column, the moment due to the eccentricity of the support force will be small. On the other hand, the capacity of the beam will be smaller if the support is close to the end section of the beam (ibid.). Since only the bottom flange is prevented, it is reasonable to assume free warping and free bending about minor axis.

BC3 & BC4

BC3 & BC4 are bolted, rigid connections that can transfer moment because of the stiffeners of the column. The difference between the connections is that the stiffeners of the column are placed between the flanges in *BC3* and on the outside of the flanges in *BC4* (see Figure 4) (ibid.). Both major and minor axis bending plus warping may be assumed prevented in these connections. *BC3* can also be made single-sided.

BC5

BC5 is a continuous connection often used in multi-storey buildings when erection of short columns (floor-by-floor) is preferred. The beam is placed on top of the column and fillet welded in the column circumference. The load from the column is transferred through the transversal stiffeners in the beam (ibid.).

BC6

BC6 is a double-sided connection of two separate beams. The beams are attached by bolts through beam endplates on both sides of the column web. The connection can be considered continuous if the connecting bolts have enough capacity and pierce through the endplates of both beams. Whether minor axis bending is free or not depends on the detailing of the bolts. If the bolts are placed in one aligned vertical column, the resistance to lateral bending is small and should be assumed free.

BC7

BC7 is a continuous connection where the web of the beam is attached with bolts to the flange of the column. The support reaction from the beam can be transferred to the column by the bolts or by a welded console on the column (ibid). The beam is fixed to the column with regard to minor axis bending by the bolts. Since the flanges are not attached to the column, the connection does not prevent warping.

For details on the design of the connections, see Treiberg (1988).

Table 2 *Rigidity of common beam-column connections.*

Boundary conditions	BC1	BC2	BC3 & BC4	BC5	BC6	BC7
Major axis bending	Free	Free	Fixed	Fixed	Fixed	Fixed
Minor axis bending (k_z)	Free	Free	Fixed	Fixed	Free	Fixed
Warping (k_w)	Free/Fixed ¹	Free	Free/Fixed ¹	Fixed	Free/Fixed ¹	Free

¹Dependent on the rigidity of the connecting structure and the end plates

Appendix B

In this appendix, the research by Serna et al. (2005) is briefly presented. This research has been used as reference in the parametric study of C_I in chapter 7 of the thesis. In B2, C_I -values from the handbooks Access Steel (2005) and ECCS (2006) are compared to reference values of Serna et al. (2005).

B1 Serna et al (2005)

In the paper “*Equivalent uniform moment factors for lateral torsional buckling of steel members*” by Serna et al. (2005), a new closed-form expression for the uniform moment factor, C_I , is presented. Not only moment distribution is taken into account by this expression, but also the lateral boundary conditions. It was derived with curve-fitting techniques based on C_I -values from finite difference analysis. These values are also presented in the paper. Later, the expression was refined by Lopez et al. (2006).

The analysis was conducted for rolled IPE500 and HEB500 section beams, with 8 meter and 16 meter spans. 4 combinations of lateral boundary conditions were considered: lateral bending free ($k_z=1.0$) or prevented ($k_z=0.5$) and warping free ($k_w=1.0$) or prevented ($k_w=0.5$).

B1.1 Conclusions made in the paper

Results from earlier studies showing that C_I varies with the length of the beam were confirmed through finite element analysis. It was also concluded that C_I is coupled to the lateral boundary conditions.

Through finite difference analysis it could be seen that

- Design codes give a poor approximation of C_I , either conservative or non-conservative, when warping and lateral bending is prevented.
- Prevention of lateral bending leads generally to lower C_I -values.
- Prevention of warping significantly increases C_I .

In design codes where C_I is based on the moment distribution only, the approximation of C_I is poor when lateral bending and warping is prevented. In these cases the proposed expression of Serna et al. (2005) gives better approximations.

B1.2 Reference values

The finite difference results used for the derivation of the proposed closed-form expression by Serna et al. (2005) are used as reference values in the parametric study of C_I in chapter 7 of the thesis.

B2 Table values from Access Steel (2005) and ECCS (2006)

In the tables below, table values of C_I from Access Steel (2005) and ECCS (2006) are compared with reference values from Serna et al. (2005).

Table 1 End moments.

End moments	ECCS (2006), IPE 500, 8m	ECCS (2006), IPE 500, 16m	Access Steel (2005)	Reference values
k	C_I	C_I	C_I	C_I
1.0	1.0	1.0	1.0	1.0
0.5	1.050	1.0	-	1.0

Table 2 Simply supported about major axis.

Concentrated load	ECCS (2006)	Access Steel (2005)	Reference values, IPE 500, 8m
k	C_I	C_I	C_I
1.0	1.35	1.348	1.359
0.5	1.05	-	1.061
Distributed load	ECCS (2006)	Access Steel (2005)	Reference values, IPE 500, 8m
k	C_I	C_I	C_I
1.0	1.12	1.127	1.131
0.5	0.97	-	0.967

Table 3 *Fixed about major axis.*

Concentrated load	ECCS (2006)	Access Steel (2005)	Reference values, IPE 500, 8m
k	C_1	C_1	C_1
1.0	-	1.683	1.713
0.5	-	-	1.044
Distributed load	ECCS (2006)	Access Steel (2005)	Reference values, IPE 500, 8m
k	C_1	C_1	C_1
1.0	-	2.578	2.605
0.5	-	-	1.733

Appendix C

In this appendix, an expression for the elastic critical moment is derived for the reference case, $M_{cr,0}$, with methods of potential energy.

$$M_{cr,0} = \frac{\pi^2 \cdot EI_z}{L^2} \sqrt{\frac{I_w}{I_z} + \frac{L^2 \cdot GI_t}{\pi^2 \cdot EI_z}} \quad (1)$$

The reference case is defined as a double-symmetric I-beam on two fork-supports subjected to end moment loading.

The derivation follows the procedures outlined by Höglund (2006, pp. 42-58). For more information about methods of potential energy, see chapter 4.1 in the thesis.

C1 Derivation of the elastic critical moment

C1.1 Definition of deformations

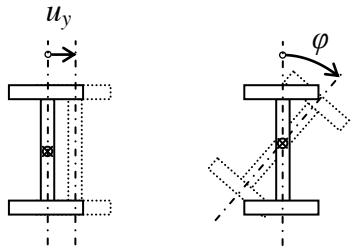


Figure 1 Definition of deformations in lateral torsional buckling.

C1.2 Identification of internal potential energy, H_i

C1.2.1 Bending about minor axis

The internal potential energy of a small beam element with area dA and length dx subjected to bending about the minor axis can be visualized as the area under the stress-strain curve.

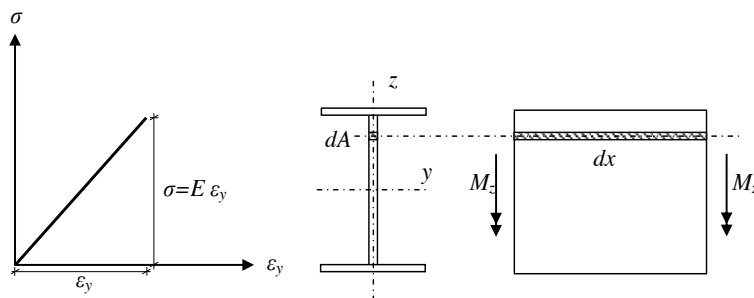


Figure 2 The area under the stress-strain curve represents the potential internal energy of a small beam element subjected to bending.

$$dH_{i,b} = \frac{1}{2} dA \cdot E \cdot \varepsilon_y \cdot \varepsilon_y dx \quad (2)$$

If

$$\varepsilon_y = \frac{\sigma_x}{E} = -\frac{1}{E} \frac{M_z}{I_z} y \quad (3)$$

The potential energy can be written as

$$dH_{i,b} = \frac{dx}{2} \cdot \frac{M_z^2}{2E(I_z)^2} \int_0^A y^2 dA = \frac{1}{2} \frac{M_z^2}{EI_z} dx \quad (4)$$

Integration along the beam yields

$$H_{i,b} = \int_0^L \frac{M_z^2}{2 \cdot EI_z} dx \quad (5)$$

Express the potential energy in terms of the lateral translation u_y instead of an applied moment. The equation of the elastic line for beams yields

$$u_y'' = -\frac{M_z}{EI_z} dx \quad (6)$$

Equation (5) and (6) yields

$$H_{i,b} = \int_0^L \frac{EI_z (u_y'')^2}{2} dx \quad (7)$$

Equation (7) describes the internal potential energy stored in a beam when subjected to bending about the minor axis

C1.2.2 Torsion

The internal potential energy of a small beam element subjected to torsion is equal to the work done by the torque T over the element length dx . Since the twisting angle increases with $d\varphi$ over dx , the work can be written as the torque times the mean twisting angle, $d\varphi/2$.

$$dH_{i,t} = \frac{1}{2} T \cdot d\varphi = \frac{1}{2} T \cdot \varphi' \cdot dx \quad (8)$$

A twisting moment that acts on a double-symmetric I-section is resisted by both Saint Venant shear stresses (as for a circular-symmetric section) and warping effects.

$$T = T_{\text{Saint Venant}} + T_{\text{warping}} \quad (9)$$

In cases of circular-symmetric sections

$$T = T_{Saint Venant} \quad (10)$$

Saint Venant torsion

The change in twisting angle over a small element subjected to a torque T is dependent on the torsional stiffness GI_t . The equation for Saint Venant torsion can be written

$$T_{Saint Venant} = GI_t \frac{d\varphi}{dx} = GI_t \varphi' \quad (11)$$

For Saint Venant torsion the torsional shear stresses is only dependent on the angle φ .

Warping

When a double-symmetric I-section rotates, shear forces will arise due to lateral deflection of the flanges (see chapter 2.1.10 in the thesis). These warping effects can be accounted for by calculating the resulting moment from the shear forces in the flanges.

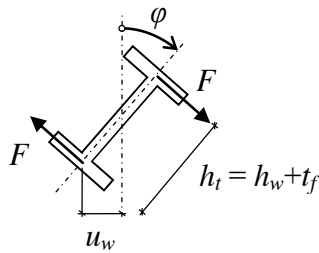


Figure 3 Shear forces induced by lateral bending of the flanges (warping).

The lateral deflection of one of the flanges due to warping, u_w , can approximately be expressed in terms of the rotation, φ . See Figure 3.

$$u_w = \frac{h_t}{2} \varphi \quad (12)$$

This lateral deflection creates a bending moment M and a shear force F in the flange. The equation of the elastic line for beams yields

$$M = -EI_{z,flange} \cdot u_w'' = -EI_{flange} \cdot \frac{h_t}{2} \varphi'' \quad (13)$$

$$F = \frac{dM}{dx} = -EI_{z,flange} \cdot \frac{h_t}{2} \varphi''' \quad (14)$$

- The contribution from the web to the second moment of inertia is very small and can be omitted in calculations.
- Since double-symmetric sections are considered the second moment of inertia is equal for both flanges.

Thus

$$I_z = 2 \cdot I_{z,flange} \quad (15)$$

This yields

$$F = -E \frac{I_z}{2} \cdot \frac{h_t}{2} \varphi''' \quad (16)$$

The two shear forces F creates the torque $T_{warping}$, see Figure 3.

$$T_{warping} = F \cdot h_t = -E \frac{I_z}{2} \cdot \frac{h_t}{2} \varphi''' \cdot h_t = -\frac{EI_z \cdot h_t^2}{4} \varphi''' \quad (17)$$

$$T_{warping} = -\frac{EI_z (h_w + t_f)^2}{4} \varphi''' \quad (18)$$

Introduce the warping constant I_w

$$I_w = \frac{I_z (h_w + t_f)^2}{4} \quad (19)$$

$$T_{warping} = -EI_w \cdot \varphi''' \quad (20)$$

With the expressions of $T_{Saint Venant}$ and $T_{warping}$ known, the total twisting moment can be written as

$$T = T_{Saint Venant} + T_{warping} = GI_t \cdot \varphi' - EI_w \cdot \varphi''' \quad (21)$$

Combining equation (21) and (8)

$$dH_{i,t} = \frac{1}{2} (GI_t \cdot \varphi' - EI_w \cdot \varphi''') \cdot \varphi' \cdot dx \quad (22)$$

Integration along the beam length

$$H_{i,t} = \int_0^L \frac{GI_t (\varphi')^2}{2} dx - \int_0^L \frac{EI_w \cdot \varphi''' \cdot \varphi'}{2} dx \quad (23)$$

Integration by parts of the second term

$$\int_0^L \frac{EI_w \cdot \varphi''' \cdot \varphi'}{2} dx = \frac{1}{2} [EI_w \cdot \varphi'' \cdot \varphi']_0^L - \int_0^L \frac{EI_w (\varphi'')^2}{2} dx \quad (24)$$

φ'' in the boundary term represents the warping degree of freedom. If $\varphi'' = 0$, no resistance to lateral deflection of the flanges exist, e.g. warping is free. See equation (13). Since warping is free for fork supports ($\varphi'' = 0$), the boundary term vanishes.

The internal potential energy for torsion and warping can now be written

$$H_{i,t} = \int_0^L \frac{GI_t (\varphi')^2}{2} dx + \int_0^L \frac{EI_w (\varphi'')^2}{2} dx \quad (25)$$

C1.3 Identification of external potential energy, H_e

When the beam twists during buckling a component $M_y \cdot \varphi$ of the bending moment is created about the weak z -axis.

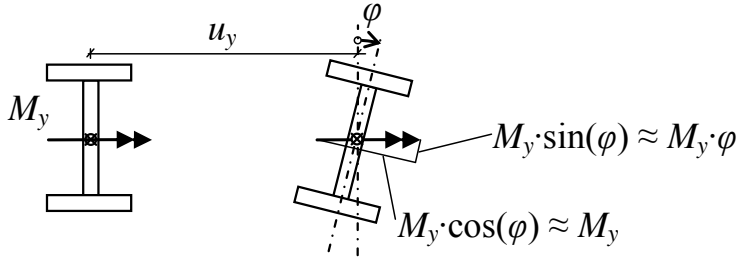


Figure 4 A component from the bending moment is created about the weak z -axis when the beam twists.

With the same reasoning as for the change in internal potential energy during bending, the change in external potential energy because of this additional moment about the weak axis can, be written

$$H_{e,M_y} = \int_0^L M_y \cdot \varphi \cdot u_y'' dx \quad (26)$$

C1.4 Total potential energy

With the internal and external potential energies known, an expression for the total potential energy can be established

$$H = H_i + H_e = H_{i,b} + H_{i,t} + H_{e,M_y} \quad (27)$$

$$H = \int_0^L \frac{EI_z (u_y'')^2}{2} dx + \int_0^L \frac{GI_t (\varphi')^2}{2} dx + \int_0^L \frac{EI_w (\varphi'')^2}{2} dx + \int_0^L M_y \cdot \varphi \cdot u_y'' dx \quad (28)$$

C1.5 Conditions for instability

The task is to find deflected shapes of u_y and φ so that the potential of the system has a minimum value.

Define a function W

$$W(u_y'', \varphi, \varphi', \varphi'') = \frac{EI_z (u_y'')^2}{2} + \frac{GI_t (\varphi')^2}{2} + \frac{EI_w (\varphi'')^2}{2} + M_y \cdot \varphi \cdot u_y'' \quad (29)$$

An equation for the minimum of the potential energy H can be written symbolically

$$H = \int_0^L W(u_y'', \varphi, \varphi', \varphi'') dx = \min \quad (30)$$

C1.6 Solution

The condition in equation (30) can be solved from Euler's equations

$$\frac{\partial W}{\partial u_y} - \frac{d}{dx} \left(\frac{\partial W}{\partial u_y'} \right) + \frac{d^2}{dx^2} \left(\frac{\partial W}{\partial u_y''} \right) = 0 \quad (31)$$

$$\frac{\partial W}{\partial \varphi} - \frac{d}{dx} \left(\frac{\partial W}{\partial \varphi'} \right) + \frac{d^2}{dx^2} \left(\frac{\partial W}{\partial \varphi''} \right) = 0 \quad (32)$$

The derivatives of W with respect to u_y and φ in equation (31) and (32) can be identified as

$$\frac{\partial W}{\partial u_y} = 0 \quad (33)$$

$$\frac{\partial W}{\partial u_y'} = 0 \quad (34)$$

$$\frac{\partial W}{\partial u_y''} = \frac{1}{2} EI_z \cdot 2u_y'' + M_y \cdot \varphi = EI_z \cdot u_y'' + M_y \cdot \varphi \quad (35)$$

$$\frac{\partial W}{\partial \varphi} = M_y \cdot u_y'' \quad (36)$$

$$\frac{\partial W}{\partial \varphi'} = \frac{1}{2} GI_t \cdot 2\varphi' = GI_t \cdot \varphi' \quad (37)$$

$$\frac{\partial W}{\partial \varphi''} = \frac{1}{2} EI_w \cdot 2\varphi'' = EI_w \cdot \varphi'' \quad (38)$$

The first of Euler's equations (31) can now be written

$$\frac{d^2}{dx^2} (EI_z \cdot u_y'' + M_y \cdot \varphi) = 0 \quad (39)$$

Derivation yields (M_y is constant with respect to x)

$$EI_z \cdot u_y^{iv} + M_y \cdot \varphi'' = 0 \quad (40)$$

The second of Euler's equations (32) can be written

$$M_y \cdot u_y'' - \frac{d}{dx} (GI_t \cdot \varphi') + \frac{d^2}{dx^2} (EI_w \cdot \varphi'') = 0 \quad (41)$$

Derivation yields

$$M_y \cdot u_y'' - GI_t \cdot \varphi'' + EI_w \cdot \varphi^{iv} = 0 \quad (42)$$

The two Euler equations (40) and (42) are coupled differential equations that describe the deflected state of equilibrium after buckling

If equation (40) is integrated twice with respect to x , the following expression is obtained

$$EI_z \cdot u_y'' + M_y \cdot \varphi = k_1 x + k_2 \quad (43)$$

Where k_1, k_2 = Constants that can be determined from the boundary conditions

For fork supports at both ends

$$u_y''(0) = u_y''(L) = 0 \quad (44)$$

$$\varphi(0) = \varphi(L) = 0 \quad (45)$$

Hence, the constants k_1 and k_2 are equal to zero and equation (43) is reduced to

$$EI_z \cdot u''_y + M_y \cdot \varphi = 0 \quad (46)$$

$$u''_y = -\frac{M_y \cdot \varphi}{EI_z} \quad (47)$$

If equation (47) is inserted in equation (42) (the second Euler equation), the following fourth order ordinary differential equation is obtained

$$M_y \cdot \left(-\frac{M_y \cdot \varphi}{EI_z} \right) - GI_t \cdot \varphi'' + EI_w \cdot \varphi^{iv} = 0 \quad (48)$$

$$EI_w \cdot \varphi^{iv} - GI_t \cdot \varphi'' - \frac{M_y^2 \cdot \varphi}{EI_z} = 0 \quad (49)$$

To solve this equation, the deflected shape must be assumed. Let the solution be on form of a sine curve

$$\varphi = A \cdot \sin\left(\frac{j \cdot \pi \cdot z}{L}\right) \quad (50)$$

Derivation gives

$$\varphi'' = -A \left(\frac{j \cdot \pi}{L} \right)^2 \cdot \sin\left(\frac{j \cdot \pi \cdot x}{L}\right) \quad (51)$$

$$\varphi^{iv} = A \left(\frac{j \cdot \pi}{L} \right)^4 \cdot \sin\left(\frac{j \cdot \pi \cdot x}{L}\right) \quad (52)$$

With the solutions inserted, equation (49) can be written as

$$A \cdot \sin\left(\frac{j \cdot \pi \cdot x}{L}\right) \cdot \left(EI_w \cdot \left(\frac{j \cdot \pi}{L} \right)^4 + GI_t \cdot \left(\frac{j \cdot \pi}{L} \right)^2 - \frac{M_y^2}{EI_z} \right) = 0 \quad (53)$$

Since

$$A \cdot \sin\left(\frac{j \cdot \pi \cdot x}{L}\right) \neq 0 \quad (54)$$

The equation is reduced to

$$EI_w \cdot \left(\frac{j \cdot \pi}{L} \right)^4 + GI_t \cdot \left(\frac{j \cdot \pi}{L} \right)^2 - \frac{M_y^2}{EI_z} = 0 \quad (55)$$

$$M_y = \sqrt{EI_z \cdot EI_w \cdot \left(\frac{j \cdot \pi}{L}\right)^4 + EI_z \cdot GI_t \cdot \left(\frac{j \cdot \pi}{L}\right)^2} \quad (56)$$

$$M_y = \frac{(j \cdot \pi)^2}{L^2} \sqrt{EI_z \cdot EI_w + \frac{EI_z \cdot GI_t}{\left(\frac{j \cdot \pi}{L}\right)^2}} \quad (57)$$

$$M_y = \frac{(j \cdot \pi)^2}{L^2} \sqrt{\frac{(EI_z)^2 \cdot EI_w}{EI_z} + \frac{(EI_z)^2 \cdot GI_t}{EI_z \cdot \left(\frac{j \cdot \pi}{L}\right)^2}} \quad (58)$$

$$M_y = \frac{(j \cdot \pi)^2 \cdot EI_z}{L^2} \sqrt{\frac{EI_w}{EI_z} + \frac{GI_t}{EI_z \cdot \left(\frac{j \cdot \pi}{L}\right)^2}} \quad (59)$$

$$M_y = \frac{(j \cdot \pi)^2 \cdot EI_z}{L^2} \sqrt{\frac{I_w}{I_z} + \frac{L^2 \cdot GI_t}{(j \cdot \pi)^2 \cdot EI_z}} \quad (60)$$

The lowest value of M_y is given by $j = 1$ and hence, an expression for the elastic critical moment for a double-symmetric I-beam on two fork-supports subjected to end moment loading can be established

$$M_{cr,0} = \frac{\pi^2 \cdot EI_z}{L^2} \sqrt{\frac{I_w}{I_z} + \frac{L^2 \cdot GI_t}{\pi^2 \cdot EI_z}} \quad (61)$$

Appendix D

In this appendix, two examples of in.-files are presented that was used for the parametric study in ADINA.

D1 IPE 500, 8m, Fork supports, $k=1.0$ - Concentrated load in mid-span

* IPE 500, 8m, Fork supports - Concentrated load in mid-span *

*****KINEMATICS*****

KINEMATICS DISPLACE=LARGE STRAINS=SMALL

KINEMATICS BEAM-ALGORITHM=V87

*****GEOMETRY*****

*-----Define points-----

COORDINATES POINT SYSTEM=0

@CLEAR

1 0 0 0

2 4 0 0

3 8 0 0

*-----Define lines-----

LINE STRAIGHT NAME=1 P1=1 P2=2

LINE STRAIGHT NAME=2 P1=2 P2=3

*-----General Cross-section-----

CROSS-SECTIO PROPERTIES NAME=1 RINERTIA=8.93E-07,

SINERTIA=0.000482 TINERTIA=2.142E-05,

AREA=0.0116 SAREA=0,

TAREA=0 CTOFFSET=0,

CSOFFSET=0 STINERTI=0,

SRINERTI=0 TRINERTI=0,

WINERTIA=1.249E-06 WRINERTI=0,

DRINERTI=0

*****MATERIAL*****

MATERIAL ELASTIC NAME=1 E=210e9 NU=0.3 MDESCRIP='STEEL'

*****BOUNDARY CONDITIONS*****

*-----Define boundaries-----

FIXITY NAME=FORK1

@CLEAR

'Y-TRANSLATION'

'Z-TRANSLATION'

'X-ROTATION'

'Y-ROTATION'

'OVALIZATION'

FIXITY NAME=FORK2

@CLEAR

'X-TRANSLATION'

'Y-TRANSLATION'

'Z-TRANSLATION'

'X-ROTATION'

'OVALIZATION'

*-----Apply boundaries-----

FIXBOUNDARY POINTS FIXITY=ALL

@CLEAR

1 'FORK1'

3 'FORK2'

*****CONCENTRATED LOAD*****

*-----Define load-----

LOAD FORCE NAME=1 MAGNITUD=100000 FX=0 FY=0 FZ=-1

*-----Apply load-----

APPLY-LOAD BODY=0

@CLEAR

1 'FORCE' 1 'POINT' 2 0 1 0 0 -1 0 0 0 'NO' 0 0 1 0 'MID'


```

*****MESH*****
*-----Element definition-----
EGROUP  BEAM  NAME=1  SUBTYPE=THREE-D  DISPLACE=LARGE
MATERIAL=1 RINT=5 WARP=YES

*-----Subdivide line-----
SUBDIVIDE LINE NAME=1 MODE=DIVISIONS NDIV=50 RATIO=1
@CLEAR
1
2

*-----Assign cross-section to mesh-----
GLINE NODES=2 AUXPOINT=0 NCOINCID=ALL NCENDS=12,
NCTOLERA=1E-05 SUBSTRUC=0 GROUP=1 MIDNODES=CURVED,
XO=0 YO=1 ZO=0 XYZOSYST=SKEW
@CLEAR
1
2

*****DEFINE ANALYSIS*****
MASTER ANALYSIS=BUCKLING-LOADS MODEX=EXECUTE TSTART=0,
IDOF=0 OVALIZAT=NONE FLUIDPOT=AUTOMATIC CYCLICPA=1
IPOSIT=STOP REACTION=YES INITIALS=NO FSINTERA=NO
IRINT=DEFAULT CMASS=NO SHELLNDO=AUTOMATIC AUTOMATI=OFF
SOLVER=SPARSE CONTACT=CONSTRAINT-FUNCTION TRELEASE=0,
RESTART=NO FRACTURE=NO LOAD-CAS=NO LOAD-PEN=NO
SINGULAR=YES STIFFNES=0.0001 MAP-OUTP=NONE MAP-FORM=NO
NODAL-DE=" POROUS-C=NO ADAPTIVE=0 ZOOM-LAB=1 AXIS-CYC=0
PERIODIC=NO VECTOR-S=GEOMETRY EPSI-FIR=NO STABILIZ=NO
STABFACT=10E-10 RESULTS=PORTHOLE FEFCORR=NO BOLTSTEP=1
EXTEND-S=YES CONVERT=-NO DEGEN=YES TMC-MODE=NO ENSIGHT-
=NO IRSTEPS=1 INITIALT=NO TEMP-INT=NO ESINTERA=NO
OP2GEOM=NO

BUCKLING-LOA NEIGEN=1 NMODE=0 IPRINT=NO NITEMM=40
NVECTOR=DEFAULT TOLERANC=DEFAULT STARTTYP=LANCZOS
NSTVECTO=0 METHOD=CLASSICAL

```

D2 IPE 500, 8m, Fixed about major axis, $k=0.5$ - Concentrated load applied on the top flange in mid-span

* IPE 500, 8 m, Fixed, $k=0.5$ - Concentrated load on top flange in mid-span *

*****KINEMATICS*****

KINEMATICS DISPLACE=LARGE STRAINS=SMALL

KINEMATICS BEAM-ALGORITHM=V87

*****GEOMETRY*****

*-----Define points-----

COORDINATES POINT SYSTEM=0

@CLEAR

1 0 0 0

2 4 0 0

3 8 0 0

4 4 0 0.25

*-----Define lines-----

LINE STRAIGHT NAME=1 P1=1 P2=2

LINE STRAIGHT NAME=2 P1=2 P2=3

*-----Define rigid link-----

RIGIDLINK NAME=1 SLAVETYP=POINT SLAVENAM=2 MASTERTY=POINT
MASTERNA=4, DISPLACE=LARGE OPTION=0 SLAVEBOD=0 MASTERBO=0
DOF=ALL DOFSI=123456

*-----General Cross-section-----

CROSS-SECTION PROPERTIES NAME=1 RINERTIA=8.93E-07,
SINERTIA=0.000482 TINERTIA=2.142E-05,
AREA=0.0116 SAREA=0,
TAREA=0 CTOFFSET=0,
CSOFFSET=0 STINERTI=0,
SRINERTI=0 TRINERTI=0,
WINERTIA=1.249E-06 WRINERTI=0,
DRINERTI=0

*****MATERIAL*****

MATERIAL ELASTIC NAME=1 E=210e9 NU=0.30 MDESCRIP='STEEL'

*****BOUNDARY CONDITIONS*****

*-----Define boundaries-----

FIXITY NAME=FIX1

@CLEAR

'X-TRANSLATION'

'Y-TRANSLATION'

'Z-TRANSLATION'

'X-ROTATION'

'X-ROTATION'

'Y-ROTATION'

'Z-ROTATION'

'BEAM-WARP'

'OVALIZATION'

FIXITY NAME=FIX2

@CLEAR

'Y-TRANSLATION'

'Z-TRANSLATION'

'X-ROTATION'

'X-ROTATION'

'Y-ROTATION'

'Z-ROTATION'

'BEAM-WARP'

'OVALIZATION'

*-----Apply boundaries-----

FIXBOUNDARY POINTS FIXITY=ALL

@CLEAR

1 'FIX1'

3 'FIX2'

*****CONCENTRATED LOAD*****

*-----Define load-----

LOAD FORCE NAME=1 MAGNITUD=100000 FX=0 FY=0 FZ=-1

*-----Apply load-----

APPLY-LOAD BODY=0

@CLEAR

1 'FORCE' 1 'POINT' 4 0 1 0 0 -1 0 0 0 'NO' 0 0 1 0 'MID'

*****MESH*****

*-----Element definition-----

EGROUP BEAM NAME=1 SUBTYPE=THREE-D DISPLACE=LARGE
MATERIAL=1 RINT=5 WARP=YES SECTION=1

*-----Subdivide line-----

SUBDIVIDE LINE NAME=1 MODE=DIVISIONS NDIV=50 RATIO=1

@CLEAR

1

2

*-----Assign cross-section to mesh-----

GLINE NODES=2 AUXPOINT=0 NCOINCID=ALL NCENDS=12
NCTOLERA=1E-05 SUBSTRUC=0 GROUP=1 MIDNODES=CURVED XO=0
YO=1 ZO=0 XYZOSYST=SKEW

@CLEAR

1

2

*-----Add node of rigid link-----

GPOINT NODE=102 NCOINCID=ALL NCTOLERA=1E-05 SUBSTRUC=0

@CLEAR

4

@

*****DEFINE ANALYSIS*****

MASTER ANALYSIS=BUCKLING-LOADS MODEX=EXECUTE TSTART=0,
IDOF=0 OVALIZAT=NONE FLUIDPOT=AUTOMATIC CYCLICPA=1
IPOSIT=STOP REACTION=YES INITIALS=NO FSINTERA=NO
IRINT=DEFAULT CMASS=NO SHELLNDO=AUTOMATIC AUTOMATI=OFF
SOLVER=SPARSE CONTACT=CONSTRAINT-FUNCTION TRELEASE=0,
RESTART=NO FRACTURE=NO LOAD-CAS=NO LOAD-PEN=NO
SINGULAR=YES STIFFNES=0.0001 MAP-OUTP=NONE MAP-FORM=NO
NODAL-DE=" POROUS-C=NO ADAPTIVE=0 ZOOM-LAB=1 AXIS-CYC=0
PERIODIC=NO VECTOR-S=GEOMETRY EPSI-FIR=NO STABILIZ=NO
STABFACT=10E-10 RESULTS=PORTHOLE FEFCORR=NO BOLTSTEP=1
EXTEND-S=YES CONVERT=-NO DEGEN=YES TMC-MODE=NO ENSIGHT-
=NO IRSTEPS=1 INITIALT=NO TEMP-INT=NO ESINTERA=NO
OP2GEOM=NO

BUCKLING-LOA NEIGEN=1 NMODE=0 IPRINT=NO NITEMM=40
NVECTOR=DEFAULT TOLERANC=DEFAULT STARTTYP=LANCZOS
NSTVECTO=0 METHOD=CLASSICAL

Appendix E

In appendix E, results from the parametric study are presented.

E1 Parametric study of C_I

E1.1 Simply supported about major axis

E1.1.1 Serna et al. (2005)

End moments

(Section properties from ArcelorMittal)

Length [m]	k	C ₁	M _{cr_ref} [kNm]	M _{cr} [kNm]
8	1	1,000	279,448	279,448
8	0,7			
8	0,5	1,000	805,645	805,645
16	1	1,000	119,423	119,423
16	0,7			
16	0,5	1,000	279,448	279,448

Concentrated load in mid-span

(Section properties from ArcelorMittal)

Length [m]	k	C ₁	M _{cr_ref} [kNm]	M _{cr} [kNm]
8	1	1,359	279,448	379,770
8	0,7			
8	0,5	1,061	805,645	854,789
16	1	1,355	119,423	161,818
16	0,7			
16	0,5	1,059	279,448	295,935

Distributed load

(Section properties from ArcelorMittal)

Length [m]	k	C ₁	M _{cr_ref} [kNm]	M _{cr} [kNm]
8	1	1,131	279,448	316,056
8	0,7			
8	0,5	0,967	805,645	779,058
16	1	1,130	119,423	134,948
16	0,7			
16	0,5	0,966	279,448	269,947

E1.1.2 ADINA

End moments

Length [m]	k	M_cr/M_cr_ref	M_cr_ref [kNm]	M_cr [kNm]
8	1	1,023	279,448	285,848
8	0,7	1,011	467,941	472,937
8	0,5	0,983	805,645	791,797
16	1	1,023	119,423	122,176
16	0,7	1,010	181,193	183,043
16	0,5	0,982	279,448	274,415

Concentrated load in mid-span

Length [m]	k	M_cr/M_cr_ref	M_cr_ref [kNm]	P_cr [kN]	M_cr [kNm]
8	1	1,393	279,448	194,576	389,152
8	0,7	1,308	467,941	305,928	611,856
8	0,5	1,066	805,645	429,444	858,888
16	1	1,388	119,423	41,444	165,776
16	0,7	1,293	181,193	58,548	234,192
16	0,5	1,063	279,448	74,235	296,940

Distributed load

Length [m]	k	M_cr/M_cr_ref	M_cr_ref [kNm]	q_cr [kN/m]	M_cr [kNm]
8	1	1,157	279,448	40,423	323,384
8	0,7	1,117	467,941	65,316	522,528
8	0,5	0,965	805,645	97,131	777,048
16	1	1,156	119,423	4,313	138,016
16	0,7	1,110	181,193	6,285	201,120
16	0,5	0,962	279,448	8,399	268,768

E1.1.3 COLBEAM

End moments

Length [m]	k	C_1	M_cr_ref	M_cr [kNm]
8	1	1,000	279,890	279,890
8	0,7	1,030	468,534	482,590
8	0,5	1,050	806,429	846,750
16	1	1,000	119,660	119,660
16	0,7	1,030	181,524	186,970
16	0,5	1,050	279,886	293,880

Concentrated load in mid-span

Length [m]	k	C_1	M_cr_ref	M_cr [kNm]
8	1	1,350	279,889	377,85
8	0,7	1,170	468,530	548,18
8	0,5	1,050	806,429	846,75
16	1	1,350	119,667	161,55
16	0,7	1,170	181,521	212,38
16	0,5	1,050	279,886	293,88

Distributed load

Length [m]	k	C_1	M_cr_ref	M_cr [kNm]
8	1	1,120	279,893	313,48
8	0,7	1,030	468,825	482,89
8	0,5	0,970	806,423	782,23
16	1	1,120	119,661	134,02
16	0,7	1,030	181,524	186,97
16	0,5	0,970	279,887	271,49

E1.1.4 COLBEAM with the option “advanced calculation of C1”

End moments

Length [m]	k	C1_ "advanced"	M_cr_ref [Nm]	M_cr [kNm]
8	1	-		-
8	0,7	-		-
8	0,5	-		-
16	1	-		-
16	0,7	-		-
16	0,5	-		-

Concentrated load in mid-span

Length [m]	k	C1_ "advanced"	M_cr_ref [Nm]	M_cr [kNm]
8	1	1,256	279,976	351,650
8	0,7	1,127	468,385	527,870
8	0,5	1,031	806,469	831,470
16	1	1,256	119,697	150,340
16	0,7	1,127	181,464	204,510
16	0,5	1,031	279,903	288,580

Distributed load

Length [m]	k	C1_ "advanced"	M_cr_ref [Nm]	M_cr [kNm]
8	1	1,134	279,947	317,460
8	0,7	1,07	468,654	501,460
8	0,5	1,015	806,305	818,400
16	1	1,134	119,691	135,730
16	0,7	1,07	181,570	194,280
16	0,5	1,015	279,852	284,050

E1.1.5 LTBeam

End moments

Length [m]	k	M_cr/M_cr_ref	M_cr_ref [kNm]	M_cr [kNm]
8	1	1,000	279,348	279,340
8	0,7	1,002	468,078	468,930
8	0,5	1,000	806,355	806,340
16	1	1,000	119,275	119,270
16	0,7	1,001	181,036	181,290
16	0,5	1,000	279,348	279,340

Concentrated load in mid-span

Length [m]	k	M_cr/M_cr_ref	M_cr_ref [kNm]	M_cr [kNm]
8	1	1,362	279,348	380,400
8	0,7	1,295	468,078	605,960
8	0,5	1,067	806,355	860,040
16	1	1,357	119,275	161,900
16	0,7	1,281	181,036	231,840
16	0,5	1,064	279,348	297,290

Distributed load

Length [m]	k	M_cr/M_cr_ref	M_cr_ref [kNm]	M_cr [kNm]
8	1	1,131	279,348	316,020
8	0,7	1,106	468,078	517,820
8	0,5	0,970	806,355	782,230
16	1	1,130	119,275	134,760
16	0,7	1,101	181,036	199,240
16	0,5	0,969	279,348	270,630

E1.1.6 SAP2000

End moments

Length [m]	k	C_1	M_cr_ref [kNm]	M_cr [kNm]
8	1	1,000	279,466	279,466
8	0,7	1,000	468,240	468,240
8	0,5	1,000	806,580	806,580
16	1	1,000	119,338	119,338
16	0,7	1,000	118,123	118,123
16	0,5	1,000	279,466	279,466

Concentrated load in mid-span

Length [m]	k	C_1	M_cr_ref [kNm]	M_cr [kNm]
8	1	1,316	279,422	367,719
8	0,7	1,316	468,166	616,106
8	0,5	1,316	806,451	1061,289
16	1	1,316	119,318	157,023
16	0,7	1,316	181,093	238,319
16	0,5	1,316	279,422	367,719

Distributed load

Length [m]	k	C_1	M_cr_ref [kNm]	M_cr [kNm]
8	1	1,137	279,370	317,644
8	0,7	1,137	468,080	532,207
8	0,5	1,137	806,304	916,768
16	1	1,136	119,376	135,611
16	0,7	1,136	181,180	205,821
16	0,5	1,136	279,555	317,575

E1.2 Fixed about major axis

E1.2.1 Serna et al. (2005)

Concentrated load in mid-span

(Section properties from ArcelorMittal)

Length [m]	k	C_1	M_cr_0 [kNm]	M_cr [kNm]
8	1	1,713	279,448	478,694
8	0,7			
8	0,5	1,044	805,645	841,093
16	1	1,702	119,423	203,258
16	0,7			
16	0,5	1,033	279,448	288,670

Distributed load

(Section properties from ArcelorMittal)

Length [m]	k	C_1	M_cr_0 [kNm]	M_cr [kNm]
8	1	2,605	279,448	727,962
8	0,7			
8	0,5	1,733	805,645	1396,182
16	1	2,596	119,423	310,022
16	0,7			
16	0,5	1,711	279,448	478,135

E1.2.2 ADINA

Concentrated load in mid-span

Length [m]	k	M_cr/M_cr_0	M_cr_0 [kNm]	P_cr [kN]	M_cr [kNm]
8	1	1,761	279,448	492,210	492,210
8	0,7	1,446	467,941	676,606	676,606
8	0,5	1,070	805,645	862,437	862,437
16	1	1,750	119,423	104,503	209,006
16	0,7	1,413	181,193	128,039	256,078
16	0,5	1,060	279,448	148,100	296,200

Distributed load

Length [m]	k	M_cr/M_cr_0	M_cr_0 [kNm]	q_cr [kN/m]	M_cr [kNm]
8	1	2,667	279,448	139,740	745,280
8	0,7	2,286	467,941	200,572	1069,717
8	0,5	1,762	805,645	266,095	1419,173
16	1	2,658	119,423	14,880	317,440
16	0,7	2,243	181,193	19,053	406,464
16	0,5	1,740	279,448	22,795	486,293

E1.2.3 COLBEAM

Concentrated load in mid-span

Length [m]	k	C_1	M_cr_0 [kNm]	M_cr [kNm]
8	1	1,565	279,891	438,030
8	0,7	1,189	468,452	556,990
8	0,5	0,938	806,429	756,430
16	1	1,565	119,661	187,270
16	0,7	1,189	181,497	215,800
16	0,5	0,938	279,889	262,536

Distributed load

Length [m]	k	C_1	M_cr_0 [kNm]	M_cr [kNm]
8	1	1,285	279,891	359,660
8	0,7	0,941	524,352	440,980
8	0,5	0,712	806,419	574,170
16	1	1,285	119,665	153,770
16	0,7	0,941	203,151	170,850
16	0,5	0,712	279,888	199,280

E1.2.4 COLBEAM with the option "advanced calculation of C1"

Concentrated load in mid-span

Length [m]	k	C_1_"advanced"	M_cr_0 [kNm]	M_cr [kNm]
8	1	1,381	279,826	386,440
8	0,7	1,109	468,323	519,370
8	0,5	0,948	806,688	764,740
16	1	1,381	119,638	165,220
16	0,7	1,109	181,443	201,220
16	0,5	0,948	279,979	265,420

Distributed load

Length [m]	k	C_1_"advanced"	M_cr_0 [kNm]	M_cr [kNm]
8	1	2,419	279,876	677,020
8	0,7	1,918	468,425	898,440
8	0,5	1,654	806,378	1333,750
16	1	2,419	119,657	289,450
16	0,7	1,918	181,486	348,090
16	0,5	1,654	279,873	462,910

E1.2.5 SAP2000

Concentrated load in mid-span

Length [m]	k	C_1	M_cr_0 [kNm]	M_cr [kNm]
8	1	1,923	279,477	537,435
8	0,7	1,923	468,259	900,462
8	0,5	1,923	806,612	1551,115
16	1	1,923	119,343	229,496
16	0,7	1,923	181,130	348,313
16	0,5	1,923	279,477	537,435

Distributed load

Length [m]	k	C_1	M_cr_0 [kNm]	M_cr [kNm]
8	1	2,383	279,418	665,852
8	0,7	2,383	468,159	1115,623
8	0,5	2,383	806,439	1921,745
16	1	2,381	119,335	284,137
16	0,7	2,381	181,119	431,245
16	0,5	2,381	279,461	665,396

E2 Parametric study of C_2

E2.1 Simply supported about major axis

E2.1.1 ADINA

Concentrated load in mid-span

	Length [m]	k	C_1	M_cr [kNm]	C_2
Top	8	1	1,393	273,460	0,574
Bottom	8	1	1,393	550,326	0,573
Top	8	0,7	1,308	424,208	0,491
Bottom	8	0,7	1,308	868,056	0,474
Top	8	0,5	1,066	593,376	0,437
Bottom	8	0,5	1,066	1238,722	0,436

Distributed load

	Length [m]	k	C_1	M_cr [kNm]	C_2
Top	8	1	1,157	214,326	0,674
Bottom	8	1	1,157	381,829	0,273
Top	8	0,7	1,117	346,745	0,554
Bottom	8	0,7	1,117	610,211	0,208
Top	8	0,5	0,965	529,228	0,455
Bottom	8	0,5	0,965	876,554	0,141

E2.1.2 COLBEAM

Concentrated load in mid-span

	Length [m]	k	M_cr [kNm]	C_2
Top	8	1	194,500	0,590
Bottom	8	1	399,100	0,590
Top	8	0,7	316,900	0,524
Bottom	8	0,7	687,800	0,524
Top	8	0,5	537,700	0,480
Bottom	8	0,5	1204,000	0,480

Distributed load

	Length [m]	k	M_cr [kNm]	C_2
Top	8	1	211,300	0,450
Bottom	8	1	367,400	0,450
Top	8	0,7	347,300	0,396
Bottom	8	0,7	627,600	0,396
Top	8	0,5	592,600	0,360
Bottom	8	0,5	1092,000	0,360

E2.1.3 LTBeam

Concentrated load in mid-span

	Length [m]	k	C_1	M_cr [kNm]	C_2
Top	8	1	1,362	269,300	0,561
Bottom	8	1	1,362	534,090	0,560
Top	8	0,7	1,295	421,720	0,486
Bottom	8	0,7	1,295	856,020	0,468
Top	8	0,5	1,067	594,210	0,438
Bottom	8	0,5	1,067	1240,500	0,436

Distributed load

	Length [m]	k	C_1	M_cr [kNm]	C_2
Top	8	1	1,131	238,720	0,451
Bottom	8	1	1,131	417,990	0,461
Top	8	0,7	1,106	390,650	0,374
Bottom	8	0,7	1,106	682,620	0,373
Top	8	0,5	0,970	603,910	0,302
Bottom	8	0,5	0,970	1005,000	0,296

E2.2 Fixed about major axis

E2.2.1 ADINA

Concentrated load in mid-span

	Length [m]	k	C_1	M_cr [kNm]	C_2
Top	8	1	1,761	216,726	1,463
Bottom	8	1	1,761	1095,447	1,434
Top	8	0,7	1,446	316,138	1,100
Bottom	8	0,7	1,446	1399,695	1,049
Top	8	0,5	1,070	427,761	0,879
Bottom	8	0,5	1,070	1698,676	0,850

Distributed load

	Length [m]	k	C_1	M_cr [kNm]	C_2
Top	8	1	2,667	269,626	1,922
Bottom	8	1	2,667	1539,071	1,276
Top	8	0,7	2,286	421,064	1,412
Bottom	8	0,7	2,286	2032,786	0,91
Top	8	0,5	1,762	633,710	1,038
Bottom	8	0,5	1,762	2375,161	0,626

E2.2.2 COLBEAM

Concentrated load in mid-span

	Length [m]	k	M_cr [kNm]	C_2
Top	8	1	117,500	1,565
Bottom	8	1	660,300	1,565
Top	8	0,7	207,700	1,189
Bottom	8	0,7	1049,000	1,189
Top	8	0,5	384,000	0,938
Bottom	8	0,5	1685,000	0,938

Distributed load

	Length [m]	k	M_cr [kNm]	C_2
Top	8	1	117,700	1,562
Bottom	8	1	659,500	1,562
Top	8	0,7	229,700	1,016
Bottom	8	0,7	948,900	1,016
Top	8	0,5	470,600	0,652
Bottom	8	0,5	1375,000	0,652

E2.2.3 LTBeam

Concentrated load in mid-span

	Length [m]	k	C_1	M_cr [kNm]	C_2
Top	8	1	1,722	214,980	1,431
Bottom	8	1	1,722	1055,800	1,403
Top	8	0,7	1,420	314,300	1,080
Bottom	8	0,7	1,420	1359,800	1,031
Top	8	0,5	1,054	425,720	0,866
Bottom	8	0,5	1,054	1657,100	0,836

Distributed load

	Length [m]	k	C_1	M_cr [kNm]	C_2
Top	8	1	2,607	305,370	1,572
Bottom	8	1	2,607	1698,900	1,536
Top	8	0,7	2,249	476,530	1,155
Bottom	8	0,7	2,249	2279,400	1,128
Top	8	0,5	1,741	721,510	0,829
Bottom	8	0,5	1,741	2687,200	0,810